UNIVERSITA' DEGLI STUDI DI PADOVA

Dipartimento di Scienze Chimiche

Corso di laurea magistrale in Chimica Industriale

TESI DI LAUREA MAGISTRALE

Sustainable synthesis of coumarins catalyzed by Au(I)/Au(III) complexes in ionic liquids

Relatore: Prof. Biffis Andrea

Correlatore: Prof. Bourissou Didier

Controrelatore: Prof. Santi Saverio

LAUREANDO: Ravera Francesco

2021829

ANNO ACCADEMICO 2021/2022

Index

Abbreviations

TMs	Transition metals
ILs	Ionic liquids
r.d.s.	Rate determining step
TFA	Trifluoroacetic acid
DCM	Dichloromethane
DCE	1,2-Dichloroethane
API	Active pharmaceutical ingredient
BMIM	Butyl methyl imidazolium
TMB	1,3,5-Trimethoxybenzene

Abstract

The possibility to directly activate C-H bonds is nowadays one of the most interesting perspectives, concerning the direct functionalization of organic substrates. Achieving a sufficient knowledge on the fundamental mechanisms that allow these transformations, will make possible to get access to new methodologies for more sustainable processes. Since the beginning of the new century, gold catalysis has received a lot of consideration in modern organometal-focused research environments. The strong affinity of gold for unsaturated organic systems opens a new avenue to explore as a potential tool for organic synthesis: the π-acid catalysis. This project deals with the activation of alkynes toward the hydroarylation reaction, performed by cationic Au(I)/Au(III) complexes. Moreover, the use of ionic liquids (ILs) as reaction media give us the possibility to explore a new and interesting catalytic system, which combines a positive solvent effect, enhancing the catalytic performance of the active species, with a sustainable choice. Indeed, ILs open a series of other features to be explored, such as the potential recyclability of the system, which constitutes a very attractive perspective to lower costs and process wastes, avoiding at the same time the use of conventional halogenated solvents (dichloromethane, dichloroethane).

The process I have focused on, developed by the *Applied Organometallic Chemistry* group (DiSC-UNIPD, Prof. Biffis), has been applied for the synthesis of coumarins, organic products of interest for their bioactivity and optical properties. In collaboration with the LBPB group of Toulouse (LHFA-UPS, Prof. Bourissou), the potential application of (P,C)Au(III)X_2 complexes has been also explored on this system, with the aim of expanding the reaction scope.

Chapter 1
Introduction to gold chemistry and π-acid catalysis

1. π-σ coordinative bond and π-systems activation

1.1 Introduction to π-acid catalysis

The organometallic chemistry of the last century saw an incredible development, pushed by the driving force of new applications in organic synthesis. In particular, the second half of the 20th century has been led by some of the most relevant discoveries in term of catalytic transformations. The disclosure of Heck and cross-coupling reactions,[1] together with alkene/alkyne metatheses[2][3] and stereoselective hydrogenations/oxidations of unsaturated bonds[4][5] have all been awarded the Nobel prize on the first decade of the 21st century: respectively in 2010, 2005 and 2001. In the middle of the such a blooming period for organic synthesis, we see emerging a new concept for organometallic catalysis, which does not involve redox steps at the metal center. Lewis acids as activators for chemical transformations have a long history. The principal novelty of this new trend is the rediscovery of metals such as Pt and Au, which were believed unreactive until few decades ago, as extremely efficient carbophilic π-acids. The main interests in these systems fall on their ability to totally outperform classic stochiometric reagents either in the context of atom-economy or in the extent of applications in term of substrates and reactivities. Nevertheless, in the literature are reported others transition metals (TMs: Cu, Pd, Ti, Hf, Zn)[6] and even lanthanoids that are able to activate π systems. The particular affinity of a metal toward multiple C-C bonds can be successfully rationalized by the HSAB theory,[7] introduced by Pearson in order to describe the empirical reactivity patterns between Lewis acids and bases, evaluating their relative polarizability. According to this last aspect, the metal oxidation state and the presence of a net charge on the acid species play a fundamental role on these transformations. The metal-unsaturated bond interaction for TMs is described as well by the Dewar-Chatt-Ducanson (DCD) model.[8] According to this description (see ***figure 1.1.1***), the frontiers molecular orbitals of the ligand overlap with the metal d orbitals forming a stable adduct enforced by σ-donation and π back-donation synergism. However, as in all the models some approximation have been performed: it is indeed important to consider also the electrostatic contribution to the coordinative bond formation, which may amount to around 50% of the total bond energy according to computational studies on Cu, Ag and Au complexes bearing an acetylene and ethylene moiety.[9] In the model for alkynes, other two interactions involving the $\pi_{\perp}$ and $\pi^{*}_{\perp}$ out-of-plane orbitals are also reported, but they give a negligible apport to bond formation in the case of Pt(II) and Au(I).[6] In particular, the last interaction is limited by symmetry issues.

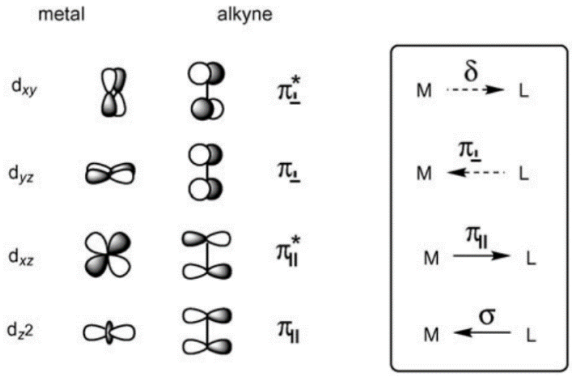

Figure 1.1.1 DCD model for Pd/Au-alkyne bond rationalization [6]

However, the important concept to learn about this interpretation for the alkene/yne coordinative bond to π acidic metal centers is directly related to the relative contributions of the before mentioned interactions to the bond formation. Considering the Au(I)-acetylene coordinative bond, the main contribution to orbital overlapping comes from the L→M σdonation (~65%) against the M→L back-donation to the alkyne (~27%).[9] So acetylene can be classified as a two electrons donor with low tendency to undergo π back donation. The same conclusion may be postulated in the case of ethylene, revealing to be even a slightly better donor than acetylene.[10] The oxidation state of the metal center can drastically change the relative weight of the different interactions contributing to the coordinative bond. For instance, picking up a Pt(0) complex, the metal center will be for sure more electron rich and so more prone to back donate electron density to the anti-bonding orbital of the alkyne. In that case, the DCD model would to be reconsidered in favor of a metallacyclopropene bond model, which takes into account the deformation in the ligand structure, with loss of planarity. The selection of the correct model is though not so obvious. The electron distribution over the complex can change according to the substrate substituents, the geometry, possible ring strain and also metal-related contributes, such as the electronic configuration, free coordination sites or even the presence of a net charge on the complex. Independently from this, we define as π acid any species that may act as a template for redistributing the alkyne electron density. The overall consequence is to

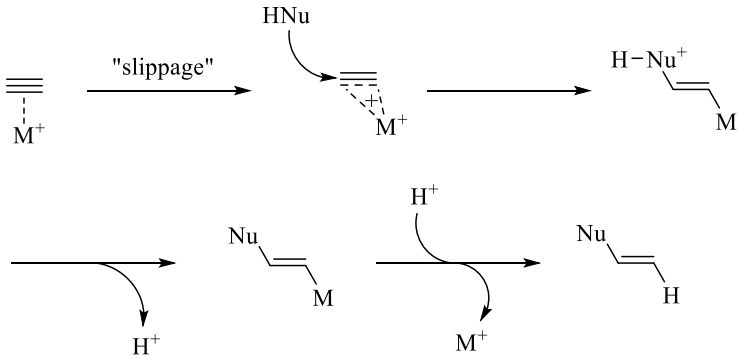

Figure 1.1.2 Carbophilic activation mechanism by π catalysis

withdraw part of it and generate a site for a nucleophilic attack: a simplified representation of the mechanism is reported in ***figure 1.1.2***. The illustration reports a classic carbophilic activation process of acetylene toward functionalization by a generic protic nucleophile HNu. The final product consists in a *trans* addition of the H^+ and Nu^- moieties over the former alkyne. In absence of available protons, any suitable electrophile may perform the terminal demetallation step. This is not the only possible pathway. In fact an inner sphere mechanism should be also considered possible. In this case, at first the nucleophile fragment coordinates to the metal center, then it migrates to the activated alkyne through a concerted mechanism. Indeed, it has already been observed in the case of alkyne hydroarylation reactions the presence of metalated arene and/or the syn addition product.[11] Another interesting perspective is the activation of alkynes toward other olefins nucleophilic attacks, often generating complex and unpredictable structures. In ***figure 1.1.3*** is reported a synthetic step over the total synthesis for streptorubin B, a prodigiosin alkaloid.[12]

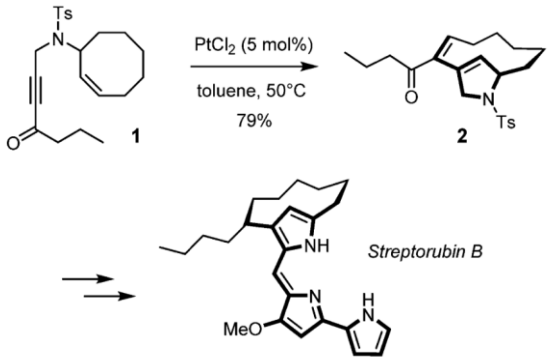

Figure 1.1.3 Platinum catalyzed enyne cycloisomerization as key step on streptorubin B synthesis [13]

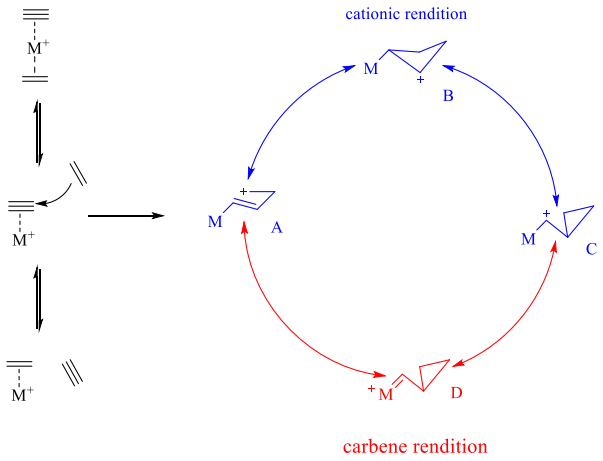

Figure 1.1.4 Carbene-carbocation hypothesis on ene-yne cycloisomerization reactions [13][14]

The reported transformation involves a complex rearrangement after the instauration of the new C-C bond. The group of Fürstner, the same which proposed the former synthesis, gave also a unified mechanism in order to describe the behavior of those transformations (***figure 1.1.4***). Once the olefin binds the activated metal-alkyne complex by slippage of the metal moiety, a series of resonance structures contributes to stabilize the carbocation-carbenoid that is forming. The specific prevalence of a structure with respect to another is dependent on the specific structure of the substrate and the possibility to form stable products. Moreover, we see that the attack is selective by the alkene to the alkyne and not vice versa. This comes from kinetic reasons, since we saw in case of the ethylene/acetylene that the alkene can even be a better ligand than the analogous alkyne. The situation of both the molecules coordinated represent as well a probable unreactive path, coming from the excess of donating electron density at the metal center; in this condition, the carbophilic activation fails for an increasing back-donation at the alkyne moiety. In conclusion, the activation of π-systems toward nucleophilic attacks by soft electrophilic centers can be a formidable tools for generating new complex structures. However, the complex mechanistic variables are many, determining a difficult prevision of the reaction outcome. Thus, the application of gold and platinum chemistry in synthesis are still rather limited if compared to the impressive number of mechanistic studies aimed to understand reactivity and selectivity of such processes.

1.2 Relativistic effects in late transition metals catalysis

Although the introduction of the carbene-carbocation hypothesis was not supported by clear experimental evidence, it is now extensively accepted by the scientific community. In particular, by these model it was possible to predict the particular affinity of soft and hardly-oxidizable late transition metal cations toward unsaturated C-C molecules. The effect of the charge and the coordination number is as well predicted, anticipating cationic monocoordinated $LAu(I)^+$ complexes as the best scaffold for alkyne coordination and activation. All these features have been explained taking into account the relativistic contraction of the 6s orbital (***figure 1.2.1***), which affects the 5d orbitals energy and enhances their diffuse character, since they are more screened. This phenomenon can be experimentally put in evidence considering the high energy of the L-Au coordinative interaction,

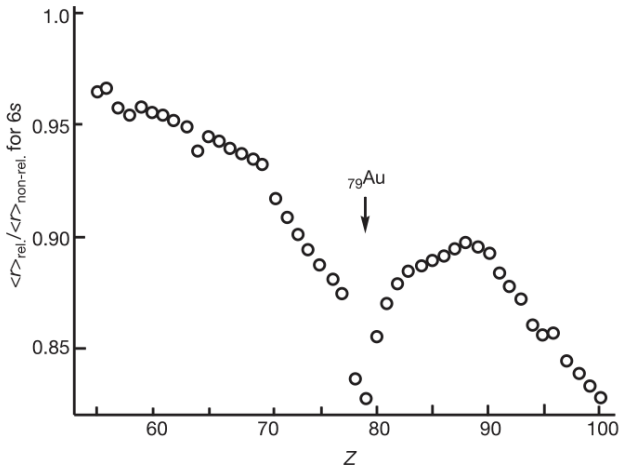

Figure 1.2.1 6s orbitals relative contraction in function of the atomic number Z

with L a phosphine or carbene ancillary ligand. As well, this effect contributes to determine the large value of the gold first ionization potential (9.22 eV against 7.57 eV for Ag). Lastly, it determines the formation of really singular Au-Au interactions with energy similar to a H-bond.[15] A computational analysis of the different coordination number and geometries on d^{10} configuration metals highlights the tendency of Au(I) to be involved in di-coordinated complexes of linear geometry. The reason of this behavior is demonstrated to match with the high deformation energy needed for bending the linear geometry of di-coordinated species and free another coordination site. On the other hand, the interaction contribute to the formation energy of tricoordinated complexes is negligible in order to explain differences in the behavior of 11^{th} group metals. Indeed, considering the same set of ligands (with the same charge), the calculated association energies are similar for all the monovalent cations of the 11^{th} group.[16]

These features have a fundamental implication in gold(I) catalysis, that exclude the formation of tricoordinated-Au(I) complexes as first step of catalytic transformations. It is indeed necessary to liberate a coordination site, often by removing a halide, in order to obtain carbophilic activity. However, once the coordinative site is free, the catalyst can be extremely reactive: the potential deactivation by coordination of more alkene/yne moieties is indeed inhibited. Summarizing all these aspects together: Au(I) metal centers constitute an extremely efficient electrophilic scaffold due to its soft character and the limited back-donation toward alkynes antibonding orbitals. The unfavorable oxidative addition at the metal center and its soft character make possible for Au(I) complexes to tolerate a notable range of functional groups, extending the variety of substrates on which we can apply these transformations.

1.3 C-H bond functionalization and the Fujiwara reaction

The direct functionalization of a C-H bond has always been one of the most fascinating perspectives in the field of synthetic organic chemistry. Thinking about these processes, it is present a strict analogy with cross-coupling reactions. For example, in a generic Suzuki coupling an organic halide RX is activated by oxidative addition at the Pd(0) catalytic center, to give a residue that may be coupled to another organic fragment, carried by an organoborane species in this case. Taking any organic molecule, likely, it would be rich of C-H bonds as "functional groups" over all its backbone. The possibility to selectively activate one of those bonds as it were a C-X bond could lead to new atom economic and convenient paths to afford important molecular targets. Notwithstanding, the challenges to achieve the desired reactivity are extremely tough to face. A hydrocarbon bond is indeed rather stabler than a generic C-X bond. The low difference in electronegativity and good orbitals overlap ensure a poorly polarized bond with low zero-point energy, even considering differences depending on the formal carbon hybridization state. The history of C-H bond functionalization is quite recent and sees its major developments in the last two decades. From a mechanistic point of view, different activation modes have been proposed and the energetic demand for each of them

depend on the substrate and catalyst. In the literature, four different classes have been proposed, each one containing other sub-cases: electrophilic activation, oxidative addition, σ-bond metathesis and 1,2-addition.[17] Inherently to the electrophilic properties of catalysts that are able to perform carbophilic activation, we can focus only on the first class. The oxidative addition at Au(I) centers is indeed a rather rare reaction[18][19] and the last two activation modes are limited to some specific compounds and early TMs complexes bearing multiple-bonded ligands (only for the 1,2-addition mechanism).

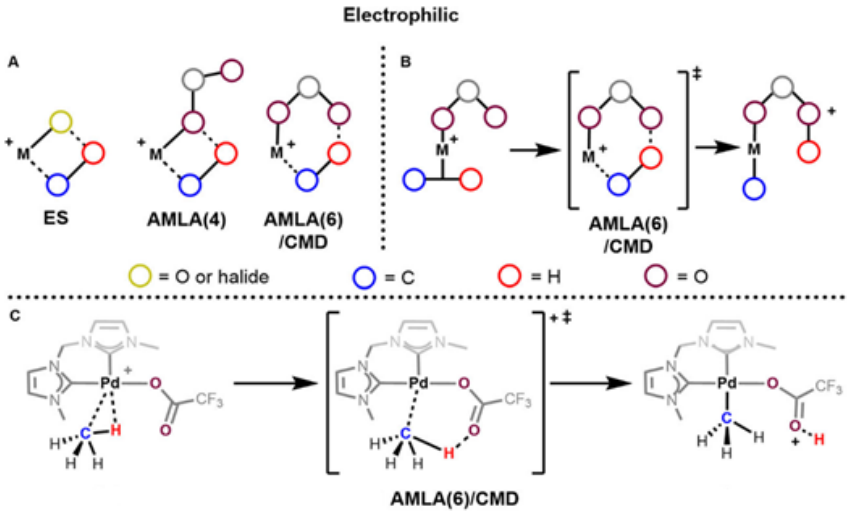

Figure 1.3.1 C-H activation by electrophilic substitution mechanism; A) Common transition states for electrophilic C-H activation: ES (electrophilic substitution), AMLA/CMD (amphiphilic metal-ligand activation or concerted metalation-deprotonation); B) AMLA/CMD mechanism with 6-membered transition state; C) DFT-predicted mechanism for methane activation [17][20]

In ***figure 1.3.1*** are reported the main activation modes for electrophilic C-H functionalization. As it is put in evidence, the presence of halides or an heteroatom able to abstract the proton is fundamental, taking the transition state to assume also 4 or 6-membered ring geometry. In the case of ES mechanism, for aromatic substrates it is commonly named electrophilic metalation (EM), since the reaction develops by a Wheland-type intermediate. The proton abstraction often represents the rate determining step (r.d.s.) of the process; it has to be assisted by an external base (intermolecular mechanism).

Despite all the attempts to classify the experimental evidence and computational studies into precise overviews on the mechanism of these reactions, exceptions always exist. In 2000 Fujiwara and co-workers reported an interesting system for the alkenylation of arenes via direct C-H functionalization.[11][21] The scheme reported in ***figure 1.3.2*** showcases an unusual type of reactivity toward alkyne hydrofunctionalization. It is well known that palladium acetate can perform metalation of arenes (reaction A) and subsequent functionalization of alkenes (the so called Fujiwara-Moritani reaction).

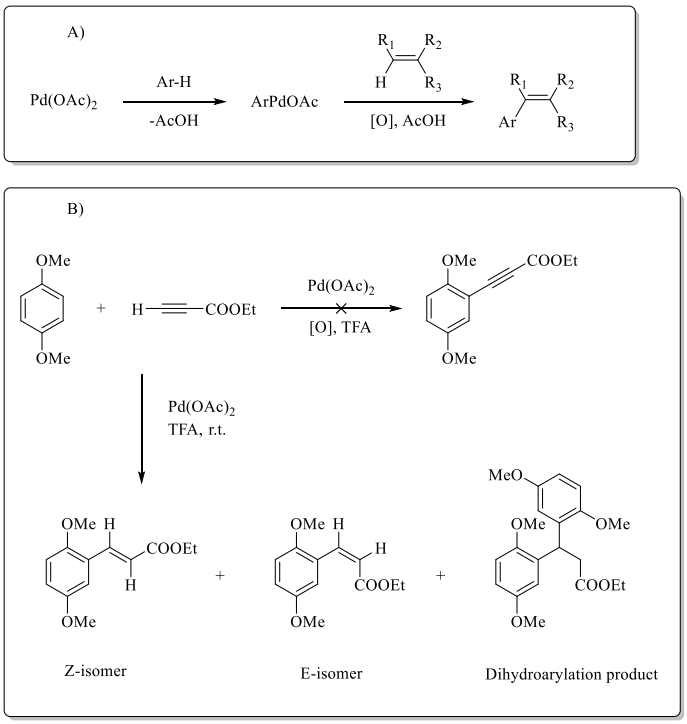

Figure 1.3.2 A) Oxidative functionalization of alkenes; B) Catalytic hydroarylation of ethyl propiolate with 1,4-di-methoxybenzene

The same reaction attempted on alkyne substrates provided unusual reactivity. Indeed the reaction B achieves only the addition product to the alkyne, with particular selectivity toward the Z-isomer. Some of the product undergoes a further cycle to afford the double addition product formation and complete saturation of the former olefin. Anyway, this last product is obtained only at high catalyst loading (5 mol%). A screening of catalysts outlined Pd(II) species to be abundantly superior with respect to Pd(0) complexes, such as $Pd(PPh_3)_4$ or Pd/C. The TFA environment is fundamental for maintaining the metal center bound only to labile ligands and favoring the formation of the reactive cationic species. The same reaction undergoes an evident decrease in rate changing either the solvent or the counter-anion: an unsuccessful attempt was done using $PdCl_2$/AgOTf. Only the addition of a small amount of DCM in 1:4 v/v ratio with respect to TFA was found to improve the substrate solubility, without losing activity. Adding an external ligand (1 eq. to Pd) was shown to slightly improve the final yield, but an excess generates the opposite effect. The analysis of the scope of this reaction show very good tolerance toward a broad variety of electron-donating functional groups, while maintaining high selectivity for the Z-isomeric product. Interestingly, the product regioselectivity is uniquely dependent on the nature of the substituents on the alkyne. Indeed, electron-withdrawing groups orients the aryl addition on distal position (anti-Markovnikov product).

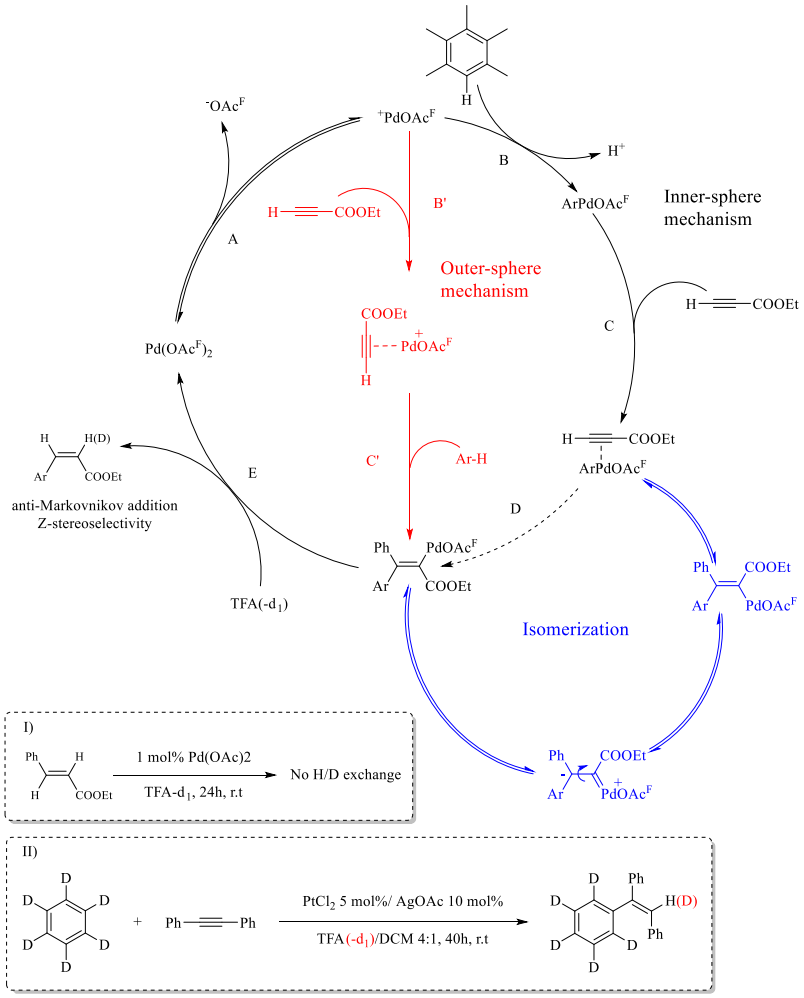

Figure 1.3.3 Proposed mechanism by Fujiwara and co-workers and experimental isotopic experiments

While, electron-donating groups have the opposite behavior, favoring the vicinal addition of the aryl with respect to the substituent (Markovnikov regioselectivity). In ***figure 1.3.3*** is reported the mechanism proposed by the authors basing on the experimental evidence. The first step of the cycle is the electrophilic metalation by the cationic Pd species (**B**) after detachment of one TFA moiety (**A**). The hypothesis is partially corroborated by ^{1}H NMR analysis of equimolar pentamethylbenzene and $Pd(OAc)_2$ in TFA mixture, observing the disappearance of the signal of the substrate aromatic proton. Nevertheless, the most controversial step is represented by the trans-addition of the aryl group to the olefin (**D**). It is known by many mechanistic studies that this process should result in a *cis* addition and consequently lead to the E-product. On this basis, Alper et al. proposed a kinetically driven isomerization of the vinylic complex, passing through a di-polar intermediate.[22] Another hypothesis postulates an outer-sphere activation mechanism (red mechanism of the scheme) in order to afford directly the Z-product, by an intermolecular

nucleophilic attack of the arene to the electrophilic center generated on the alkyne (**C'**). The transformation probably passes through a Wheland-type intermediate. The cycle is closed by protonolysis of the metallavinyl complex and regeneration of $Pd(OAc^F)_2$ (**E**). Isotopic experiments confirmed the protic demetallation performing the reaction in TFA-d_1. In this conditions the trans deuterium addition is almost completely selective. On the other hand, hydroarylation of deuterated benzene in normal TFA (reaction **II**) yields only a negligible amount of deuterated product. Moreover, a control test (reaction **I**) excludes a H/D exchange in the hydroarylation product.[23][24]

2. Gold-catalyzed processes

2.1 Hydrofunctionalization of alkynes

As outlined in the former sections, gold complexes constitute an extremely valuable choice as catalysts for a broad range of applications.[25][26] Regardless its high price, the elevate stability of Au species and their broad range in terms of electron properties contributed taking gold at the center of a large number of studies in the last two decades. Since costs in the chemical industry are a non-negligible aspect to be considered, a solid methodology and prevision of the system behavior is needed before going to proper applications. The unique alkynophilicity of Au(I) complexes could indeed be a powerful tool for the activation of such compounds toward nucleophilic attacks. but the interpretation of the mechanistic-path that leads to products is not often clear or experimentally supported. The carbocation-carbenoid formalism (f***igure 1.1.4***) could give some hint for the interpretation of the following reactions.

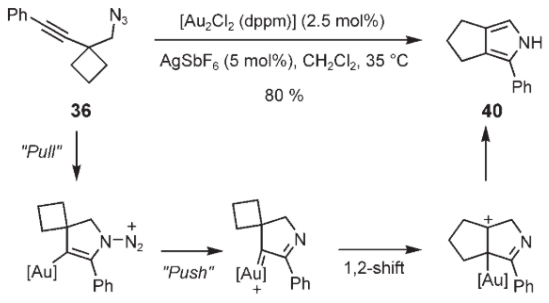

Figure 2.1.1 Pull and Push mechanism in Schmidt reaction for pyrrole synthesis [27]

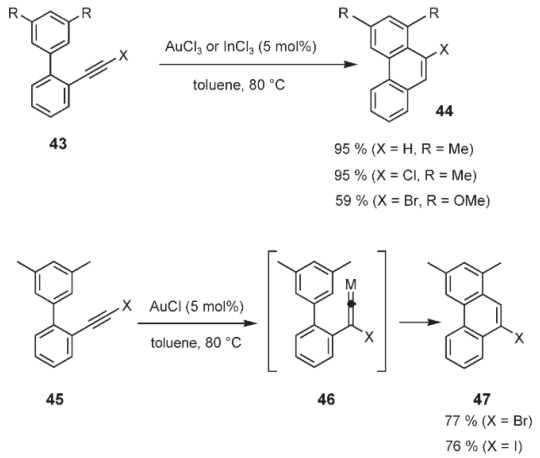

Figure 2.1.2 Change of selectivity by vinylidene intermediate formation in phenanthrenes synthesis [28]

The first example (***figure 2.1.1***) report an acetylenic-adapted Schmidt reaction, catalyzed by a binuclear Au(I) complex. The alkyne electron density is pulled by the metal center, according to the carbophilic activation mechanism, favoring the nitrogen nucleophilic attack and the slippage of gold along the triple-bond axis. On this particular framework, the carbenoid rendition suites perfectly in order to explain the role of the metal back-donation in the electrophilic cleavage. After nitrogen liberation, the carbocation can be regenerated by 1,2-shift and isomerization to achieve the desired product. In the case of ***figure 2.1.2***, it is reported a curious change in selectivity varying the catalyst. In order to explain the halogen shift during the cyclization, the Au(I) alkyne complex may pass through a vinylidene intermediate formation. Also in the case of $AuCl_3$ we have some possibility for the vinylidene intermediate formation, which leads to the 5-exo-isomer formation.[29]

The two former examples are merely illustrative. The important concept that has to pass through is that the reactivity of those systems is extremely various and deeply linked to the specific nature of substrates. The lack of prevision and the difficulties on mechanism interpretations are still now the main concerns that limit their synthetic applications. Moreover, in the literature such processes are often limited to their “simplified" intramolecular version. Keeping the focus on intermolecular alkyne functionalization by protic nucleophiles HNu, the reaction mechanism can be typically reduced to the one reported in ***figure 2.1.3***.

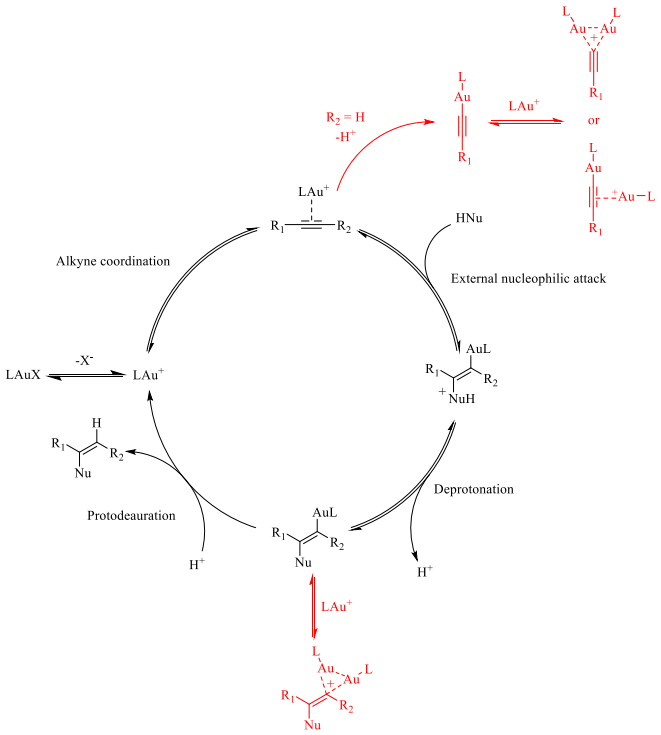

Figure 2.1.3 General mechanism for cationic gold(I)-catalyzed alkynes hydrofunctionalization

The cycle completely resembles the outer-sphere mechanism proposed for the Fujiwara reaction. Moreover, the tendency of gold to form geminal alkynyl and vinyl complexes leads to unreactive species toward the desired reaction. The nature of the nucleophile could be different (heteroatom-based or carbon-based nucleophiles) with obvious implications on the activation parameters in the catalytic cycle. Keeping the focus on alkynes hydroarylation reactions, it is not possible to unambiguously define the r.d.s, of the process. Initial studies conducted by Reetz confirmed the general selectivity trends reported for the Pd-catalyzed process.[30] The hydroarylation of ethyl propiolate with mesitylene in nitromethane was addressed with a broad variety of catalysts. As result of this screening, gold(I) complexes show to be more effective than simple salts such as AuCl or $AuCl_3$, regarding both activity and product selectivity. The process does not request the presence of an acid co-catalyst but an increase of the equivalents of arenes is needed in order to achieve high yields. In general, the most favorable conditions for this reaction see the activation of electron-poor alkynes toward electron-rich arenes. The right choice of the ligand is fundamental in order to modulate the catalytic performance of the process. Strong electron-donating ligands support the protonolysis step[31] and improve the complex stability. On the other hand, increasing the electron density on the gold center enhances the π back-donation to the alkyne, with possible issues on the substrate activation. The activation of electron rich olefins by Au(I) catalysis is as well possible using poorly-donating cationic ligands, as reported by Alcarazo with its cationic pyridinophosphine ligands.[32]

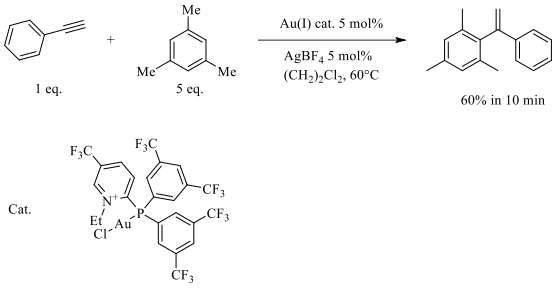

Figure 2.1.4 Hydroarylation of phenyl acetylene with mesithylene catalyzed by Alcarazo catalyst

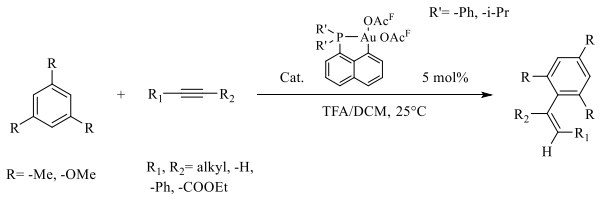

Figure 2.1.5 Gold(III) cyclometalated (P,C) complexes as catalyst for electron rich alkynes activation

The catalyst reported in ***figure 2.1.4*** is also able to perform hydroarylation of phenyl acetylene with mesitylene in DCE under mild conditions. Indeed, even the gold oxidation state plays a role on the activation of such challenging substrates. Simple salt $AuCl_3$, suitably activated by exchange of the chloride with a non-coordinating anion, was already known to be able to perform hydroarylation of alkynes, also in absence of acid conditions.[30][33] Recently, Bourissou and co-workers reported cyclometallated (P,C)Au(III) complexes with excellent results on their application in catalysis. The hydroarylation of the electron-rich phenyl- and diphenyl-acetylene with 1,3,5-tri-methoxybenzene (TMB) and mesitylene leads to almost complete

conversion in short reaction times at 5 mol% of catalyst loading and Fujiwara-type conditions (***figure 2.1.5***). For this system, the presence of TFA is necessary in order to unlock activity.

2.2 Role of the counter anion and the "silver effect"

As it was anticipated in the previous sections, the cleavage of one coordinative bond at the gold(I) center is fundamental for generating the monocoordinated, cationic active species. This concept is common for all electrophilic gold catalysts and it is already reported in the literature.[35][36] However, in the process optimization the role of the counter ion is often considered marginal with respect to other parameters (nature of the ligand, temperature, solvent, etc). In ***figure 2.2.1*** is reported a pie chart collecting the data on experimental studies on gold catalysis published in 2017. It is evident that the study of the counter anion effect are limited only to 14% of the studies that have been undertaken. Under this framework, the screening study conducted by Hashmi and co-workers aims to furnish a solid procedure for the counter-ion selection.[34] As overall result, the authors outlined that the pattern of reactivity on a benchmark reaction by changing counter anion is similar for different complexes. Thus, the counter-ion screening should precede the selection of the ligand for a target reaction. The species that allows to reach the highest reactivity are typically noncoordinating and rigid anions such as NTf_2^- or SbF_6^-.

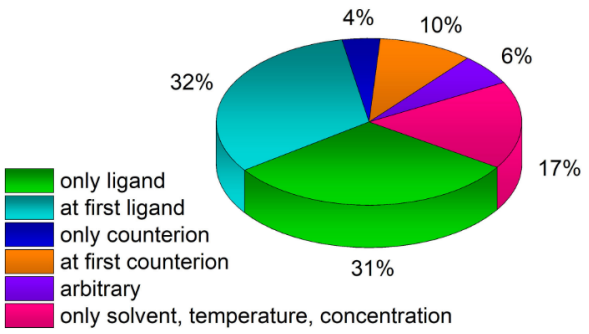

Figure 2.2.1 Catalytic process optimization basing on the procedures in 2017 (116 publications at 16.11.2017, Scifinder, keyword: gold catalyzed) [34]

Classically, the more convenient method to afford the anion exchange is the substitution of a halido ligand (often a chloride) by reaction with a silver salt. This method is easy and effective, even though it leads to some disadvantages. First of all, the catalyst could undergo only partial activation, regardless the anion exchange is assisted by precipitation of AgCl. As second and more important drawback, silver species cannot be considered as innocent. The presence of silver in solution could involve the gold complex in formation of bimetallic species with detrimental or even advantageous effects in catalysis. The formation of silver-vinyl gold complexes has been reported by Zdhanko and Maier, and the silver effect has been tested in hydroalkoxylation reactions.[37] Before them, in 2009, mechanistic studies on these species were carried out in the context of the intramolecular hydroarylation of allenes.[38] To make an example, it is evident the case of diphenylacetylene hydration catalyzed by $IPrAuCl/AgSbF_6$ (***figure 2.2.2***).[37] In absence of the silver salt precipitate, the cationic gold complex cannot yield the desired ketone. A control test excludes either the possibility of $AgSbF_6$ to perform the addition of water at the triple bond.

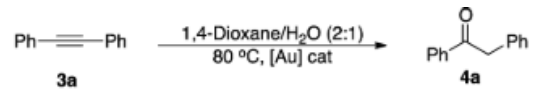

	catalyst	time	yield
A	[(IPr)Au]Cl/AgSbF$_6$ 2%, **no filtration**	2 h	97%
B	5% [(IPr)Au]$^+$SbF$_6^-$	24 h	0%
C	5% AgSbF$_6$	24 h	0%
D	2% [(IPr)Au]$^+$SbF$_6^-$ + 2% AgSbF$_6$	12 h	95%
E	2% [(IPr)Au]$^+$SbF$_6^-$ + 1% AgSbF$_6$	24 h	88%
F	2% [(IPr)Au]$^+$SbF$_6^-$ + 0.5% AgSbF$_6$	24 h	67%

Figure 2.2.2 Bimetallic Au/Ag catalysis for the diphenylacetylene hydration [39]

This reaction is a clear case of Au/Ag bimetallic catalysis, that, together with the purely gold catalyzed processes, represents the extremes of a broad number of cases. Most commonly it is observed a simple silver-assisted catalysis, where either the gold complex, the silver salt or their mixture can perform the same reaction (examples are reported in figure 2.2.3).

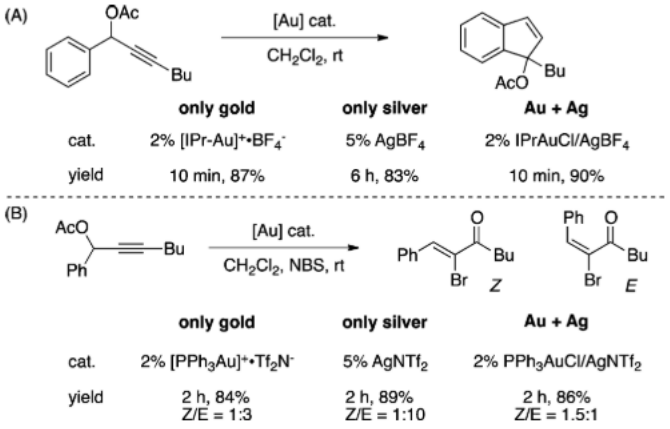

Figure 2.2.3 Ag-assisted gold catalysis of an electron-rich alkyne A) intramolecular hydroarylation B) hydration

In order to evaluate the performance of the gold complex upon a selected reaction, it is indeed needed to ensure that the silver salt does not participate. The easier method is by filtration of the solid precipitate after activation or even by substituting silver with another Lewis acid as chloride extractor such as $BF_3{\cdot}Et_2O$.[37] Other silver-free methods involve the use of protic polar solvents (water or alcohols) or Deep Eutectic

solvents (mixtures of an halide salt and an hydrogen bond-donor) as reaction media. Under these conditions, the chloride anion can liberate the active site to perform carbophilic activation at the gold center.

3. Ionic Liquids as reaction media for cationic gold-catalysis

3.1 Definition and interest in ionic liquids

Since before of the beginning of the century ionic liquids, or molten salts, were described as fluids that are completely comprised of ions.[40] By this definition, any ionic compound above its melting point could have been included in this category. Nowadays the term "ionic liquids" is referred only to salts with melting temperature under 100°C. They can be liquid even at room temperature, colorless and poorly viscous. The chemical nature of these species is quite broad and the cation or anion moiety can be changed independently. In ***figure 3.1.1*** are reported examples of ionic liquids and a table reporting the melting points of some imidazolium-based salt.

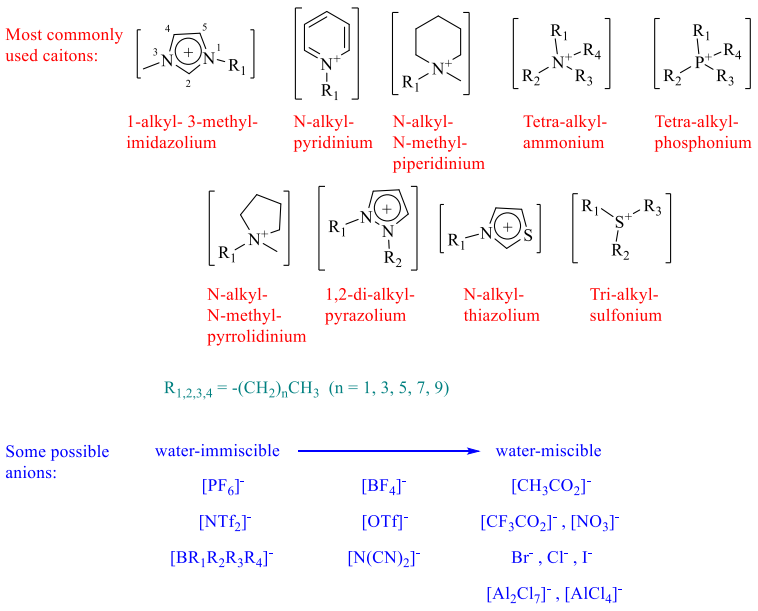

R	X	mp/°C
Me	Cl	125
Et	Cl	87
n-Bu	Cl	65
Et	NO_3	38
Et	$AlCl_4$	7
Et	BF_4	6
Et	CF_3SO_3	-9
Et	$(CF_3SO_3)_2N$	-3
Et	CF_3CO_2	-14
n-Bu	CF_3SO_3	16

Figure 3.1.1 Chemical nature of cations and anions in ionic liquids and melting points of some imidazolium-based salt [41]

The principle behind their physical state has to be allocated to the scarce intermolecular interactions between the oppositely charged ions. The cation is typically an asymmetric and hindered organic molecule, with low ability as H-bond donor. The anion could be either an halide or, as it is often the case for room temperature

ionic liquids, a noncoordinating fluorinated anion.[41] In the last two decades the interest in these fluids is increased as sustainable reaction media, in substitution to classic organic solvents. The wide range of chemical, physical and electrochemical-stability, together with the lower polarity with respect to water, makes these species extremely appealing for the immobilization of homogeneous catalysts.[42] Moreover, their polarity and other physical properties, such as the relative solubility of organic substrates or gases, can be finely modulated by selection of the cation and anion moieties. The application of ILs media for homogeneous or, more often, biphasic catalysis is already reported in the literature for a broad variety of reactions and methodologies for catalyst recovery and recycling.[41][43][44] From a mechanistic point of view, it is hard to observe if the catalytic process occurs in the IL phase, in the organic one or even in both of them. However, since the organic solvents are not capable to extract the complex, it is more probable that the product forms in the ionic medium through a similar mechanism observed in classic solvents. All these concepts can generally be applied also to gold catalysis. The cationic active species formation is indeed favored by charge stabilization and weak intermolecular interaction. As appointed by Chauvin's work on alkene hydroformylation, hydrogenation and isomerization catalyzed by phosphine rhodium complexes, the cationic active species are not solvated by ionic liquids.[45] The catalytically active species reported in ***figure 3.1.2*** is supposed to be in equilibrium with the monohydride neutral complex after deprotonation.

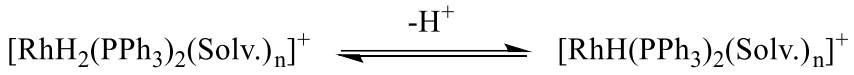

Figure 3.1.2 Protonation equilibrium of the catalytic active species for catalytic hydrogenations

Dissolving the complex in BMIM SbF_6 only one signal has been observed by ^{31}P NMR, indicating the presence of only one symmetric species: probably the di-hydride complex with two free coordinating sites. This feature could explain why, in some cases, the IL environment leads to improvements in terms of catalytic activity and even selectivity. This effect has been recorded also by Biffis and co-workers in the case of the hydroarylation of ethyl propiolate with mesitylene catalyzed by IPrAuCl/$AgNTf_2$ (***figure 3.1.3***).[46]

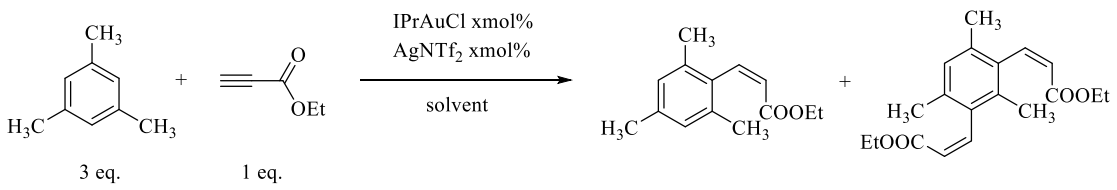

Conditions	Alkyne conversion	Mono-/Di-hydroarylation products molar ratio
BMIM NTf_2, 0.5 mol% cat. , 3h	> 90 %	5 : 1
$(CH_2)_2Cl_2$, 60°C , 5 mol% cat. , 4h	> 90 %	2 : 1

Figure 3.1.3 Effect of the IL media on propiolic acid hydroarylation with mesitylene

The same reaction is reported to be much more efficient in BMIM NTf_2, achieving more than 90% of alkyne conversion and improved selectivity toward the single adduct formation. In order to have a comparable result in solvent DCE, the catalyst loading has to be increased from 0.5 to 5 mol% and the reaction performed for longer times at higher temperature. As shown in the reaction mechanism reported in ***figure 1.2.3***, the different cationic species involved in the catalytic cycle can benefit from the stabilization by the IL medium. Moreover, the ionic environment is thought to favor the proton transfer, lowering the energy barrier to overcome the protonolysis and afford the hydroarylation product. Both these effects contribute to an overall improvement in the catalytic performance.

4. Coumarins as synthetic target

4.1 State of the art in coumarins synthesis and transition metal-based approaches

Coumarins are a specific class of heterocycles, recognized by the typical structure reported in ***figure 4.1.1***. The interest in these specific compounds falls on their potential biological activity, thus their implementations as possible Active Pharmaceutical Ingredients (API) in pharmaceutical industry. The planar, rigid structure can lead also to luminescent features, a characteristic that make them appealing for formulation in paints or even for optoelectronic devices and chemical sensors[47].

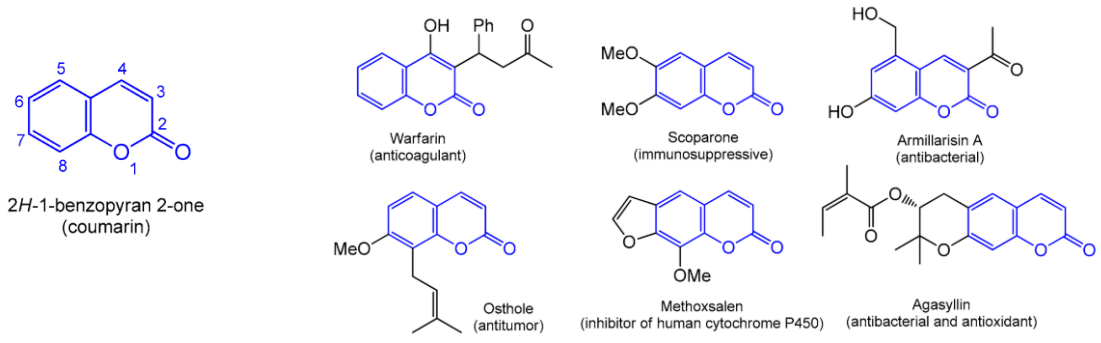

Figure 4.1.1 Coumarin backbone and some example of biologically active coumarins and chromophores[48]

Regardless that most of these species can be found in nature, a synthetic approach is more indicated in order to obtain precise molecular targets. The nature and position of the substituents over the heterocycle leads to a fine modulation of the physico-chemical properties. It is well known that natural coumarins tether an oxidized group in position C-7. Together with functionalization in position 4 and 6, a pronounced inhibitory activity toward acetylcholinesterase and anti-inflammatory properties have been recorded. Analogously, substituents in positions C-3 and C-4 may enhance anticancer activity.[48] However, the direct functionalization of the aromatic moiety can be quite challenging, since the aromatic ring is less active than a benzene one. On the other hand, the unsaturated 3,4 bond is reactive and organometallic based methods have been developed for the selective functionalization of this site. Methods involving cross-coupling are well suited for the scope, but an halogen moiety is needed in order to activate the position. Another route involves the direct C-H activation by electrophilic metalation. Nevertheless, if the selective functionalization of position C-3 is performed by electrophilic palladium complexes, reaction at position 4 is less facile and dependent on the nature of the fragment we want to couple. The direct synthesis of coumarins could solve the problem at the origin. Starting from Perkin in 1868, organic methods have been developed and implemented to the synthesis of coumarins (***figure 4.1.2***). However, consistent presence of by-products is inevitable using these traditional approaches, principally focused on acid/base catalysis or strong base activation of reactive species, such as enolates or Wittig-type reagents. A catalytic methodology based on TMs chemistry should improve the overall atom-economy of the process. The available approaches are many and all of them involve as substrates a phenol derivative and a functionalized olefin. The same reaction can be proposed with intermolecular or intramolecular mechanisms (***figure 4.1.3***).

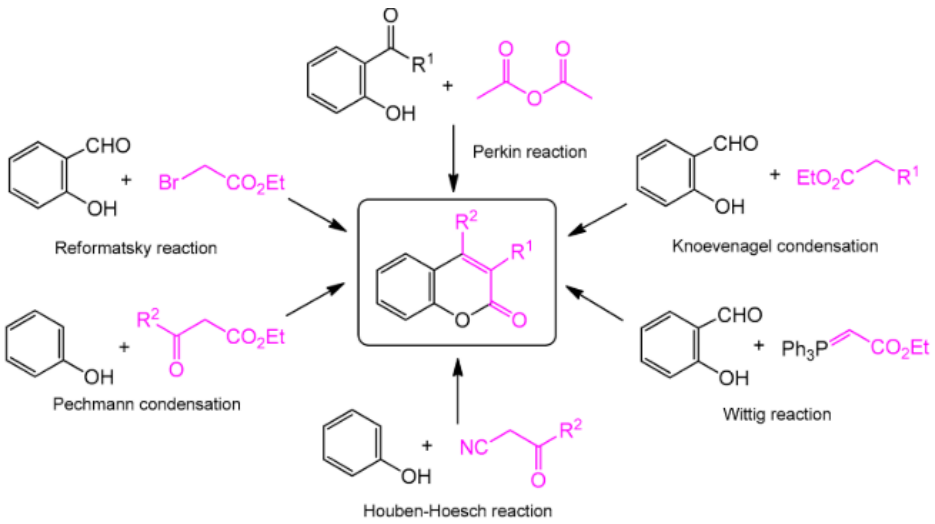

Figure 4.1.2 Synthetic methods based on traditional organic chemistry[48]

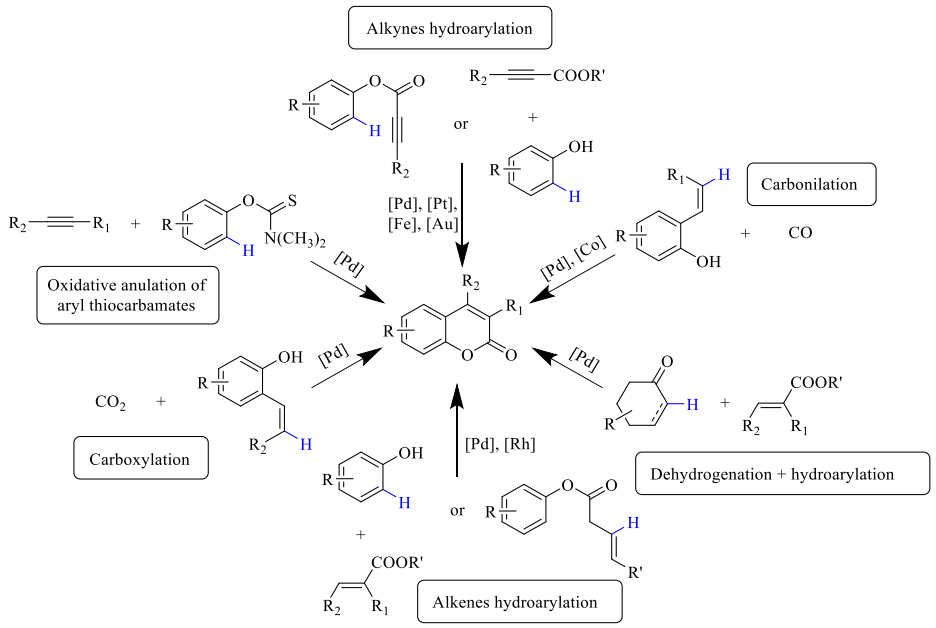

Figure 4.1.3 Overview on organometallic-based approaches for coumarin synthesis[48]

Since the discovery of the alkyne hydroarylation processes by Fujiwara, coumarins were targeted as synthetic challenge, in order to put into evidence the technological relevance of palladium and platinum complexes on C-H bond functionalization.[49][50] Nowadays the focus is more directed on gold-catalyzed approaches, due to the excellent carbophilicity of this metal and stability of its species towards moisture and air. In the literature, an intramolecular approach is mainly reported. The group of Banwell put into evidence the excellent performance of Echavarren's catalyst for the cyclization of aryl alkynoates and others heterocycles formation (***figure 4.1.4***).[51][52] Moreover, a standard method was provided for the synthesis of these substrates, bearing a terminal alkyne moiety. On the other hand, intermolecular approaches are quite rare and principally based on Pd(II) and Pt(II) catalysts, but also on Fe(III) in DCM/TFA mixtures.

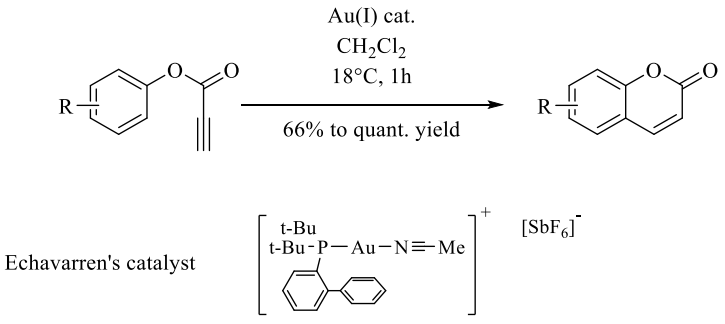

Figure 4.1.4 Intramolecular hydroarylation of aryl propiolates proposed by Banwell and co-workers[52]

4.2 Aim of the project

Now that the theoretical bases have been settled down, it is important to define the questions this thesis want to address. As outlined in the former section, coumarins are a very attractive target for pharmaceutical industry and TMs chemistry furnish a series of different strategies in order to yield these species in good to excellent yields. The use of organic solvents is extensive and varies consistently with the chosen synthetic approach. Hydroarylation of alkynes are rather frequently performed under Fujiwara-type condition (DCM/TFA mixture), in order to ensure the cationic active species formation and good homogeneity of the system. The activation of electron rich arenes is particularly successful in these conditions, while higher temperatures and more electrophilic catalysts are required for non-activated arenes and electron-rich alkynes. The present work aims to formalize a sustainable approach concerning the synthesis of coumarins by hydroarylation of propiolic acid derivatives. The use of ionic liquids has been already reported to provide improved activity and selectivity in Au(I)-catalyzed intermolecular hydroarylation of alkynes with arenes and heteroarenes.[53] The same system has been adapted for our process, making possible a two steps/one-pot synthesis of coumarinic targets. Being all the components commercially available, the thesis will mainly focus on understanding how the reaction parameters affect the system behavior in term of activity and selectivity. The presence of an acid source may be fundamental in order to accelerate the reaction rate to an appreciable extent, assisting both the protodeauration step (***figure 2.1.3***) and even the lactonization step that leads to the coumarin (***figure 4.2.1***). The system will be tested on different and challenging substrates (e.g. electron-rich alkynes) for expanding the reaction scope to a significative extent. Under this framework, (P,C)-cyclometalated Au(III) complexes will be also evaluated as potential catalyst for the activation of unreactive substrates toward Au(I) catalysts. Since Bourissou's (P,C)-catalysts have been tested only under Fujiwara conditions on selected electron-rich arenes (TMB, mesitylene),[54] a step-by-step process will be followed in order to evaluate the response to the change of substrates and media.

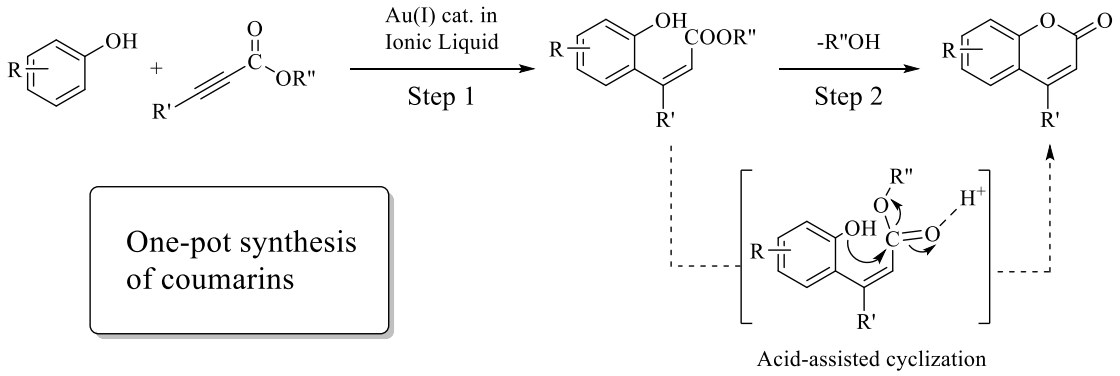

Figure 4.2.1 Direct synthesis of coumarins by alkynes intermolecular hydroarylation in ILs

Chapter 2

Gold(I) catalyzed processes

1. The starting point

1.1 Selection of the ionic liquid

The research group of Applied Organometallic Chemistry has shown keen interest on these systems in the past few years, studying how IL environments could benefit the catalytic performance in gold catalyzed hydroarylations. Before starting to report the results of the last research activity, it is indeed opportune to introduce the former experimental evidence. The systematic study on the main parameters that affect the catalytic performance was carried out by Sara Bonfante (A.A. 19/20), who clarified the dependence of the system reactivity on the nature of the IL.[55]

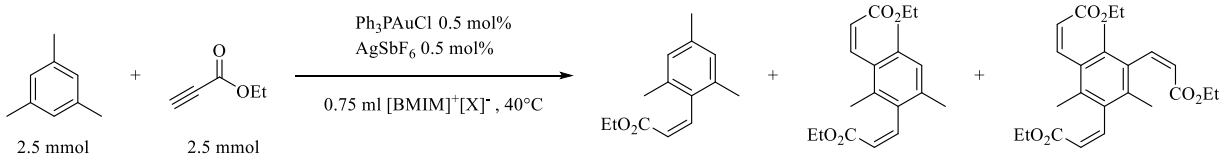

[X]$^-$	**Alkyne conversion [%]**
$[NTf_2]^-$	96
$[OTf]^-$	0
$[BF_4]^-$	<1
$[PF_6]^-$	1

Figure 1.1.1 Hydroarylation of ethyl propiolate by mesitylene after 3h of reaction

The effect of the counterion in cationic gold catalysis has been extensively reported in the literature.[34] In particular, a rigorous evaluation of the electron density distribution, H-bonding basicity and coordination ability of the anion is fundamental for the catalyst selection and optimization of a determined process. This effect is obviously confirmed also in IL media, where the anion component nature determines drastic changes in the system reactivity, as outlined in ***figure 1.1.1***. Confirming former studies,[53] NTf_2^- is by far

the best candidate for promoting the analyzed reaction. Thus, less coordinating counteranions do not succeed in the stabilization of intermediate species involved in the catalytic transformation. On the other hand, strong coordinating anions would bring the catalyst to the formation of a tight ionic couple, shutting completely down the system reactivity. Since the r.d.s. of the reaction is often not clearly defined and strongly dependent on the nature of the substrates and the gold complex electronic properties, the Brønsted basicity of the IL anion should affect only marginally the reaction rate. More incisively, being our system a biphasic heterogeneous mixture, a slight change in the substrates solubility into the reaction media could bring to a not-negligible change in reactivity. In order to quantify this aspect, the Hildebrand solubility parameter has been taken as reference (***figure 1.1.2***).

Ionic liquid	**δ [MPa$^{1/2}$]**
BMIM BF_4	31.6
BMIM PF_6	29.8
BMIM NTf_2	26.7
BMIM OTf	25.4

Figure 1.1.2 Hildebrand solubility parameter of the IL in function of the anion reported by Lee and Marciniak [56][57]

In order to be miscible, two different substances should interact by similar intermolecular modes. This aspect can be translated as a similarity of their solubility parameters. Coming back to the reaction of ***figure 1.1.1***, it is now more clear why the system shows higher activity in BMIM NTf_2 than, for example, in BMIM BF_4. The two counter anions have similar features concerning the Lewis and Bronsted basicity, but BMIM BF_4 has a higher δ value which is likely less compatible with the ones of the substrates. About the contribution of the cation, it is much less strong, since it does not affect Lewis and Bronsted basicity but only the Hildebrand solubility parameter, and to a relatively limited extent: thus, the system is much less sensitive to the choice of the cation and its optimization is strictly substrate-dependent.

1.2 Screening of the operating conditions

The selection of the catalyst, and the preliminary screening of the reaction conditions and scope was carried out by Pietro Bax (A.A. 20/21).[58] At the very beginning, Au(I) complexes with ligands with different basicity were tested on a benchmark reaction such as the formation of coumarin upon hydroarylation of 3-phenylpropiolic acid with sesamol (***figure 1.2.1***). Since the first tests, the 3-phenylpropiolic acid showed

higher activity than the ethyl 3-phenylpropiolate. This behavior is probably linked to the acidic proton of the carboxylic acid, which accelerates the protodeauration step and, in general, the reaction rate. Moreover, the acidic conditions assist the subsequent cyclization step (***figure 4.2.1***, in Chapter 1), in order to obtain the desired product. Nevertheless, if the influence of the functional group seems quite clear, the analysis of the behavior of the different complexes gave unexpected results.

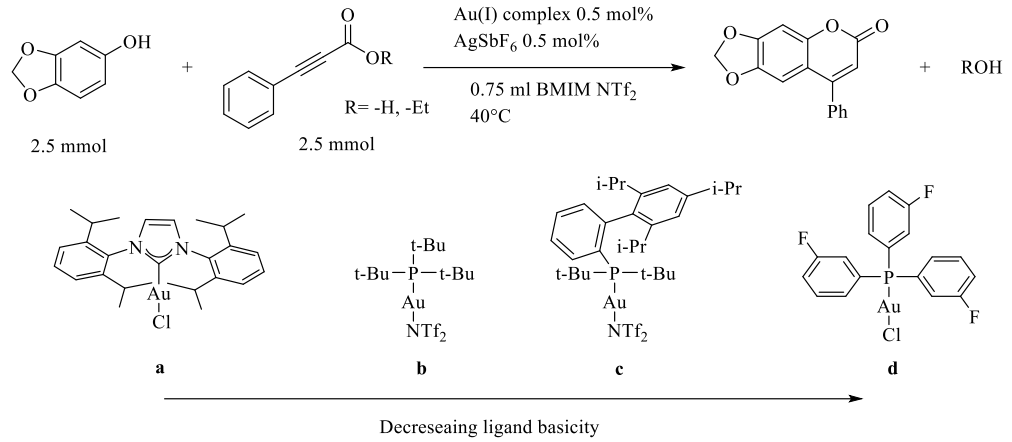

Catalysts [a]	Sesamol conversion [b, c] [%]	Alkyne conversion [b, c] [%]	Coumarin yield [b, c] [%]
IPrAuCl (a)	69 (54)	78 (61)	60 (32)
$(t\text{-}Bu)_3PAuNTf_2$ (b)	65 (48)	66 (75)	53 (29)
$tBuXPhosAuNTf_2$ (c)	55 (48)	63 (59)	43 (29)
$(FC_6H_5)_3PAuCl$ (d)	2 (2 [d])	48 (2 [d])	2 (2 [d])

Figure 1.2.1 Catalysts screening for the synthesis of coumarins by intermolecular hydroarylation; [a] The catalysts with NTf_2^- counter anion do not need to be activated in situ by $AgSbF_6$; [b] conversions and yields are calculated by ^1H NMR at 24 hours of reaction time; [c] the reported data in parentheses are referred to ethyl phenylpropiolate as substrate, otherwise they are referred to phenyl propiolic acid; [d] data referred to 72 hours reaction time

In contrast to former studies on the hydroarylation of simple alkynes, the more electrophilic complex **d** gave the poorest results in terms of catalytic activity, determining only 2% of sesamol conversion after 72 hours reaction time. Instead, the more electron-rich complexes **a**, **b** and **c** showed good activity, reaching

the best results with the IPrAuCl, which afforded the desired product in 60% yield after 24 hours. From these results is quite clear that the carbophilic activation of the alkyne is not the r.d.s. of the process. On the other hand, the Au-C bond cleavage seems to be more energy-demanding. This hypothesis further corroborates the role of the acidic proton in determining the different reactivities observed for the phenylpropiolic acid and the ethyl phenyl propiolate.

After the best catalyst has been selected, the effect of the temperature on the catalytic performance was extensively studied. In general, the best working conditions for these type of processes revealed to be in the range between 40-60°C. In fact, for lower temperature values the process starts to become too slow with these substrates, and above 60°C the stability limit of the gold complex is reached, corresponding to low product yield due to the catalyst decomposition. As last feature, varying the molar ratio of the two substrates was considered a valuable option to supply the loss of alkyne during the process; In fact, due to the side-reactions of decarboxylation and/or hydration of the propiolic substrate, unactive species toward the hydroarylation reaction are formed. Unfortunately, the first attempts to increase the molar ratio of the alkyne to the arene afforded a worse process selectivity (***figure 1.2.2***). Consistently with the increase of the alkyne loading, phenylacetylene and acetophenone are produced in 41% yield already after 3 hours of reaction. Moreover, despite the increase in the final coumarin yield, the hydroarylation rate does not increase as observed for the by-products formation processes. A possible explanation to this behavior deals with the relative solubility of the substrates into the reaction medium. Consistently with this hypothesis, an increase of one substrate quantity can result in the drop in solubility of the other one, explaining why the reaction ratio slows down. However, further evidence is needed in order to understand this phenomenon.

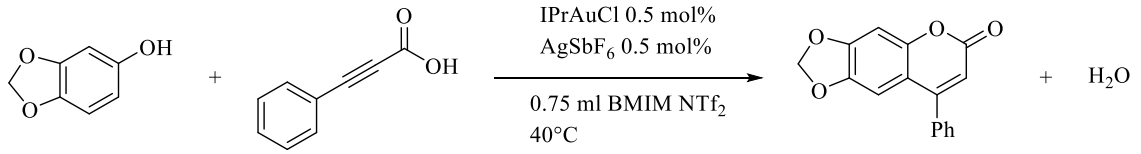

2.5 mmol x mmol

Molar ratio sesamol : alkyne	Time [h]	Sesamol conversion [a] [%]	Alkyne conversion [a] [%]	Coumarin yield [a] [%]	Decarboxylation and hydration products yields [a, b] [%]
1 : 1 x = 2.5 mmol	3	37	54	22	32
	24	51	64	42	22

1 : 2 **x = 5 mmol**	3	25	52	22	41
	24	67	75	63	43

Figure 1.2.2 Effect of the molar ratio on phenylpropiolic acid hydroarylation; [a] conversions and yields are calculated by ^{1}H NMR analysis and referred at 24 hours of reaction time; [b] yields quantified on the signals of phenylacetylene (singlet at 3.08 ppm, 1H) and acetophenone (singlet at 2.59, 3H)

2. Intermolecular hydroarylation of 3-phenylpropiolic acid for the synthesis of 4-substituted coumarins

2.1 Protocol optimization

Once the preliminary studies were completed and a starting protocol was developed, we started with the optimization of a designed process. For convenience, we kept sesamol as aryl substrate: since we got already a large amount of data on this substrate, it allows an easier screening and interpretation of the effect of changing the reaction parameters. Initially, we introduced $HBF_4{\cdot}Et_2O$ as an acid co-catalyst, with the aim to increase the process activity and selectivity. Indeed, the acidic proton should increase the rate of the protodeauration step and assist the cyclization of the hydroarylation product, in order to afford the final coumarin in higher yields. Moreover, keeping protonated the carboxylic functional group, it should be possible to depress alkyne decarboxylation. On this last point, also the use of the ester is obviously a valuable choice in order to definitely avoid this side-path.

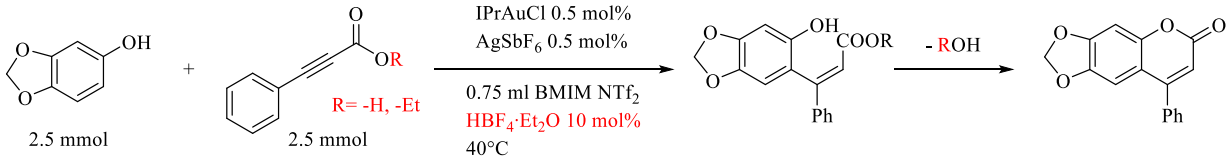

Conditions	**Time [h]**	**Sesamol conversion [%]**	**Alkyne conversion [%]**	**Coumarin yield [%]**	**Z-alkene yield [%]**
R= -H	1	9	27	8	1
	3	20	47	14	5
	24	26	56	16	10
R= -H,	1	59	83	56	-

$HBF_4 \cdot Et_2O$ 10 mol%	3	61	92	59	-
	24	61	94	61	-
R= -Et $HBF_4 \cdot Et_2O$ 10 mol%	1	47	51	14	33
	3	54	56	19	35
	24	65	86	52	14

Figure 2.1.1 Screening of the acid co-catalyst effect on the system and varying the substrate; yields and conversions are calculated by ^1H NMR analysis;

The results of the conducted test are reported in the ***figure 2.1.1***. As expected, the presence of the strong Brønsted acid strongly affect the reaction rate, affording 59% of product in only three hours. Even the cyclization step turns to be so fast that the direct hydroarylation product is not observed anymore in the NMR spectra while using phenylpropiolic acid as substrate. Unluckily, we did not obtain an analogous effect concerning the process selectivity. In particular, even if we succeeded in limiting phenyl acetylene formation through decarboxylation, the alkyne hydration rate dramatically increased. As it is reported in ***figure 2.1.2***, we clearly see that the characteristic singlet at 3.1 ppm of the phenyl acetylene alkynyl proton is not present in the test containing the acid co-catalyst.

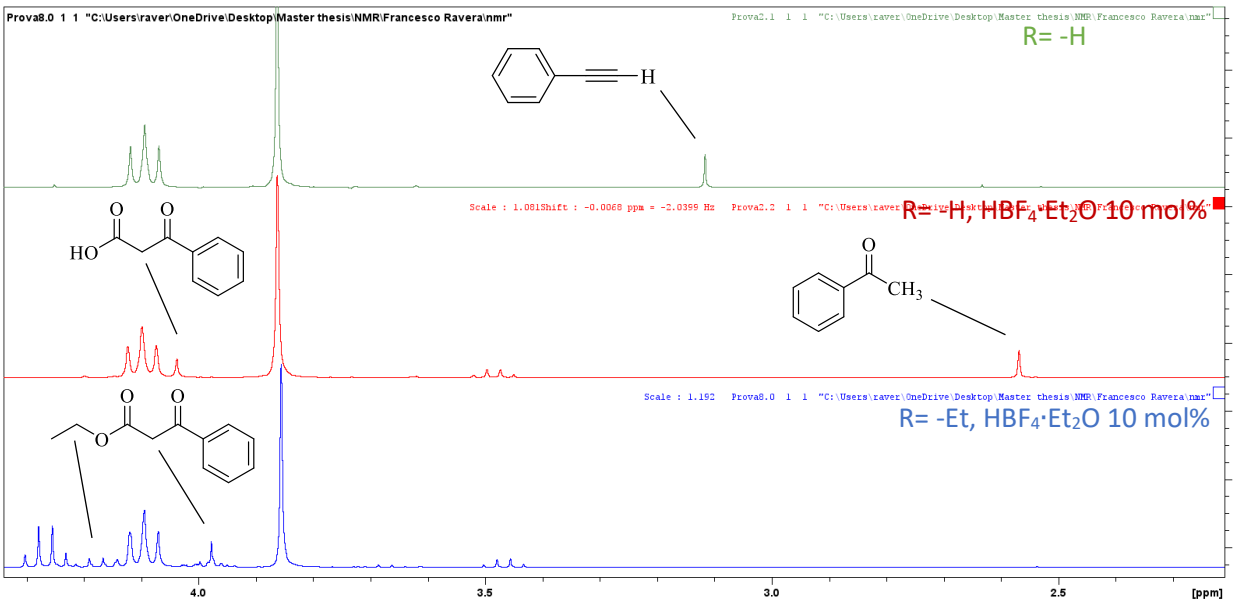

Figure 2.1.2 ^1H NMR (300 MHz, $CDCl_3$) of the crudes after 1h of reaction; the highlighted region contains all the characteristic signals of the by-products coming from the alkynes hydration and/or decarboxylation

At the same time, a signal matching with the $–CH_3$ protons of the acetophenone is evident. A reliable explanation is that it is formed by decarboxylation of 3-oxo-3-phenylpropanoic acid. This last species is indeed present in the reaction mixture containing HBF_4. It is recognizable by the singlet at 4 ppm (red-lined spectrum), which disappears upon time: after 24h the signal is not present anymore. In the case of the ester, the hydration product forms in minor quantities with respect to the process involving the carboxylic acid and the hydroarylation reaction proceeds at a comparable rate; on the other hand, the subsequent cyclization step is more difficult in that case. However, we need further experimental evidence in order to clarify the exact mechanism for acetophenone formation,

In order to exclude the possibility that the acid can catalyze alone the reaction, a blank test was performed. At 3h of reaction a ^1H NMR spectrum was recorded and 0.5 mol% of $AgSbF_6$ were added for determining a potential contribute. Another ^1H NMR spectrum was taken after further 3h reaction time. None of the two spectra reported product traces or, interestingly, even by-products signals. This reveals that is the gold complex that assist the decarboxylation, probably via an intermediate with the carboxylate group coordinated to the Au(I) center.[59] Now, it is clear the catalyst is also responsible for the alkyne degradation that we observe in the course of the reaction. Consequently, we thought to lower the catalyst loading for limiting the direct hydration of the phenylpropiolic acid; moreover, 4Å molecular sieves were used to dry the employed IL and were also added in the reaction mixture to sequester the water coming from the cyclization step. In order to increase the homogeneity of the system and avoid issues concerning the mixture stirring, the system was diluted by doubling the IL volume. The results of the test are reported in ***figure 2.1.3*** and it is clear that introducing the molecular sieves at lower catalyst loading the hydration reaction rate slows down. At the same time, we achieved to obtain analogous results concerning the final product yield. Comparing these data to the ones reported in ***figure 2.1.1*** for phenylpropiolic acid susbtrate, the new system shows to be as active as the test performed with 0,5 mol% of gold complex and the acid co-catalyst. Indeed, both the experimented conditions allow to reach almost 60% of sesamol conversion after only 3 hours of reaction. At the same time, the alkyne conversion is markedly decreased (76% instead of 92% for the former test) as effect of the limited by-products formation. This test was repeated during my stay in Toulouse, using an internal standard for the quantitative calculations: 1 mmol of 1,2.dichloroethane or 1,2-di-methoxyethane. The results is curious because we obtain system with a different behavior in terms of reactivity and stability. In such type of system we afforded a higher coumarin yield at 24 hours of reaction (72%), revealing the catalyst to have a long life-time. At the same time, the catalytic activity decreases, since we recorded only 27% sesamol conversion after 3 hours. This effect could be due to the increased phase separation between the ionic liquid phase (mainly containing the catalyst) and the organic phase (mainly made out of the substrates and standard), or even to an interaction of the internal standard

coordinating with $IPrAu^+$. As further result, we do not see changes in reactivity or selectivity toward the hydration products.

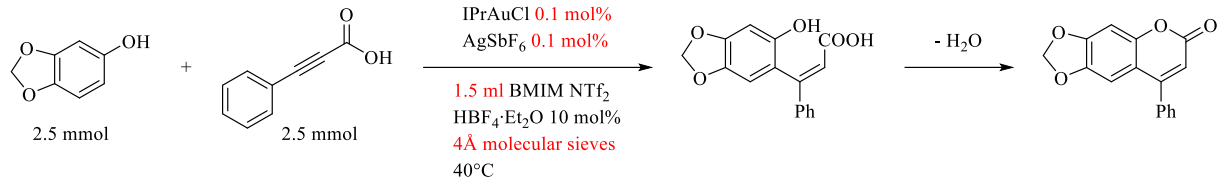

Time [h]	Sesamol conversion [%]	Alkyne conversion [%]	Coumarin yield [%]	Z-alkene yield [%]
1	30	31	30	-
3	57	76	57	-
24	63	85	63	-

Figure 2.1.3 Yields and conversion grades basing on ^1H NMR analysis

2.2 Expanding the reaction scope to other arenes and electron rich alkynes

Next step was to evaluate the possibility to activate different type of substrates. Firstly, we attempted to activate more electron rich triple bonds, such as the 2-hexynoic acid. This species is indeed more challenging to get involved in the hydroarylation process, due to the electron donating aliphatic chain. The substrate showed reactive toward the hydroarylation reaction (see ***figure 2.2.1***). Using 0.1 mol% of catalyst sesamol conversion is limited to 12% in the first hours of reaction. At longer reaction times the process loses selectivity, affording only 12% coumarin yield after 24 hours. An increase of IPrAuCl loading to 0.5 mol% allows the system to reach 44% coumarin yield after 3 hours, while at 24 hours no further improvement is recorded. This behavior is probably due to the side-reactions of decarboxylation/hydration involving the 2-hexynoic acid. In fact, the higher the catalyst loading, the faster the characteristic signal at 2.06 ppm, that corresponds to the 2-pentanone alpha protons, is detected by ^1H NMR. Further experiments with excess 2-hexynoic acid as substrate are planned. Interestingly, the collected spectra of the test at 0.1 mol% IPrAuCl loading present other signals which are responsible for the low yield of the reaction. This species presents signals similar to the ones of sesamol but located at higher frequencies. Further tests are needed in order to establish both the exact chemical identity and the mechanism of formation of this by-product.

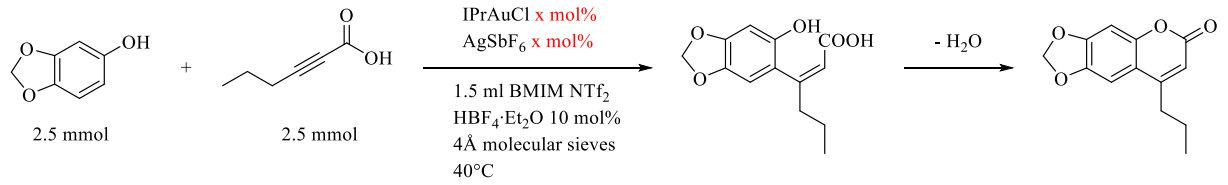

IPrAuCl x mol%	Sesamol conversion [%]	Coumarin yield [%]
0.1 mol%	12 (52)	7 (12)
0.5 mol%	50 (48)	44 (43)

Figure 2.2.1 Yield and conversion calculated by ^{1}H NMR analysis of reaction crudes at 3 hours of reaction (in parenthesis are reported the calculated data at 24 hours)

Changing the focus to other type of phenols, the system starts to show its true limitations. The causes are often related to the limited solubility of the phenols in BMIM NTf_2. In order to better clarify this aspect, we chose three electron rich phenols with different polarities. The pattern of reactivity seems to be quite clear, since the more polar phenols got the better conversion with respect to the 4-tert-butylphenol, which did not afford any product. For the same reason, the 3,4,5-tri-methoxyphenol showed higher yields than the analogous 3,4,5-tri-methylphenol. In this last case, we achieved better results by reverting to the protocol developed in the case of sesamol (***figure 2.1.1***). In these conditions, the reaction affords 56% hydroarylation product yield after 24h of reaction, even though the selectivity of the process toward the alkyne conversion decreases (33% of the substrate undergoes hydration and decarboxylation to afford acetophenone). Moreover, it was already clear by previously reported results that the cyclization step for more hindered phenols than sesamol starts to be challenging. This is even more pronounced for those substrates with substituents next to the C-H bond interested in the hydroarylation. Coming back to the 3,4,5-tri-methylphenol, the hydroarylation product obtained in 53% yield has to undergo the final lactonization to afford the coumarin. The solution to this problem is apparently trivial, since it is sufficient to increase the temperature after hydroarylation to promote substrate lactonization. However, increasing the temperature compromises catalyst stability; under these circumstances recycling of the catalytic system becomes more difficult.

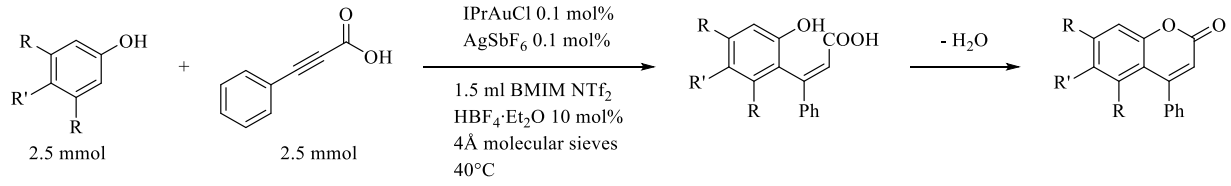

Conditions	Phenol conversion [%]	Coumarin yield [%]	Z-alkene yield [%]	Acetophenone yield [%]
R, R' = -Me	15 (57) [a]	5 (53) [a]	10 (3) [a]	15 (33) [a]
R, R' = -OMe	51	46	5	9
R = -H , R' = t-Bu	-	-	-	9

Figure 2.2.2 Conversions and yields analysis by ^1H NMR varying the phenol substituents; [a] reaction conditions: IPrAuCl/$AgSbF_6$ 0.5 mol% , HBF_4·Et_2O 10 mol% , 0.75 ml BMIM NTf_2 at 40°C

3. Adapting the process to terminal alkynes

3.1 Coumarins and late-stage functionalization at position 4

Until now, we considered synthetic methodologies involving internal alkynes in the intermolecular hydroarylation process. This methodology is particularly convenient, in order to afford coumarins with simple substituents at the position C-4 of the final product. Ideally, the alkyne moiety can even be prefunctionalized through a simple Sonogashira coupling (figure 3.1.1), so to extend the complexity of the structures we can obtain.

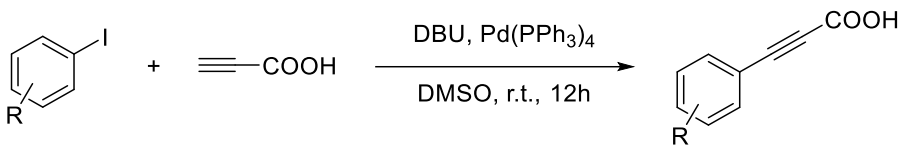

*Figure 3.1.1 Copper-free Sonogashira coupling for the synthesis of 3-arylpropiolic acid derivatives, according to Chem. Comm. **2017**, 53,* 10136[60]

Obviously, the more we modify the substrates, the less predictable is their behavior in the hydroarylation reaction. In that case, a post-functionalization of the 4-H coumarin would be a convenient choice, in order

to generate precise synthetic targets with potential bio-active features. Selective processes for specific substitution at the position 4 of the coumarin ring are already reported in the literature.[48] A further factor supporting the post-functionalization strategy is that terminal alkynes present usually higher reactivity than the analogous internal ones towards direct coumarin synthesis. In particular, the propiolic acid revealed to be so far the most reactive species among all the other alkynes we tested.

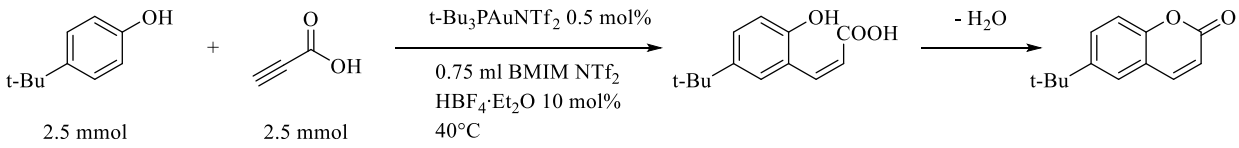

Time [h]	Phenol conversion [%]	Coumarin yield [%]	Z-alkene yield [%]
1	66	22	-
3	75	27	-
24	86	30	-

Figure 3.1.2 Propiolic acid hydroarylation by 4-tertbutyl phenol C-H bond activation; yields and conversions were calculated by ^{1}H NMR(300 MHz, DMSO-d_6) analysis

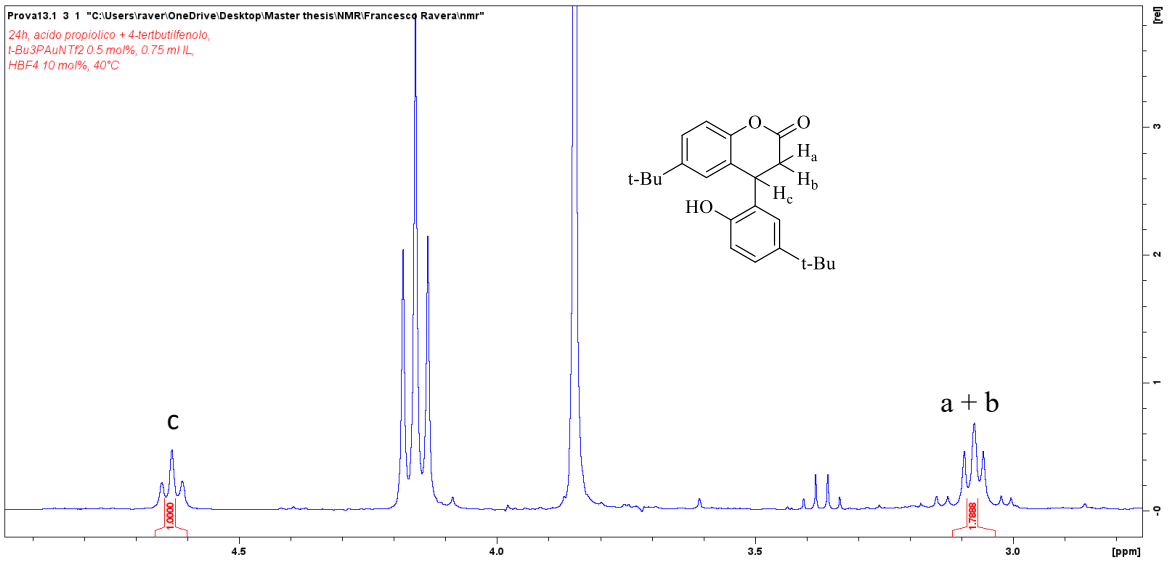

Figure 3.1.3 Highlighted region cointaining the most characteristic signals of the di-hydroarylation product

As it is reported in ***figure 3.1.2***, using the catalyst t-BuPAuNTf$_2$, analogous in reactivity to the carbene one, we succeeded in activating a species that previously seemed to be unreactive in our IL medium. Surprisingly, more than a half of the substrate was already converted in only one hour of reaction. Nevertheless, in order to evaluate the catalytic performance of the system, we cannot neglect an important issue related to process selectivity. Indeed, compared to the high conversions of the arene, we obtain poor yields of the desired product. The most abundant species is indeed the one formally deriving from an additional hydroarylation of the α,β-unsaturated bond of the coumarin product. This species is recognized in the ^{1}H NMR spectrum by the typical pattern of signals due to the diasterotopic protons at position 3 and the proton at the stereocenter (position 4), that originate respectively two doublet of doublets and a triplet of relative intensities 2:1 (see ***figure 3.1.3***). The mechanistic hypothesis for the by-product formation has been developed on the reaction that involves sesamol as aromatic substate and catalyst IPrAuNTf$_2$. As reported in ***figure 3.1.4***. we tested the reactivity of the isolated coumarin 6H-[1,3]dioxolo[4,5-g]chromen-6-one in equimolar amount with respect to sesamol, evaluating systematically all the components of the system.

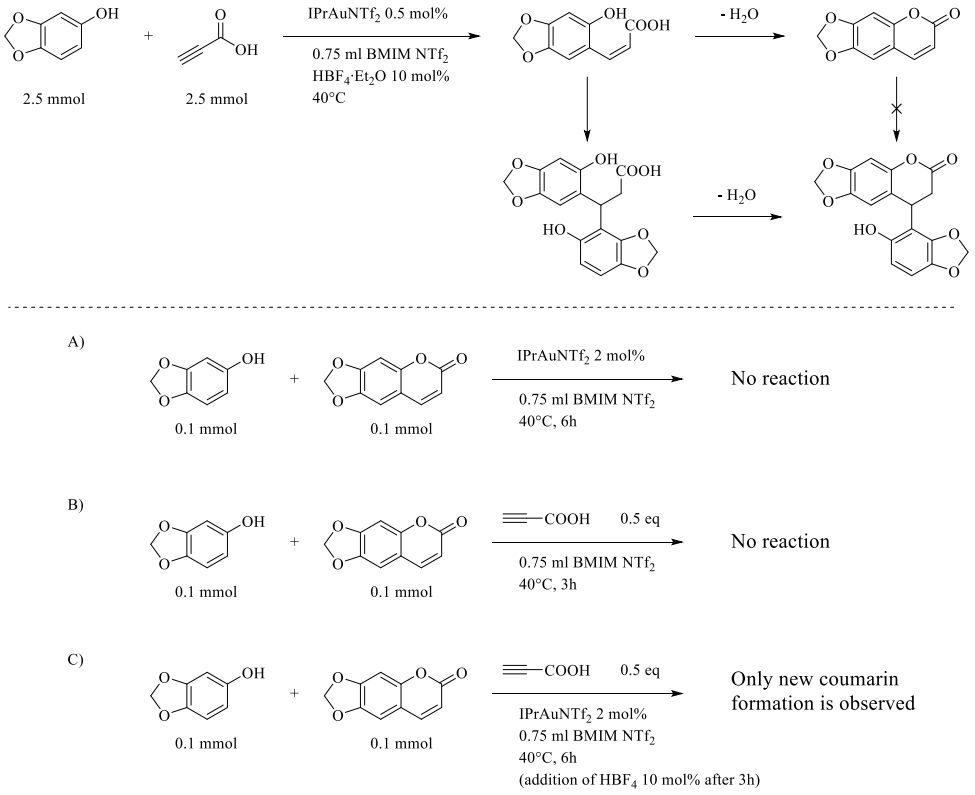

Figure 3.1.4 Hypothesis for the formation path for the di-hydroarylated product and experimental observations

As indicated by the different experiments, we did not afford the di-hydroarylated product starting from preformed coumarin under any of the reported conditions. In the tests A and B the situation appeared static for all the observation time, while for experiment C we could detect an increase of the coumarin signals intensity and again no formation of the di-hydroarylation product. A potential contribution by the acid co-catalyst was also evaluated on the experiment C, adding 10 mol% of HBF_4 after 3 hours of reaction. After this addition, the hydroarylation rate increased until taking the reaction to quantitative conversion of the alkyne. Basing on these experimental evidence, we can finally conclude that the second hydroarylation has to precede the lactonization step. A complete representation of the catalytic cycle is reported in ***figure 3.1.5***.

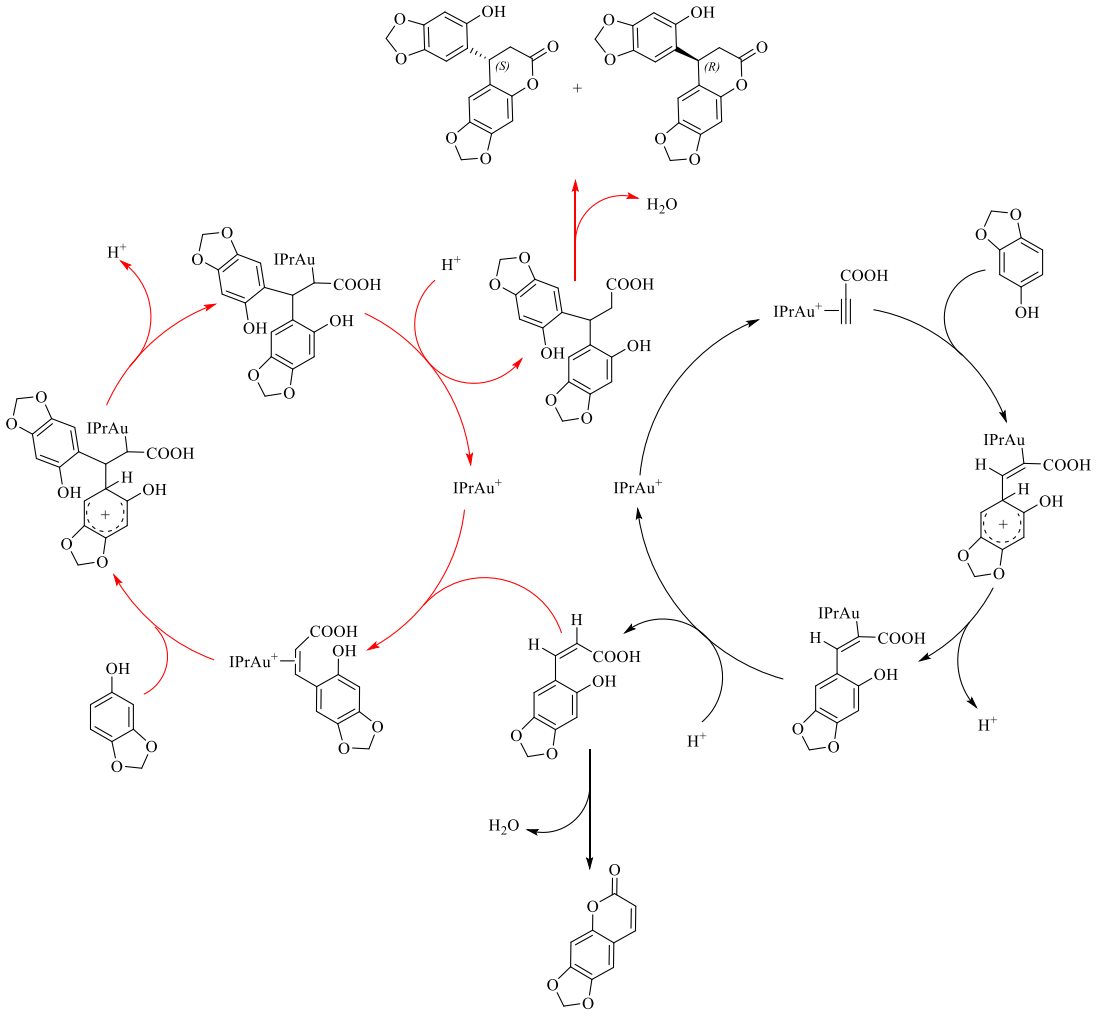

Figure 3.1.5 Catalytic cycle for the intramolecular hydroarylation of propiolic acid

3.2 Overlook on the process optimization and scope

Once understood the mechanism of formation that lead to the by-product, we focused on trying to increase the reaction selectivity with respect to the coumarin yield. Since the catalyst IPrAuCl has been extensively tested in former experiments, obtaining as best result a product distribution coumarin/dihydrocoumarin 1:1 with 0.5 mol% of catalyst and no acid co-catalyst at 40°C, we initially tried substitute the IPrAuCl catalyst with the phosphine complex $(t\text{-Bu})_3PAuNTf_2$, which revealed to be less active but more selective for the single hydroarylation in the process involving sesamol. Also the effect of the temperature was verified, but it seems to play a marginal role on the selectivity. All these results have been rationalized on the reaction involving 4-tert-butylphenol as aromatic substrate (***figure 3.2.1***).

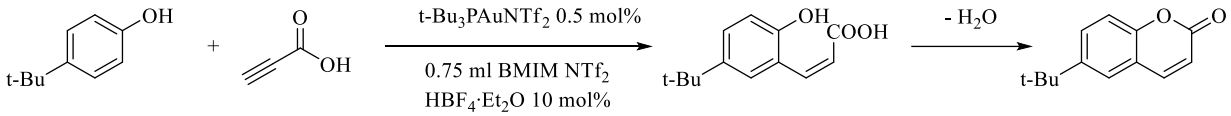

Conditions	Phenol conversion [%]	Coumarin yield [%]	Molar ratio coumarin/di-hydrocoumarin
40°C, no HBF_4	9 (15) [a]	9 (12) [a]	Full selectivity (7:1) [a]
40°C	57 (78) [a]	22 (20) [a]	3:4 (1:2) [a]
60°C	83	18	1:2

Figure 3.2.1 Screening of the reaction selectivity under different conditions; the reported data are referred to ^1H NMR analysis of crudes at 3h of reaction; [a] collected data at 24h of reaction

Even with the different catalyst we did not succeed to obtain consistent improvements in selectivity. The presence of the acid co-catalyst revealed to be fundamental in order to obtain good reactivity. The last factor we can change consists in the substrates molar ratio. As it is well known, the alkyne coordination at the gold center should be preferred with respect to the alkene one. Furthermore, the mass-effect of the alkyne should also increase the reaction rate, allowing us to perform the process at room temperature. From former experiments using IPrAuCl as catalyst, with a molar ratio arene/alkyne of 1:2 the process did not show a tangible improvement, so we increased it to 1:5.

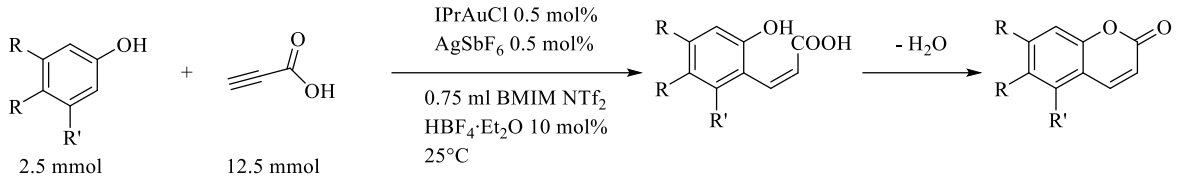

Conditions	Phenol conversion [%]	Coumarin yield [%]	Molar ratio coumarin/di-hydrocoumarin
R' = -H, R = -O-CH$_2$-O-	91 (92) [a]	81 (83) [a]	17:1 (19:1) [a]
R, R' = -Me	100	100	Full selectivity

Figure 3.2.2 ^{1}H NMR conversions and yields analysis at 3h of reaction, varying the aromatic substrate in propiolic acid hydroarylation; [a] calculated data at 24h of reaction

The first test was performed with sesamol as aryl substrate and the result was surprising, reporting high conversion of the substrate in only 3 hours of reaction, and high selectivity using IPrAuCl/AgSbF$_6$. The quantitative yields and conversions are reported in ***figure 3.2.2***. Changing the substrate to 3,4,5-trimethylphenol the reaction performed even better, affording quantitatively the coumarin in the same amount of time. This effect could be determined by the presence of a hindering substituent near the unsaturated bond that should coordinate the gold complex, favoring instead the lactonization step.

3.3 Conclusion and future aims

On this chapter it has been reported how intermolecular hydroarylations could represent a powerful synthetic tool applied to organic chemistry. The gold(I) catalytic active species takes furthermore advantage from the unique nature of the IL medium, improving the reactivity and stability of the system, even at low loadings of catalyst and mild conditions. Nevertheless, the ionic liquid environment leads to some disadvantage, mainly related to the poor solubility of less polar substrates into the media. The scope of the reaction has indeed to be better explored, trying also to improve the process outcome for those substrates that are more challenging, such as alkyl substituted phenols. On the other hand, the activation of electron-rich alkynes represents an important achievement related to the versatility of the system on the synthesis of 4-substituted coumarins. The suppression of the contribution of the hydration/decarboxylation side-paths is a crucial point that has to be further explored, in order to achieve higher yields. Meanwhile, the process involving propiolic acid hydroarylation showed very good reactivity and enhanced selectivity by employing

an excess of alkyne in the reaction mixture. The defined protocol has anyway to be extended to other type of phenols, in order to confirm the relevance of the reaction under these new conditions. The quantity of wasted alkyne per reaction is indeed relevant, especially on the hypothesis of scaling-up of the process. Under these considerations, the possibility to recycle or even reuse the same system for another batch-reaction would be extremely interesting.

Chapter 3

Gold (III)-catalyzed intramolecular hydroarylation

1. (P,C)Au(III) cyclometallated complexes as hydroarylation catalysts

1.1 The state of the art on intermolecular hydroarylation catalyzed by (P,C)-gold(III) complexes

As already anticipated in the introductive chapter, gold-catalyzed hydroarylations present a case where two different oxidation states of the same metal are shown to have the same ability to promote these reactions. Treating this as a tool for organic synthesis, we see increased the assortment of gold complexes we can use in term of different electronic properties. Hence, we are ideally able to extend the scope of the substrates we can hydrofunctionalize. Under this framework, the (P,C)-cyclometalated catalysts[19] developed in the LBPB team at the University of Tolouse, led by Prof. Didier Bourissou, represent singular species bearing a ligand with no reported analogous for gold(I) counter-parts. Under the reaction conditions reported by Fujiwara in the early 2000s, in his first work on arenes alkenylation,[11] these Au(III) catalysts were shown to be incredibly active in the intermolecular hydroarylation of alkynes.

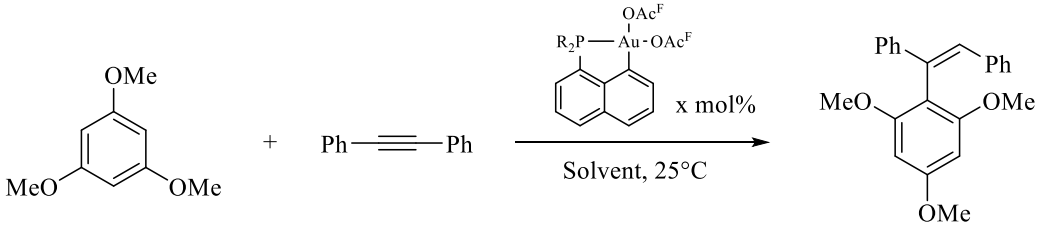

Solvent	Cat. loading [mol%]	NMR Yields	
		R = i-Pr	R = Ph
CD_2Cl_2	5	0 % (24h)	0 % (24h)
TFA/ CD_2Cl_2 (1:20) [a]	5	82 % (4h)	90 % (24h)
TFA/ CH_2Cl_2 (4:1) [b]	5	99 % (0.5h)	99 % (0.5h)
AcOH/ CH_2Cl_2 (4:1) [b]	5	0 % (1h)	0 % (1h)

TFA/ CH_2Cl_2 (4:1) [b]	1	99 % (1h)	99 % (1h)
TFA/ CH_2Cl_2 (4:1) [b]	0.1	91 % (4h)	98 % (3h)

[a] 1 eq. of TMB, [alkyne] = 0.2 M ; [b] 2 eq. of TMB, [alkyne] = 1M

Figure 1.1.1 Intermolecular hydroarylation of di-phenylacetylene with TMB under optimized conditions[54]

The higher electrophilicity of the Au(III) metallic center enables the activation of electron-rich alkynes, such as the di-phenylacetylene (***figure 1.1.1***). On this system, a crucial role is played by the TFA/DCM environment that ensures a fast cleavage of the Au-C bond, which likely is the r.d.s. of the process. Lowering the acid content in the TFA/DCM media, from a ratio 4:1 to 1:20, the catalytic activity sensibly decreases. Meanwhile, changing the nature of the acid to the more coordinating acetic acid totally shuts down catalysis. This effect indicates that we need a labile ligand in order to form the active tri-coordinated species. The different substituents on the phosphorus atom of the ligand further modulate the electronic properties of the complex, influencing the catalytic performance. Indeed, the complex bearing the ligand with P-isopropyl substituents sees its electrophilicity decreased and performs worse in activating the di-phenylacetylene. The stability of the system was also tested, performing the reaction in technical solvents under air, obtaining only a marginal decrease in activity. Interestingly, the control tests concerning a potential silver effect on the gold catalysis led to a zero-dependence by the adopted methodology, i.e. in-situ activation or pre-formation of the catalytic active species with filtration of the AgI precipitate. The system showed to be really robust for potential applications. In the same work, the authors showed how their system at 5 mol% catalyst loading in TFA/CD_2Cl_2 1:20 is comparatively better than the state of art in gold(III)-catalyzed hydroarylation. In particular, a series of selected Au(III) complexes bearing a PCP pincer and (N,C) type ligands were shown to perform worse than the considered (P,C) cyclometalated species. In fact, the reaction was reported to yield traces up to 59% of product on the best performance, after 3 days of reaction with 5-10 mol% of catalyst loading. Moreover, the importance of the ligand architecture and the gold oxidation state was highlighted by comparison with the simple $AuCl_3$/AgOTf and the analogous Au(I) complexes bonding only the phosphorous moiety of the (P,C) ligand: 66% and 47% product yield in 24 hours of reaction were obtained respectively by these two species. In conclusion, the (P,C)Au(III) cyclometalated complexes developed in Toulouse represent an interesting species to be applied on coumarin synthesis. The higher oxidation state could allow us to further expand the reaction scope, activating either electron-rich alkynes or electron-poor arenes, whereas Au(I)-based catalysts do not enable reaction of the latter. Some example of hydroarylation of terminal or alkyl phenyl substituted alkynes

has been already reported, achieving excellent results. On the other hand, some feature concerning the reaction mechanism are still to be explored, due to the presence of isomers that may imply an inner-sphere hydroarylation pathway.

1.2 Adapting the new complexes to coumarins synthesis via intermolecular hydroarylation

Before approaching the direct application of such complexes in ILs media, we followed a step-by-step process in order to better evaluate the response of the catalysts to the change of substrates. The catalytically active species was prepared from (P,C)AuI_2 by anion-exchange assisted by AgI precipitation, and tested on the ethyl phenylpropiolate hydroarylation with TMB (***figures 1.2.1*** and ***1.2.2***). Since the reaction was shown ineffective in AcOH/DCM media, we excluded the possibility to use the 3-phenylpropiolic acid as substrate. The reaction achieved quantitative conversion of the alkyne in 1 hour and 99% of NMR calculated yield, with respect to the internal standard hexamethylbenzene.

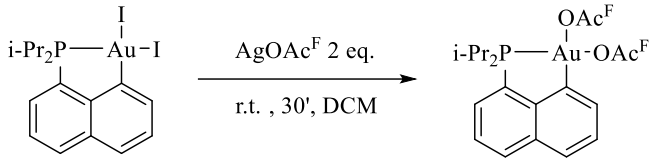

Figure 1.2.1 Activation of the active complex by anion exchange

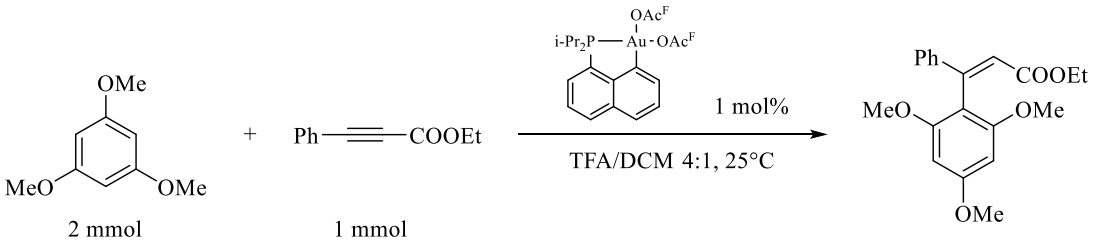

Figure 1.2.2 Intermolecular hydroarylation of ethyl phenylpropiolate with TMB [54]

At this point, we tried to integrate a phenol as aromatic substrate inside the process. In order to have a comparison with the work done in Padova, we chose sesamol. Surprisingly, the reaction did not yield any product. Conducing the same test with 5 mol% catalyst loading led to the same outcome. Recording a ^{31}P NMR spectrum of the reaction crude, we could notice the peak of the phosphorus disappearing and two new signals downfield growing up in presence of the phenol in solution (***figure 1.2.3***). It is quite clear that

sesamol leads to a change in the catalyst structure. Indeed, the final proof comes by a competitive test were sesamol and TMB are inserted in the same mixture together to the alkyne and the (P,C) complex (***figure 1.2.4***).

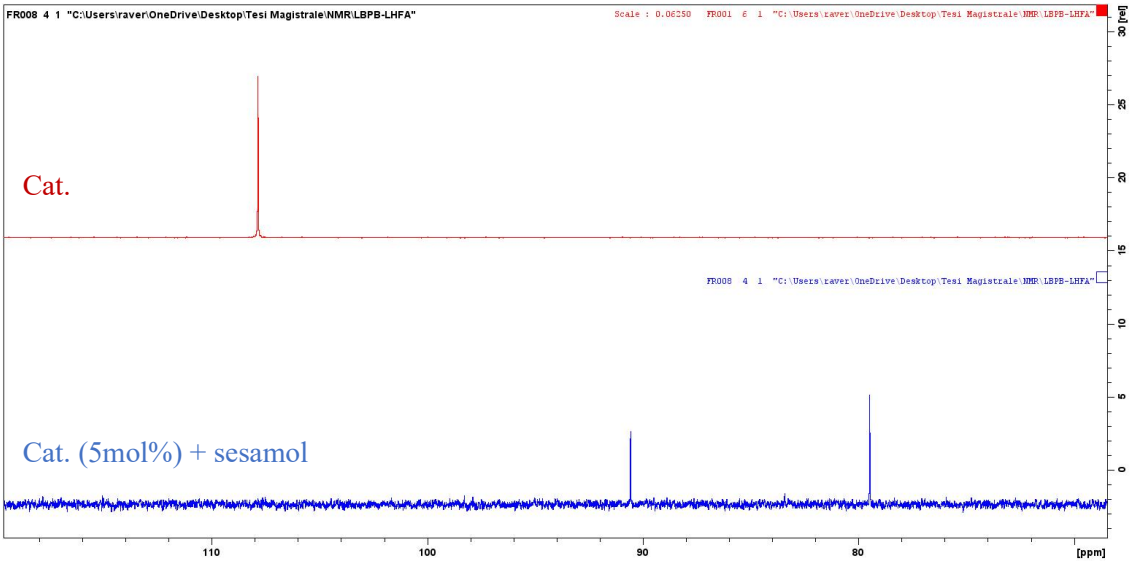

Figure 1.2.3 ^{31}P NMR(121 MHz, $CDCl_3$) of the reaction crude with sesamol compared to the isolated catalyst spectrum

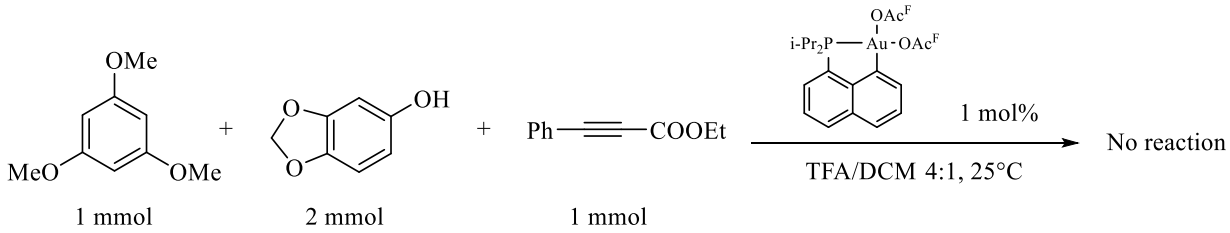

Figure 1.2.4 Hydroarylation of ethyl 3-phenylpropiolate with TMB inhibited by the presence of sesamol

The reaction again achieved no product in 2 hours of reaction. None of the substrates undergoes degradation during this time. Having confirmed that the process inefficiency deals with the hydroxyl moiety of sesamol, we did not conduct further studies for determining the mechanism of the catalyst deactivation. The easier explanation to this behavior sees a possible coordination of the phenol at the metal, forming two different phenolate complexes (cis and trans isomers with respect to phosphorus). Even if the ligation by oxygen-donating groups to gold is quite rare, these species have already been reported in the literature in the case of NHC Au(I) complexes, and the bond nature was analyzed by computational DFT and NBO studies.[61] Moreover, the higher oxidation state leads to an increased oxophilicity of the gold center, favoring the

formation of a coordinative bond with the phenolate. In these condition, the formation of the tri-coordinated active species would be quite energy demanding, and so the coordination of the alkyne becomes disfavored. Under these considerations, we tried to assist the Au-O bond cleavage by increasing the temperature to 40°C, however it resulted ineffective. Once learned that the process with free phenols is not possible, even testing the catalyst in IL media results pointless. We then turned to evaluate the possibility of coumarin formation by an intramolecular approach, in order to avoid the presence of the free hydroxyl functional group before the hydroarylation step.

2. Intramolecular hydroarylation

2.1 Aryl alkynoate synthesis and intramolecular hydroarylation in Fujiwara conditions

The first step was to find an efficient method for the aryl alkynoate synthesis. After a careful screening of the reported methodologies, we opted for a standard esterification assisted by DCC and DMAP as basic catalyst (***figure 2.1.1***). The DDC-alkyne adduct formation at 0°C is typically recognized by a change in the solution color, that turns from colorless to orange. The ester is formed together with the precipitation of the solid dicyclohexyl urea. The presence of the base DMAP in catalytic amount allows the formation of small quantities of phenolate that reacts faster in the nucleophilic addition/substitution. The desired aryl alkynoate has been obtained pure after filtration and further work-up by flash-column chromatography.

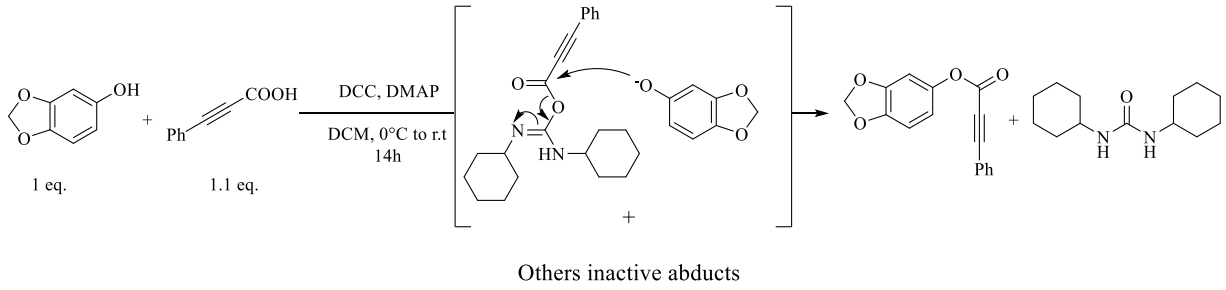

Figure 2.1.1 Synthesis of 3,4-(methylenedioxy)phenyl 3-phenylpropiolate according to [62]

Since this product has not yet been reported in the literature, a full characterization routine by NMR and HRMS was required. In particular, the connectivity of the molecule has been established by COSY, HMBC and HMQC experiments, while the correct mass end elemental composition of the species was determined by HRMS, detecting the molecular ion signal enhanced by chemical ionization (chemical formula $C_{16}H_{10}O_4$, MM = 266.05 g/mol). Once we isolated pure the desired molecule, we were ready to test it on the cyclization

reaction in order to afford the analogous coumarin (***figure 2.1.2***). The reaction revealed to be extremely efficient, enabling the quantitative cyclization of the product within 1 hour, even at low catalyst loadings and mild reaction conditions. The di-phenyl substituted catalyst showed again to be superior concerning the activity, yielding total conversion of the substrate at 25°C and 0.1 mol% of complex. In these condition, the di-isopropyl analogous finds its first limitations, leading to only 8% of product in the same time, and 55% in 24 hours of reaction. Anyway, increasing the temperature to 40°C the system is shown to regain efficiency. Regardless the better performance allowed by the biphenyl substituted complex, this species is markedly less stable, undergoing degradation with time. Therefore, it needed to be stored at low temperatures, protected from light sources.

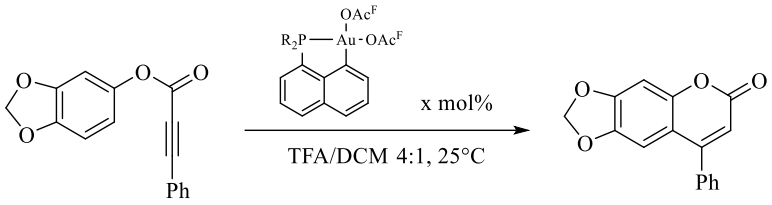

	NMR Yields [a] [%]				
	t0	**t1/2h**	**t1h**	**t3h**	**t24h**
R = i-Pr 0.5 mol%	0	93	100	-	-
R = i-Pr 0.1 mol%	0	8	19	18	55
R = i-Pr 0.1 mol%, 40°C	0	-	100	-	-
R = Ph 0.5 mol%	0	-	100	-	-
R = Ph 0.1 mol%	0	-	100	-	-

Figure 2.1.2 Catalytic test on 3,4-(methylenedioxy)phenyl 3-phenylpropiolate in Fujiwara conditions; [a] NMR calculation vs internal standard hexamethylbenzene

2.2 Adapting the process in BMIM NTf_2

Now that we have elucidated that cyclometalated (P,C) complexes can effectively afford coumarins via intramolecular hydroarylation, we can focus on integrating the ILs media on this type of process. Taking as starting point the process developed for IPrAuCl complex, we started to screen different contributes on

the reactivity, such as the acid co-catalyst role and the loading of complex. In ***figure 2.2.1*** are reported all details and yields about the performed experiments.

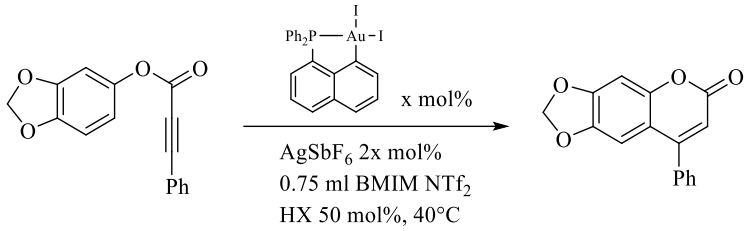

	NMR Yields [a] [%]				
	t0	**t1/2h**	**t1h**	**t8h**	**t72h**
Cat. 5 mol%	0	0	0	0	0
Cat. 5 mol% TFA	0	83	83	83	91
Cat. 5 mol% $HNTf_2$	0	100	-	-	-
Cat. 1 mol% $HNTf_2$	0	68	100	-	-

Figure 2.2.1 Aryl alkynoate cyclization in IL and screening of the reaction conditions; [a] quantitative calculations are made vs internal standard 1,2-di-methoxyethane at different times, from 0 to 72 hours

As expected, the presence of a strong Brønsted acid is necessary in order to support the protodeauration step of the catalytic cycle. Still we got an influence in reactivity varying the counter ion of the active species. The TFA co-catalyst determines lower activity compared to $HNTf_2$, probably for the higher coordination power of trifluoroacetate compared to the bis(trifluorosulfonyl)imide counteanion. This is an interesting result, because it is evident that we do not obtain the same catalytic active species in solution, despite the considerable excess of the IL anion. Moreover, comparing this system to the one in TFA/DCM solution, we notice a higher demand of complex in order to reach analogous results. This is probably due to the heterogeneous character of the system and the much lower acidic conditions. Regardless these last aspects, the IL environment could lead to some advantages concerning higher catalyst stability and easier separations of the product from the reaction media. Obtaining a performing system even with such low concentration of acid co-catalyst is indeed a feature related to the favorable nature of the medium toward proton-transfer processes.

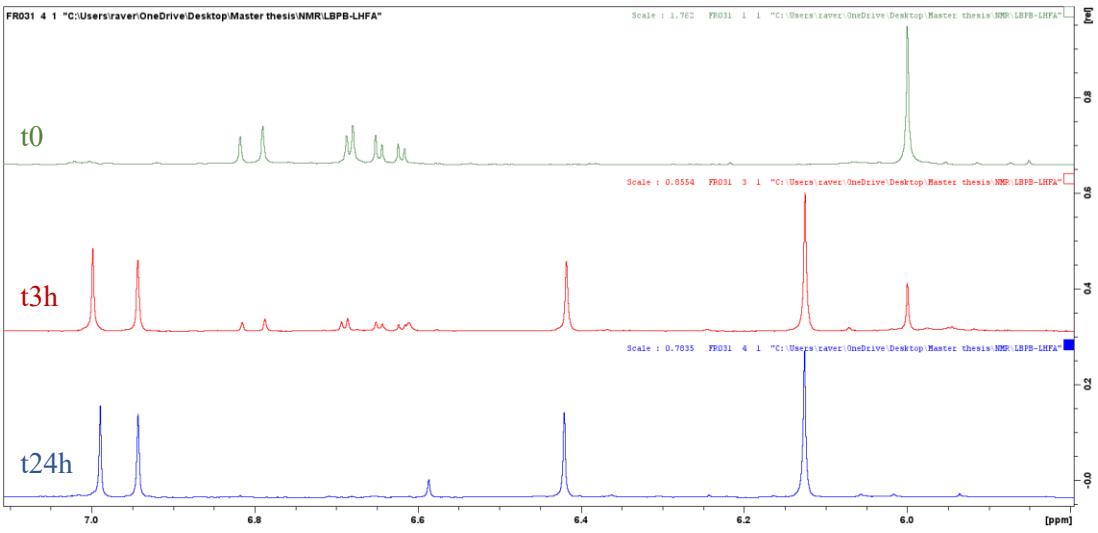

Figure 2.2.2 Blank test of the $HNTf_2$ assisted aryl alkynoate cyclization, zoom on the more relevant signals for the interested species

Concerning this last aspect, a control test about the acid contribution in the system revealed that $HNTf_2$ is able to perform the reaction even in absence of gold complex and in a not negligible rate. After 24 hours of reaction the substrate is almost quantitatively converted in product, as shown in ***figure 2.2.2***. In particular, the two singlets at 6 and 6.13 ppm are highlighted, which correspond respectively to the aryl alkynoate and to the coumarin methylene protons. Luckily, $HNTf_2$ showed to not be able anymore performing the process at lower molar ratio. Indeed, at 20 mol% of acid co-catalyst we could not detect the product, even after 24 hours of reaction. Under these new conditions, we considered to further explore the effect of the acid anion, taking as example three common acids used for the poor coordinating power of their counter-ion: $HNTf_2$, $HBF_4{\cdot}Et_2O$ and TfOH. All the analytic data are reported in ***figure 2.2.3***. As expected, the pattern of reactivity changing the acid species strictly follow the coordinating ability of the anion. This is evident for the trifluoromethansulfonate, that leads to 80% of substrate conversion in 1 hour, instead of quantitative yield as in the case of the other two acids. Again, the most electron-rich di-isopropyl substituted (P,C) complex shows lower reactivity with respect to the di-phenyl analogous, which achieve a better performance even with half of the loading (1 mol%). Although, further lowering the complex amount the process finds its limitations. As reported, at 0.5 mol% the reaction cannot achieve full conversion of the substrate anymore: after 24 hours of reaction, only 80% of product yield has been detected.

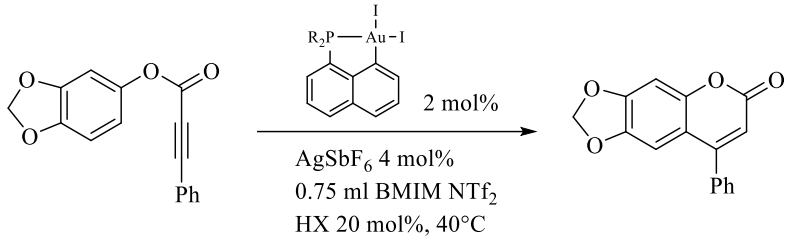

R	HX	NMR Yields [a] [%]		
		t0	t1h	t3h
Ph	**$HNTf_2$**	0	100	-
Ph	**$HBF_4 \cdot Et_2O$**	0	100	-
Ph	**TfOH**	0	80	100
i-Pr	**$HNTf_2$**	0	35	100
i-Pr	**$HBF_4 \cdot Et_2O$**	0	28	100
Ph, 1 mol%	**$HBF_4 \cdot Et_2O$**	0	67	100
Ph, 0.5 mol%	**$HBF_4 \cdot Et_2O$**	0	32	63 (80) [b]

Figure 2.2.3 Screening of the acid counter-anion effect and process optimization; [a] yields calculated vs internal standard 1,2-di-methoxyethane; [b] calculated yield at 24h

3. Expanding the reaction scope

3.1 The challenge and simple substrates

Gold(III) chemistry is still an unexplored field concerning its catalytic potential on π-acid catalysis. Moreover, in the literature are mainly reported as catalysts simple gold salts, thus, metal centers that are not addressed with specific ligands. In particular the $AuCl_3$/AgOTf system reported by He constitutes the starting point concerning Au(III)-catalyzed coumarin synthesis.[63][33] On the other hand, gold(I)-catalysis developed very quickly on this aspect and different authors got interest in potential application for new C-C bond formation paths. In particular, the works of Banwell and co-workers have been taken as reference on coumarin synthesis by gold(I) alkyne hydroarylation.[51][52][64] In order to highlight the relevance of (P,C)Au(III) complexes in the synthesis of such products, we selected a series of target molecules from the before-mentioned works (see ***figure 3.1.1***). The main aim of this part of the project is to expand the reaction scope, trying at the same time to achieve the activation of substrates that have shown to be less efficient if employed in cyclization processes.

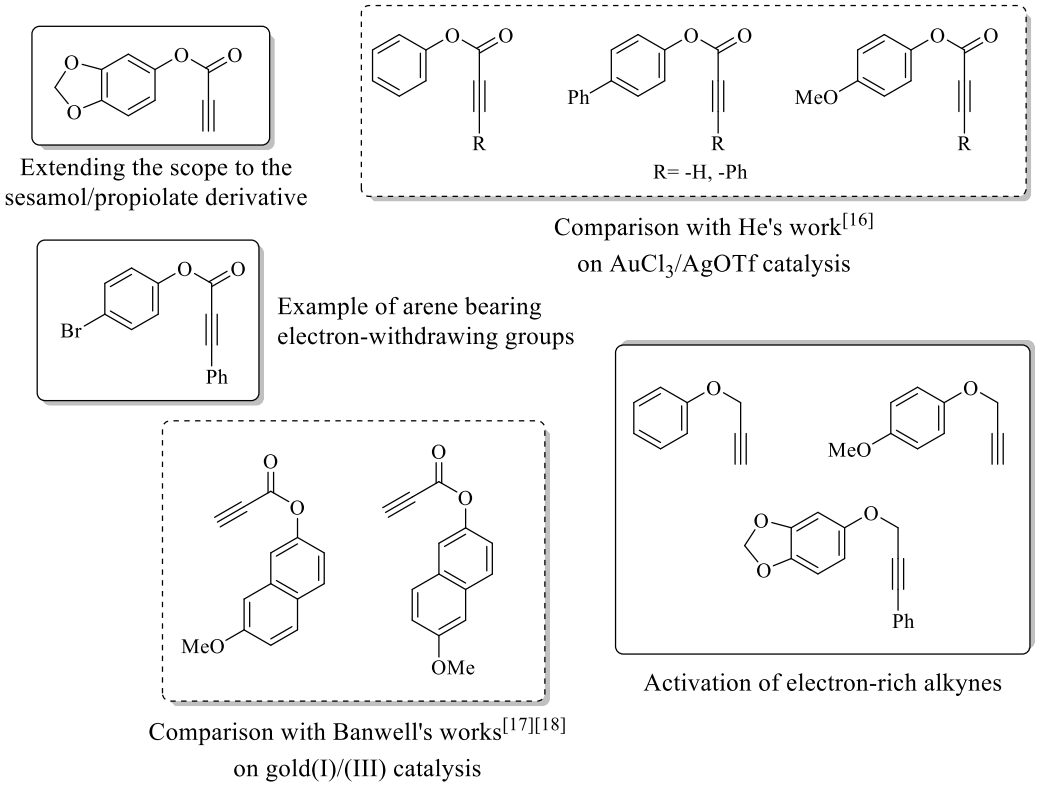

Figure 3.1.1 Target molecules for extending the reaction scope with regard to the state of the art on the synthesis of coumarins via intramolecular hydroarylation

3.2 Methoxy-substituted aryl alkynoates: reactivity and selectivity

As it has been shown and extensively discussed in the Chapter 2, the substrate polarity strongly affects the reaction outcome in ILs media. In order to simplify the results exposition, the substrates reported in ***figure 3.1.1*** have been divided with respect to the substituents on the aryl moiety of the species, starting from the more polar methoxy-substituted compounds. Firstly, the effect of the alkyne nature, if terminal or substituted, was tested on the same sesamol ester with propiolic acid.

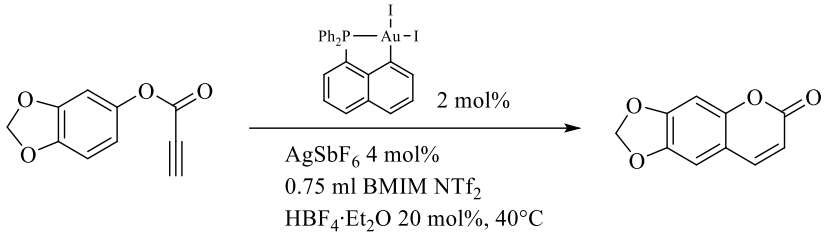

Figure 3.2.1 3,4-(Methylendioxy)phenyl propiolate cyclization on optimized conditions

The process, shown in ***figure 3.2.1***, is extremely efficient, achieving full conversion of the substrate in only 1 hour and full selectivity toward the desired coumarin, with C-H activation at position 6. Moving on methoxy-substituted coumarins the reactivity pattern is quite similar (see ***figure 3.2.2***).

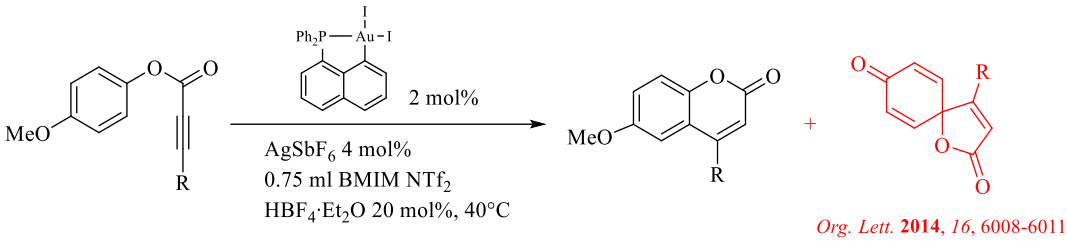

Org. Lett. **2014**, *16*, 6008-6011

R	Time [h]	NMR Conversions [a] [%]	NMR Yields [a] [%]	By-product NMR Yields [%]
H	1	100	87	15
Ph	24	100 (78) [b]	64 (42) [b]	30 (25) [b]

Figure 3.2.2 Cyclization of 4-methoxyphenyl propiolate derivatives; [a] yields and conversion calculation vs internal standard 1,2-di-methoxyethane; [b] calculated data at 3 hours;

As it was expected, the substrate bearing the terminal alkyne moiety is much more reactive than the phenyl-substituted analogous. Compared this last one to the former 3,4-(methylendioxy)phenyl 3-phenylpropiolate, the lower polarity determines longer reaction times in order to reach full conversion. Interestingly, in this process we meet issues concerning the selectivity. Indeed, the (P,C)-catalyst assists another reaction-path to afford the consequent spirocycles by the mechanism proposed in ***figure 3.2.3***. This cycle has been reported by Vadola and co-workers[65] basing on the experimental evidence on $Ph_3PAu(I)$-catalyzed ipso-cyclization processes. As reported, the amount of water in the system assists the demethylation step of the cycle. Moreover, the counter-anion of the IL (analogous to the silver salt effect in Vadola's work) could play a role concerning the stabilization of the cationic intermediate, promoting the 1,2-alkyl shift to come back on the path that would afford the coumarin. Also the alkyne substituent plays a role to determine the process selectivity, favoring the spirocycle formation in case of substituted alkynes with unhindered groups. In the conditions proposed (Ph_3PAuCl/AgOTf 5 mol% , DCM, H_2O 1eq. at room temperature) 4-methoxy propiolate yields 74% product in 3 hours, while the phenyl-substituted propiolate achieves 85% yield in only 1 hour. All these contributes on process selectivity have still to be investigated regarding (P,C)Au(III) complexes and also a possible contribute by the IL medium should be evaluated.

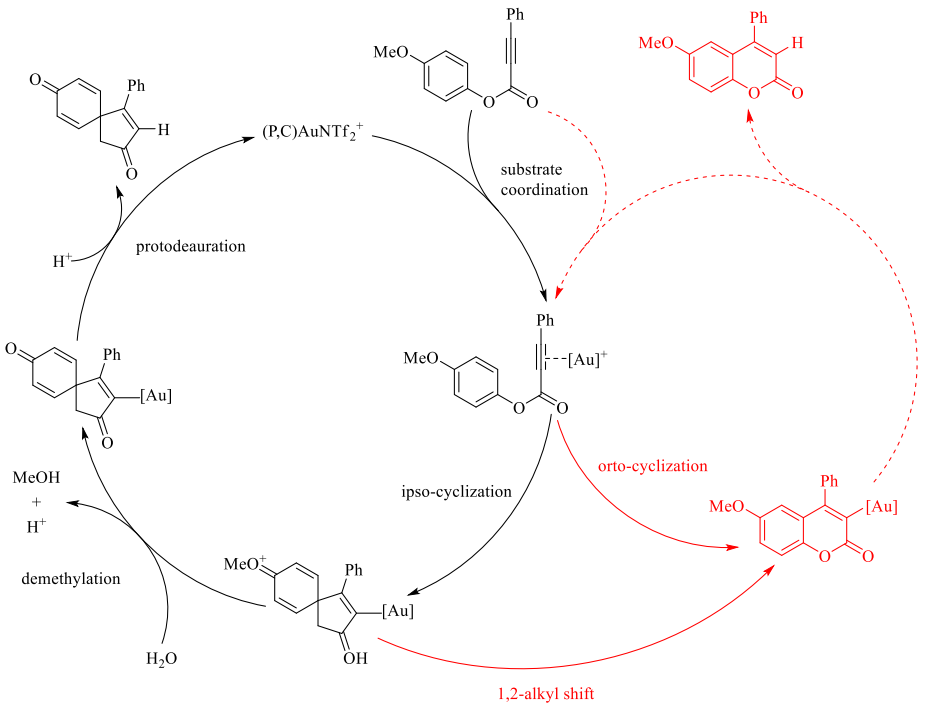

Figure 3.2.3 Proposed dearomative spirocyclization mechanism for the (P,C)Au(III) complex

The last substrates we tested are the methoxy-substituted naphthyl propiolates.

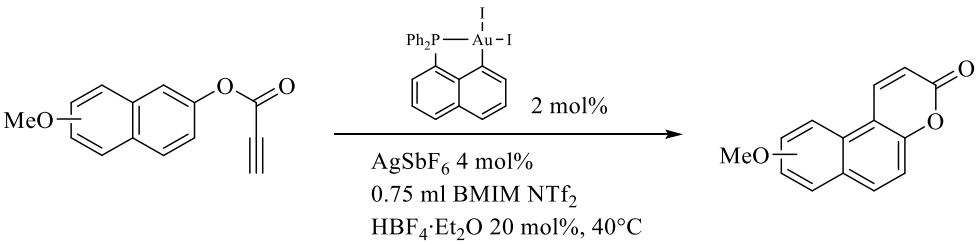

Isomer	Time [h]	NMR Conversions [a] [%]	NMR Yields [a] [%]
7-MeO	3	100	100
6-MeO	3	95	92

Figure 3.2.4 Naphthyl propiolates cyclization; [a] yields calculated vs internal standard 1,2-dimethoxyethane

We succeeded achieving the desired product with full selectivity for the vinylation at position 1. The different position of the methoxy group did not determine changes in selectivity. Instead, little variations in the substrate polarity generate a slight difference in reactivity, making the 6-methoxy substituted substrate slower in undergoing cyclization. Seen these results, it is evident the (P,C)Au(III) complex performs much better than the systems that does not tether any ligand (see ***figure 3.2.5***).

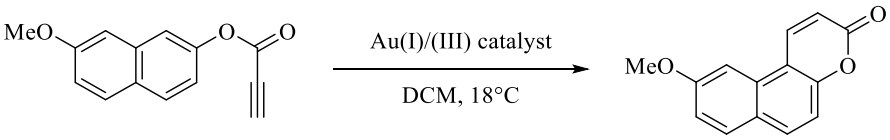

1 mmol

Catalyst	Loading [mol%]	Time	Yield [%]
IPrAu(I)Cl	3−15	48 h	no reaction
t-Bu$_3$PAu(I)Cl	3-15	48 h	no reaction
Cy$_3$PAu(I)Cl	3-15	48 h	3
Ph$_3$PAu(I)Cl	3-15	48 h	3
AuCl	3-15	48 h	18
XPhosAu(I)NTf$_2$	3	8 h	95
Echavarren's catalyst	3	10 min	100
Au(OAc)$_3$	15	16 h	8
AuCl$_3$/AgOTf	3	8 h	89

Figure 3.2.5 Data reported by Banwell and co-workers on intramolecular hydroarylation of 7-methoxynaphthyl propiolate

In fact, $AuCl_3$/AgOTf at 3 mol% in DCM could achieve 89% yield for the 7-methoxy isomer cyclization after 8 hours of reaction at 18°C. $Au(OAc)_3$ perform even worse, yielding only 6% of product after 16 hours at 15 mol% of catalyst loading in the same conditions. Moreover, the system shows competitive results even compared with the reported gold(I) catalysts. Clearly, a direct comparison is difficult to establish due to the different conditions the authors proposes in the work. Especially, Echavarren's catalyst presents such high activity that a direct comparison with the (P,C)-complex is hard to be drawn, also considering the

intrinsic dissimilarities determined by the medium and the reaction conditions; the previously tested gold(III) salts should be at least tested in presence of an acid co-catalyst in order to have a better comparison.

3.3 Less polar substrates and electron-withdrawing substituents: facing the solubility limitations

Moving the focus on less polar substrates, the firsts limitations of the system emerges. The discussion starts from the simple phenyl propiolate and phenylpropiolate (***figure 3.3.1***).

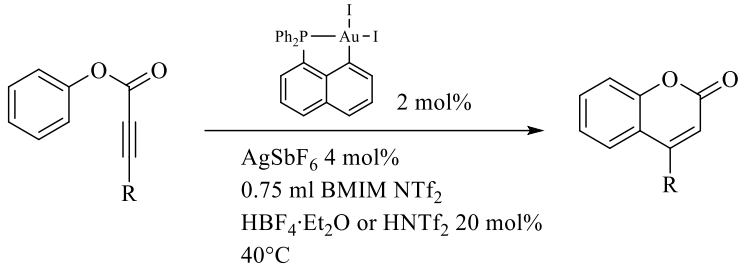

R	Time [h]	NMR Conversion [a] [%]	NMR Yield [a] [%]
H	24	70 (40-70) [b,c]	70 (100) [b]
Ph	24	93	87

Figure 3.3.1 Cyclization of phenyl propiolates in optimized conditions; [a] yields and conversions calculated vs internal standard 1,2-di-methoxyethane; [b] catalyst loading 5 mol%; [c] calculation at 3h of reaction

The first difference we can notice from the reported experimental evidence concerns the performance changing the alkyne moiety. In fact, in this case a higher activity in case of the terminal alkyne is not recorded, to the point that in the latter case an increment of the catalyst loading is necessary in order to achieve full conversion. Changing the acid to $HNTf_2$ does not influence the reaction outcome. Both the substrates show lower activity compared to the ones reported in the previous sub-chapter. The lower cyclization rate makes furthermore evident signals due to side processes such as the ester hydrolysis. In particular, the presence of free phenol in solution leads to the deactivation of the catalyst, and consequently low amounts of coumarin are produced. This problem is really relevant for aryl alkynoates bearing electron withdrawing groups, such as the 4-bromophenyl phenylpropiolate. In this case we succeed achieving only 24% coumarin yield after 24 hours and a consistent portion of substrate, almost 20%, was converted to its constituents. Increasing the catalyst loading to 5 mol% did not improve the reaction outcome. With the

biphenyl-yl propiolate derivatives the hydrolysis issue is not so evident. Instead, the main limitation to the substrate conversion is due to the poor solubility in the reaction media.

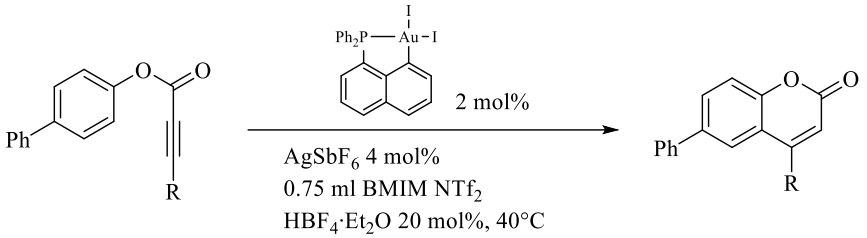

R	Time [h]	NMR Conversion [a] [%]	NMR Yield [a] [%]
H	3	64 (>90) [b]	64 (59) [b]
	24	100 (100) [b]	100 (90) [b]
Ph	24	Traces - 24	Traces - 24

Figure 3.3.2 Cyclization of biphenyl-yl propiolates in optimized conditions; [a] yields and conversions calculated vs internal standard 1,2-di-methoxyethane; [b] catalyst loading 5 mol%

Basing on the data reported in ***figure 3.3.2***, the terminal aryl alkynoate shows again higher activity than the internal one. Interestingly, increasing the catalyst loading the system activity toward the substrate conversion is improved, but the coumarin formation rate does not increase. Moreover, basing on the ^{1}H NMR recorded spectra, the alkynyl proton signal almost disappeared after 3 hours of reaction. The substrate bearing the terminal alkyne moiety is so poorly soluble that the yield is limited to 24% of substrate conversion for the best result we achieved. These two substrate perfectly represent the biphasic nature of the IL catalytic system. The process is indeed limited by the diffusion of the substrates into the IL phase, determining the independence of the reaction rate by the catalyst loading or the intrinsic activity of the gold complex to promote the reaction.

3.4 Aryl alkynyl ethers

The aryl propargyl ethers are the last class of substrates we tested in order to show the substrates extent to which we can apply our system. The preparation of these substrates was made by nucleophilic substitution of the phenolate on propargyl bromide, or by Mitsunobu reaction from the 3-phenyl-2-propynol (***figure 3.4.1***). The crudes have been suitably purified as reported by product extraction and/or flash chromatography and characterized by ^{1}H NMR (300 MHz, $CDCl_3$).

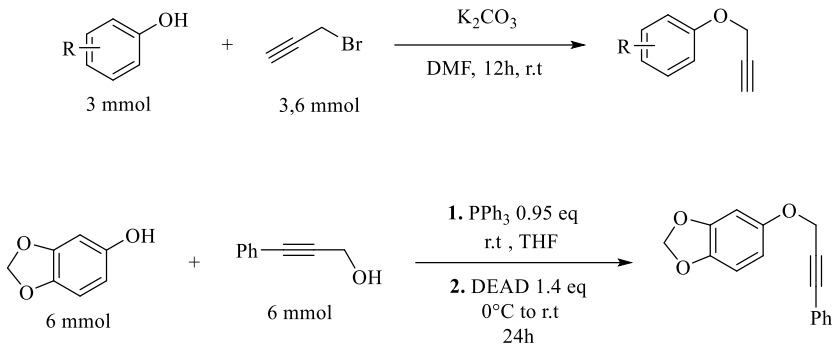

Figure 3.4.1 Synthesis of aryl alkynyl ethers [66]

The test of these compounds in the cyclization reaction gave really controversial results. The reaction reaches always complete conversion of substrates in 1 up to 3 hours. In spite of the apparent high activity of the system and the identification of 2*H*-chromene diagnostic signals in the first sample, the recorded spectra after 3 hours reaction time, surprisingly, do not report any product signal. More in specific, we could observe a broadening of reagent and product signals until their complete disappearance. What has been mentioned above is reported in ***figure 3.4.2***.

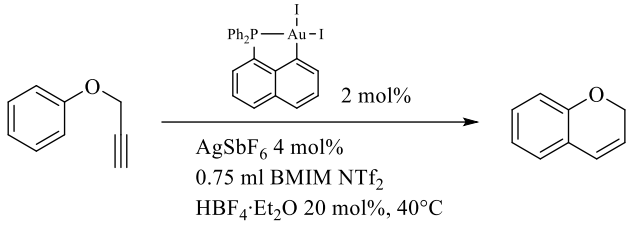

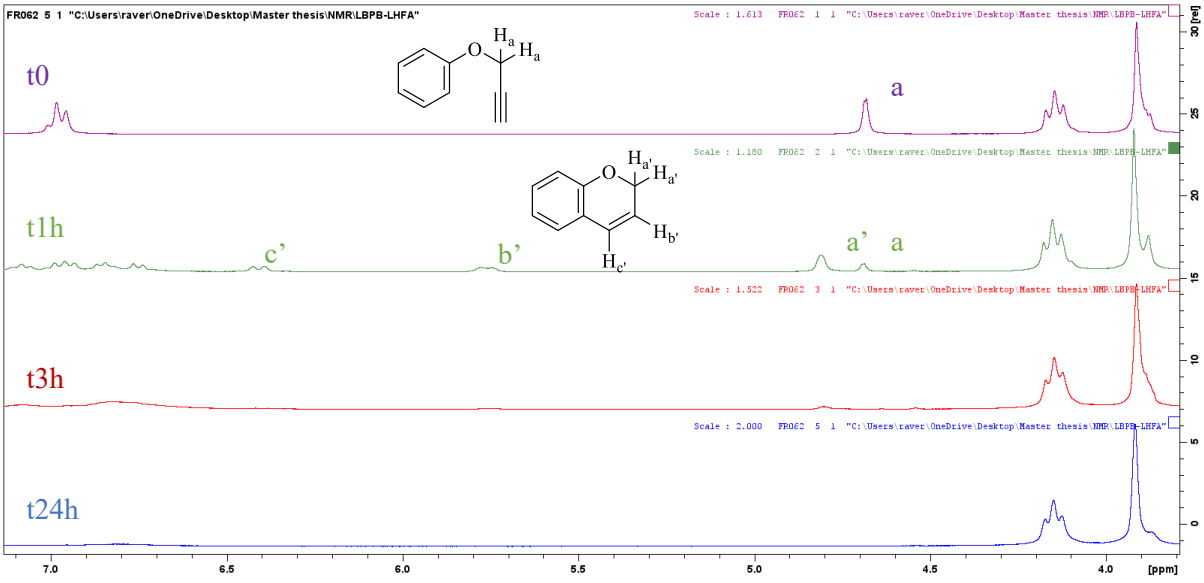

Figure 3.4.2 Evolution of the reaction followed by ^1H NMR

The most probable explanation for this behavior matches with a degradation of the product, or with the presence of another reaction path that takes the substrate to an unstable species, even not visible by proton NMR. In order to determine the origin of this phenomenon, we tried to change one by one the components and conditions of the process. The acid co-catalyst was changed to $HNTf_2$, although no improvements have been achieved. Even the effect of temperature was tested, performing the reaction at room temperature. Since in these condition the cyclization is too slow, we tried to activate the aryl moiety by the presence of an electron-donating methoxy substituent.

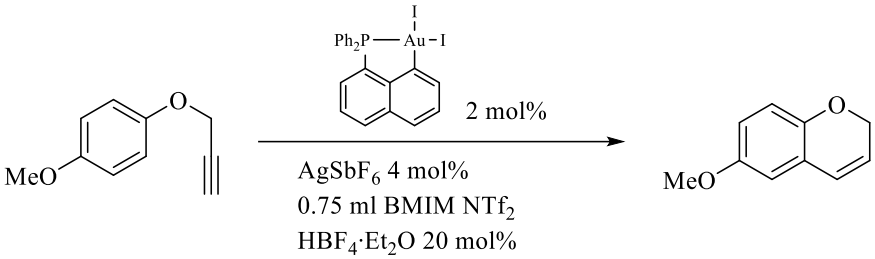

Temperature	Time [h]	NMR Conversion [a] [%]	NMR Yield [a] [%]
40 °C	1	100	0
25 °C	1	100	31

Figure 3.4.3 4-Methoxyphenyl propargyl ether cyclization: effect of the temperature; [a] yields and conversions calculated vs internal standard 1,2-di-methoxyethane

As reported in ***figure 3.4.3***, the temperature has an important role concerning the product stability. Indeed, at room temperature we achieved 31% of product in the same time of the reaction performed at 40°C. Lastly, we evaluated the effect of the alkyne electronic and steric properties, testing the sesamol derivative shown in ***figure 3.4.4***.

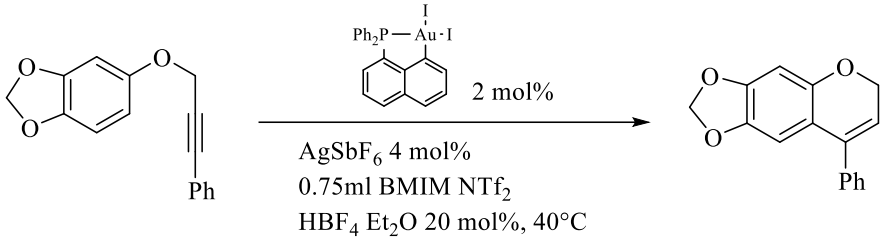

Figure 3.4.4 Sesamol 3-phenylprop-2-yn-1-yl ether cyclization

The reaction achieved 20% of product after 1 hour of reaction and 96% of substrate conversion (100% after 3 hours). In this case the reaction mixture showed several not identified species, as shown in the recorded NMR spectra (***figure 3.4.5***).

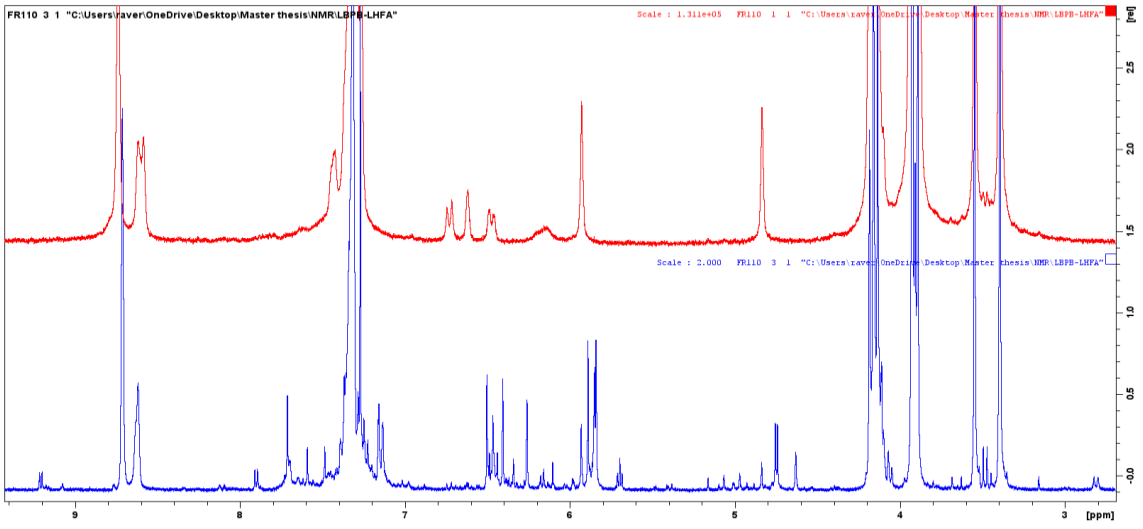

Figure 3.4.5 ^{1}H NMR(300 MHz, $CDCl_3$) of the reaction crude at time 0h (red line) and at 3h (blue line)

It is evident that other species are present in the crude, in addition to the product. This last one can be recognized by the typical signals at 4.75 (d, 2H) and 5.70 (t, 1H) ppm, which correspond to the vinylic and allylic protons of the product alkenyl moiety. In order to better define the other species, the crude has to be purified and characterized. Some by-product could even be formed by side-path catalyzed by the silver salt. This possibility has been already described in the literature. In particular, Nevado and Echavarren reported an analogous system, for the cyclization of the sesamol propargyl ether.[67] The silver salt nature showed to have a role on the formation of the product symmetric dimer (***figure 3.4.6***).

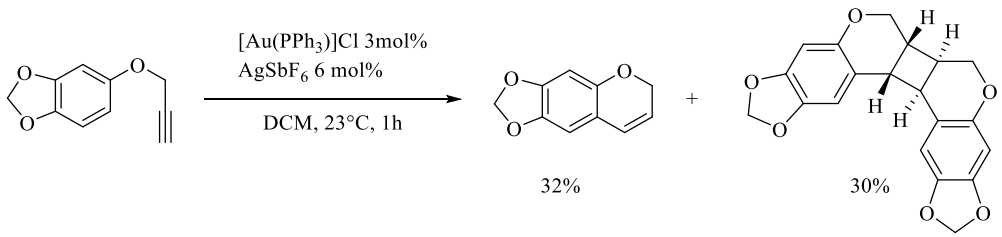

Figure 3.4.6 Silver catalyzed formation of the chromene symmetric dimer reported by Nevado and Echavarren

3. 5 Conclusions and future aims

On this last chapter it has been shown that gold(III) catalysis can be successful implemented in our system, involving BMIM NTf_2 as reaction medium. As expected, the (P,C)-catalysts are really efficient electrophiles, that have been shown working extremely well in Fujiwara conditions. Moving to ILs, the activity magnitude decreases, probably because the lower acidic conditions of the system. In order to have a direct comparison with TFA/DCM medium, we should perform some test with the same loading of acid in DCM. The nature of the co-catalyst revealed to be determining on the system activity: oxygen donating counter-anions affect negatively the catalytic performance, lowering the reaction rate and leading to lower yields. The application extent has been particularly successful concerning polar methoxy-substituted aryl alkynoate, which are not limited by solubility issues. The spirocyclization by-process for para methoxy aryl alkynoates has still to be investigated. However, the content of water in the mixture seems to be determining in directing the process selectivity toward the spirocycle. By principle, limiting the water content in the reaction-batch, even using molecular sieves for sequestering it, could enhance the substrate conversion to the analogous coumarin, but this hypothesis has still to be proved. Also changing the IL anion may be a possibility, although it could strongly affect the system activity, even shutting completely down catalysis. The activation of less polar substrates revealed more challenging than expected. We succeeded in activating simple substrates, bearing terminal alkyne moieties. Indeed, the solubility limitation seems to be difficult to overcome for strongly nonpolar substrates such as biphenyl-yl 3-phenylpropiolate, or in the case of 4-bromophenyl 3-phenylpropiolate, which undergoes hydrolysis before being activated. On the other hand, even though the activation of aryl alkynyl ethers led to highly active systems, it has to be further studied in order to understand the origins of the product degradation and other side-paths that afford the detected by-products. In general, the (P,C)-gold complexes have shown to perform better in many cases than most of Au(I) catalysts and Au(III) salts. Meanwhile, it is evident that these complexes do not seem to benefit the same advantages from the ILs media that IPrAuCl has been shown. Nevertheless, the (P,C)-cyclometallated gold complexes profit a higher stability in solution than gold(I) complexes, making possible the hypothesis of system recycling.

Conclusions and future aims

The work carried out in the frame of this thesis constitutes a further step forward on the implementation of ionic liquids in gold-catalyzed hydroarylations of alkynes. The advantages induced by these media allow to produce coumarins in a simple but effective one-pot process. Cationic $IPrAu^+$ was demonstrated to be the best scaffold leading to high conversion of substrates, using small amounts of complex (0.1 to 0.5 mol%) and mild reaction conditions. The effect of the acid functional group on the alkyne and co-catalyst $HBF_4 \cdot Et_2O$ corroborates the determining role of the protodeauration step on the reaction rate. On the other hand, the hydration side-reaction seems to receive the same benefits, while the role of the decarboxylation has to be further investigated. The activation of hexynoic acid opened the possibility to extend the scope to more electron-rich alkynes. In this framework, gold(III)-catalysis can play a complementary role for the activation of more challenging substrates. However, the attempt to implement more electrophilic (P,C)Au(III) complexes was not successful, leading to the total deactivation of the active species by the presence of phenols. ^{31}P NMR analyses and a competitive test with sesamol and TMB (***figure 1.2.3*** and ***1.2.4*** in the chapter 3) corroborated the hypothesis that it is the contribution of the arene hydroxyl moiety that shuts down the system reactivity. Unable to solve the problem, we changed the focus to the intramolecular hydroarylation of aryl alkynoates. (P,C)-gold(III) complexes showed extremely good activity and applicability for a quite large set of these substrates, whereas aryl alkynyl substrates have still to be investigated. As for gold(I) catalysis, the limited solubility of non-polar substrates is the main issue to be taken in consideration for further implementation of the IL system. Increasing the temperature could enhance the mixture homogeneity, but also leading to negative effects on the catalyst stability.

In conclusion, both intermolecular and intramolecular approaches for hydroarylation of alkynes represent a sustainable and atom economic choice for the synthesis of coumarins. Even compared with others organometallic approaches, gold-catalysis does not require pre-functionalization of substrates, and Au complexes are easy to handle and safe. The use of ionic liquids as reaction media further enhance these characteristics, opening the possibility of aimed recovery strategies for the product and recycling of the system for another life-cycle.

Experimental section

1. General remarks

Unless specified, all the experimental manipulations were carried out under argon atmosphere, using standard Schlenk technique and flame-dried glassware. Purifications were performed by flash-column chromatography on silica gel and TLC check for selecting the eluent and monitoring the isolated fractions. ^{1}H, ^{13}C, ^{31}P and ^{19}F NMR spectra were recorded on Bruker Avance 300 spectrometer at 298 K and ^{1}H and ^{13}C chemical shifts (δ) calibrated with respect to the signals of the deuterated solvent (^{13}C) and its protonated residue (^{1}H).[68] The following abbreviations and their combinations are used for the compress notation of the characterization data: br, broad; s, singlet; d, doublet; t, triplet; q, quartet; m, multiplet; hept, heptuplet. Occasionally, no-lock ^{31}P and ^{19}F experiments were recorded for monitoring reactions. HRMS analysis were performed on Waters GCT Premier spectrometer by DCI methane for the determination of the exact masses. All starting materials were purchased as high purity reagents and used as received. THF, dichloromethane, toluene and acetonitrile are dried on MBraun SPS-800 solvent purification system. (P,C)-cyclometallated complexes, aryl alkynoates and aryl alkynyl ethers were opportunely synthesized by procedures reported in the following section.

2. Synthetic procedures

2.1 Synthesis of (P,C)-ligands[19][69]

1,8-Diiodonaphtalene (1.75 mmol) was dissolved in THF (25 ml) and a solution of nBuLi (1.6 M in hexanes, 1.760 mmol, 1.05 eq.) was added dropwise at -78 °C. The reaction mixture was stirred at -78 °C for 1 h. Then Ph_2PCl or iPr_2PCl (1.75 mmol, 1 eq.) was added dropwise and the reaction mixture was allowed to warm to room temperature and stirred over-night. A no-lock ^{31}P NMR check was performed in order to verify the presence of product. All volatiles were removed in vacuo. The crude product was purified by column chromatography (SiO_2, pentane and then pentane/toluene 1:1 v/v) to yield the desired products as yellowish solids. Characterization was performed by ^{1}H and ^{31}P NMR in $CDCl_3$ or C_6D_6.

2.2 Synthesis of (P,C)AuI_2 complexes

2.2.1 Di-isopropyl substituted (P,C) complex[70]

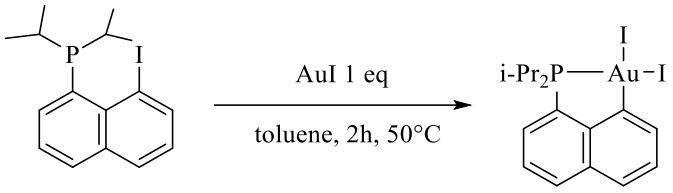

Gold iodide (437 mg, 1.35 mmol) was suspended in degassed toluene (18 ml) and a solution of ligand (500 mg, 1.35 mmol) in degassed toluene (17 ml) was added dropwise at room temperature. The reaction mixture was stirred at 50°C for 2 h. The complete conversion of the ligand was confirmed by no-lock ^{31}P NMR. All volatiles were removed in vacuo to yield the desired complex as an orange-brown powder. Crystals were obtained by layering a saturated DCM solution with pentane.

2.2.2 Di-phenyl substituted (P,C) complex[19]

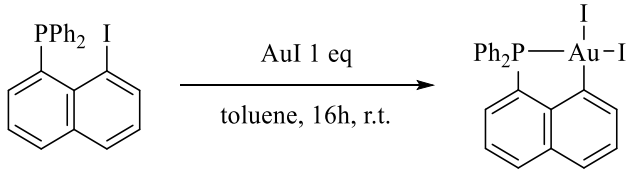

Gold iodide (19.8 mg, 0.060 mmol) was suspended in degassed toluene (3 ml) and a solution of the ligand (26.4 mg, 0.061 mmol) in degassed toluene (2 ml) was added dropwise at room temperature. The reaction mixture was stirred at room temperature for 16 h. The complete conversion of the ligand was confirmed by no-lock ^{31}P NMR. All volatiles were removed in vacuo to yield the product as an orange-red powder. Crystals were obtained by layering a saturated DCM solution with pentane.

2.3 Synthesis of (P,C)$Au(OAc^F)_2$ complexes[54]

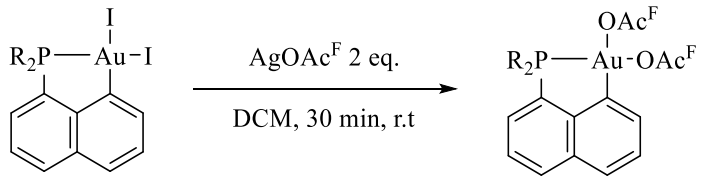

R= -Ph, -i-Pr

The right quantity of (P,C)AuI_2 complex (0.43 mmol) was dissolved in 3 ml of degassed DCM and added to a suspension of silver trifluoroacetate (191 mg, 0.86 mmol) in 3 ml of degassed DCM. The mixture was

stirred for 30 min during which AgI precipitated as the solution evolved from orange to colorless. The suspension was filtered over a Celite® pad, and evaporation of the solvent afforded the desired complexes as an air-stable solid.

2.4 General procedure for aryl 3-phenylpropiolates synthesis[60]

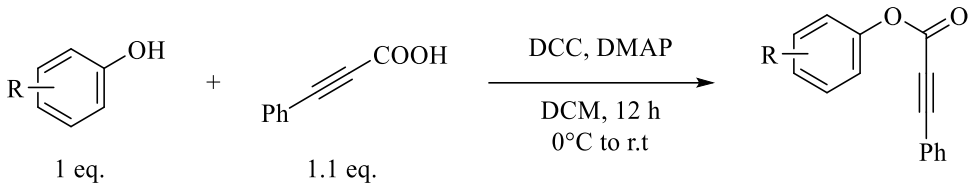

To a solution of phenol (3.0 mmol, 1.0 eq.) in DCM (12 ml) was added aryl alkynyl carboxylic acids (3.3 mmol, 1.1 eq.) at 0 °C. Then, a mixture of DCC (873.0 mg, 4.4 mmol, 1.5 eq.) and DMAP (36.0 mg, 1.5 mmol, 0.1 eq.) in DCM (6 ml) was added dropwise. The resulting mixture was stirred at room temperature for 12 hours. The crude mixture was filtered and washed with DCM (15 ml). The combined organic phase was concentrated under reduced pressure to give a residue which was purified by a silica gel column chromatography (eluent pentane/toluene 1:1 v/v or diethyl ether/pentane 1:4 v/v) to give the desired product.

2.5 General procedure for aryl propiolates synthesis[52]

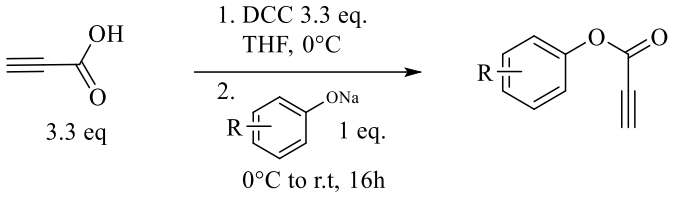

A magnetically stirred solution of the relevant phenol (1.0 mmol, 1.0 eq.) in tetrahydrofuran (10 ml) maintained at 0 °C was treated with sodium hydride (60% suspension in mineral oil, 1.1 mmol, 1.1 eq.). In a second flask, a magnetically stirred solution of propiolic acid (3.3 mmol, 3.3 eq.) in tetrahydrofuran (10 ml) was cooled to 0 °C and then treated with DCC (3.3 mmol, 3.3 eq.) followed by the mixture obtained by treating the phenol with NaH. The resulting mixture was allowed to warm to 18 °C and then stirred at this temperature for 16 h before being concentrated under reduced pressure. The residue so obtained was taken up in acetonitrile (10 ml) and filtered. The filtrate was concentrated under reduced pressure, and the residue thus obtained subjected to flash chromatography (eluent pentane/toluene 1:1 v/v or diethyl ether/pentane 1:4 v/v). Concentration of the relevant fractions gave the corresponding aryl propiolate.

2.6 Procedure for phenyl propiolate and biphenyl-4-yl propiolate synthesis[52]

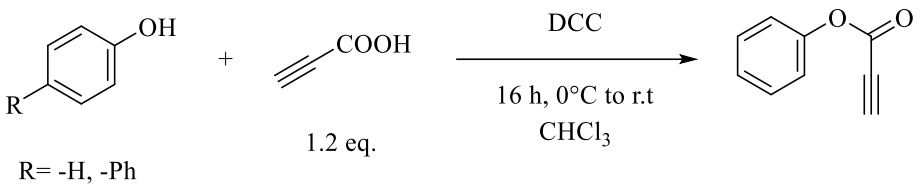

R= -H, -Ph

A magnetically stirred solution of the relevant phenol (1 mmol, 1 eq.) and propiolic acid (1.2 mmol, 1.2 eq.) in chloroform (20 ml) maintained at 0 °C was treated with DCC (1.2 mmol, 1 eq.). The solution thus obtained was allowed to warm to 18 °C and then stirred at this temperature for 16 h before being concentrated under reduced pressure. The ensuing residue was taken up in acetonitrile (20 ml), and the mixture thus formed filtered. The filtrate was concentrated under reduced pressure, and the residue was subjected to flash chromatography (silica gel, 1:1 v/v mixture of toluene/pentane). Concentration of the relevant fractions then gave the corresponding aryl propiolate.

2.7 Synthesis of aryl alkynyl ethers[66]

2.7.1 General procedure for aryl propargyl ethers

R= -H, -OMe

Phenyl and 4-methoxyphenyl propargyl ethers were prepared via the reaction of the appropriate phenol (3 mmol) with propargyl bromide (4.5 mmol, 1.5 eq.) at room temperature in 20 ml of anhydrous DMF in the presence of potassium carbonate (3.6 mmol, 1.2 eq.). Purification of the crude product was achieved via flash column chromatography.

2.7.2 Sesamol 3-phenyl-2-propynyl ether

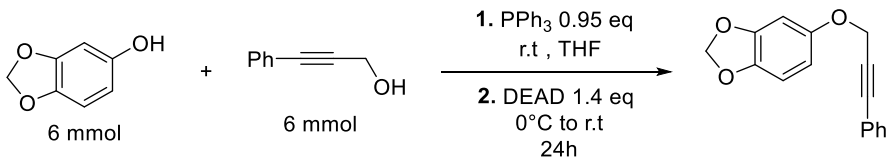

To a flame dried 150-ml round bottom flask was added phenol (1.11 g, 11.79 mmol), 3-phenyl-2- propyn-1-ol (1.56 g, 11.79 mmol), triphenylphosphine (2.94 g, 11.20 mmol, 0.95 eq.) and 50 ml of THF. The

solution was cooled to 0°C and diethyl azodicarboxylate (2.6 ml, 16.51 mmol, 1.4 eq.) was added dropwise via syringe. The ice bath was removed and stirred under argon for 24 hr. Product purification was achieved by flash column chromatography (eluent DCM/pentane 1:20 v/v).

2.8 Au(III)-catalyzed intermolecular hydroarylation of ethyl 3-phenylpropiolate with TMB[54]

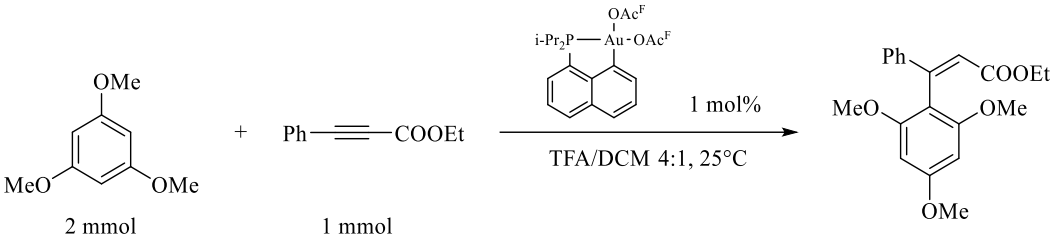

In a glovebox, arene (2 mmol) was dissolved in 0.8 ml of TFA and the solution was placed in a flame-dried Schlenk. Gold complex (0.01 mmol or 0.05 mmol) and hexamethylbenzene (25.0 mg, 0.15 mmol) were dissolved in 0.2 ml DCM and added to the Schlenk. Out of the glovebox, a t_0 NMR check was performed before cooling down to 0°C (ice bath). The alkyne (1 mmol) was added under argon flux and the mixture was stirred for 5 min at 0°C and then at 25°C for the rest of the reaction time using a 25°C thermostatic bath. The reaction was monitored by ^{1}H NMR using the arene aliphatic signals for calibration and hexamethylbenzene as the internal standard.

2.9 Procedure for the synthesis of substituted coumarins

2.9.1 Au(I)-catalyzed intermolecular hydroarylation of phenylpropiolic and hexynoic acid in BMIM NTf_2

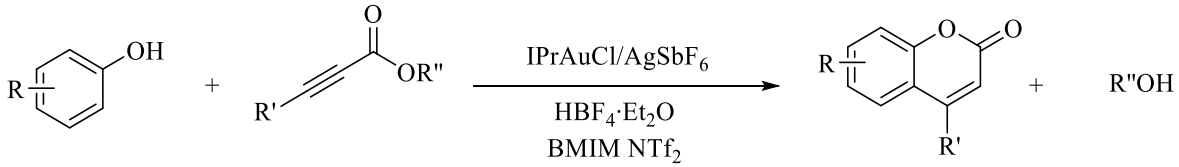

Protocol 1

The right quantity of IPrAuCl (0.012 mmol) and arene (2.5 mmol) were weighed and placed in a Schlenk-flask. Three cycle vacuum/argon were performed in order to ensure inert conditions. Propiolic acid (2.5 or 12.5 mmol) was added together to $AgSbF_6$ (0.012 mmol) in 0.75 ml of BMIM NTf_2. The flask was placed

in a thermostatic oil-bath at 25 or 40 °C and the acid co-catalyst $HBF_4{\cdot}Et_2O$ (0.035 ml, 0.25 mmol)* was added. The process was monitored by ^1H NMR sampling aliquots of the reaction crude at different times, and then dissolved in 0.5 ml of $CDCl_3$ or DMSO-d_6.

* the acid co-catalyst was not added in tests that do not specify it

Protocol 2

The right quantity of IPrAuCl (0.0025 or 0.012 mmol)*/** and arene (2.5 mmol, 1 eq.) were weighed and placed in a Schlenk flask. Three cycle vacuum/argon were performed in order to ensure inert conditions. The alkyne (2.5 mmol, 1 eq.) was added together to 0.75 ml of BMIM NTf_2 and molecular sieves 4Å, and the mixture put under stirring. At this point, $AgSbF_6$ (0.0025 or 0.012 mmol)* was added in 0.75 ml of BMIM NTf_2, and the reaction kept under stirring for 2 minutes. The Schlenk-flask was placed in a thermostatic oil-bath at 40°C and the acid co-catalyst $HBF_4{\cdot}Et_2O$ (0.035 ml, 0.25 mmol) was added. The process was monitored by ^1H NMR sampling aliquots of the reaction crude at different times, and then dissolved in 0.5 ml of $CDCl_3$ or DMSO-d_6.

* for hexynoic acid also 1 mol% of catalyst and silver salt were implemented (0.025 mmol).

** in the tests performed with the internal standard, the catalyst was added in 1 mmol of di-chloroethane or di-methoxyethane.

2.9.2 Au(I)-catalyzed intermolecular hydroarylation of propiolic acid in BMIM NTf_2

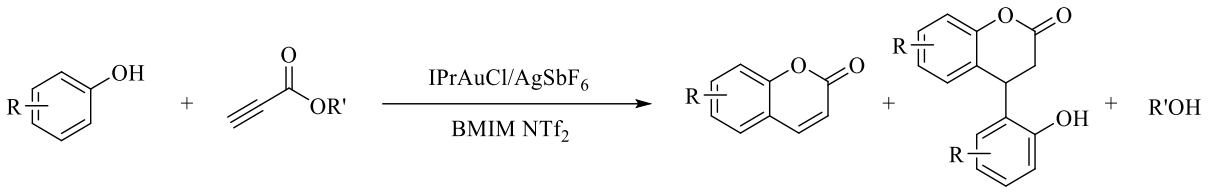

The right quantity of catalyst (0.012 mmol) and arene (2.5 mmol) were weighed and placed in a Schlenk-flask. Three cycles vacuum/argon were performed in order to ensure inert conditions. Propiolic acid (2.5 or 12.5 mmol) was added together to $AgSbF_6$ (0.012 mmol) in 0.75 ml of BMIM NTf_2. The flask was placed in a thermostatic oil-bath at 25 or 40 °C and the acid co-catalyst $HBF_4{\cdot}Et_2O$ (0.035 ml, 0.25 mmol) was added. The process was monitored by ^1H NMR sampling aliquots of the reaction crude at different times, and then dissolved in 0.5 ml of $CDCl_3$ or DMSO-d_6.

2.9.3 Cyclization of sesamol 3-phenylpropiolate catalyzed by (P,C)Au(III) complexes in Fujiwara-type conditions

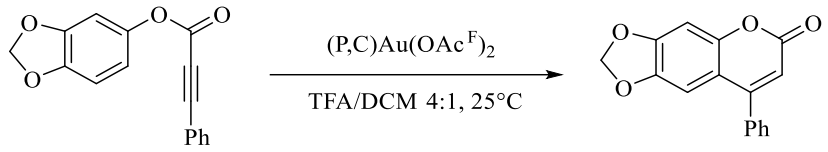

The substrate (266.3 mg, 1 mmol) and hexamethylbenzene (25.0 mg, 0.15 mmol) were weighed and placed in a flame-dried Schlenk-flask. The two solids were dissolved in 0.7 ml of TFA and 0.2 ml of degassed DCM. A t_0 NMR check was performed (solvent $CDCl_3$). Then the gold complex (0.001 mmol or 0.005 mmol) in 0.1 ml of TFA was added to the Schlenk. before cooling down to 0°C (ice bath). The flask was placed in a thermostatic bath at 25 or 40°C and the reaction was monitored by ^1H NMR taking aliquots at different times in 0.5 ml of $CDCl_3$.

2.9.4 Cyclization of aryl alkynoates catalyzed by (P,C)Au(III) complexes in BMIM NTf_2

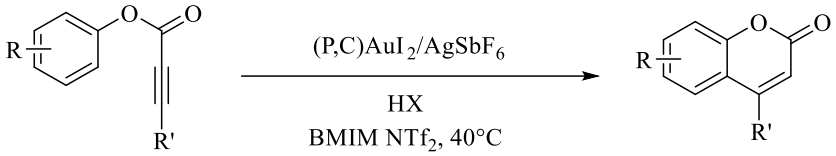

The correct quantities of substrate (0.5 mmol) and gold complex (0.01 or 0.025 mmol) were weighed and placed in a flame-dried Schlenk-flask. BMIM NTf_2 (0.75 ml) was added together to di-methoxyethane (0.05 ml, 0.48 mmol) and the acid co-catalyst (0.1 mmol)*/**. After a t_0 NMR check was performed, $AgSbF_6$ (6.9 or 17.2 mg, thus 0.02 or 0.05 mmol) was added and the mixture stirred 2 minutes at room temperature. The flask was placed in a thermostatic bath at 40°C and the reaction was monitored by ^1H NMR taking aliquots at different times in 0.5 ml of $CDCl_3$.

* $HNTf_2$, $HBF_4{\cdot}Et_2O$ or TfOH

** 50 mol% of $HNTf_2$ (73.8 mg, 0.25 mmol) or TFA (0.02 ml, 0.26 mmol) were implemented in some test with 3,4-methylendioxyphenyl phenylpropiolate

2.10 Procedure for the synthesis of 2H-chromenes

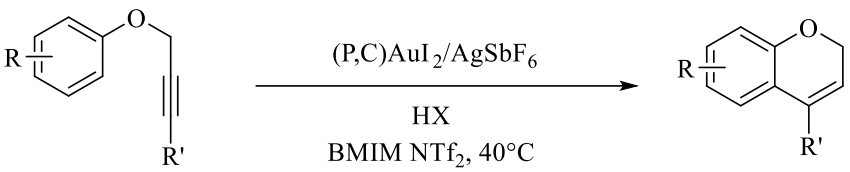

The correct quantities of substrate (0.5 mmol) and gold complex (7.6 mg, 0.01 mmol) were weighed and placed in a flame-dried Schlenk-flask. BMIM NTf_2 (0.75 ml) was added together to di-methoxyethane (0.05 ml, 0.48 mmol) and the acid co-catalyst (0.1 mmol)*. After a t_0 NMR check was performed, $AgSbF_6$ (6.9 or 17.6 mg, thus 0.02 or 0.05 mmol) was added and the mixture stirred 2 minutes at room temperature. The flask was placed in a thermostatic bath at 25 or 40°C and the reaction was monitored by ^1H NMR taking aliquots at different times in 0.5 ml of $CDCl_3$.

* $HNTf_2$ or $HBF_4{\cdot}Et_2O$

3. Blank-tests

3.1 Intermolecular hydroarylation of alkynes: evaluation of possible contributes by $HBF_4{\cdot}Et_2O$ and $AgSbF_6$

Sesamol (345 mg , 2.5 mmol) and phenyl propiolic acid (365 mg, 2.5 mmol) were weighed and placed in a Schlenk-flask. Three cycle vacuum/argon were performed in order to ensure inert conditions. BMIM NTf_2 (0.75 ml) was added together to $HBF_4{\cdot}Et_2O$ (0.035 ml, 0.25 mmol) and the flask was placed in a thermostatic oil-bath at 25 or 40 °C and the acid co-catalyst was added. After 3h a sample was taken and dissolved in 0.5 ml of $CDCl_3$ for ^1H NMR. At this point, $AgSbF_6$ (0.012 mmol) in 0.75 ml of BMIM NTf_2 was added and another ^1H NMR spectrum was taken after further 3h reaction time.

3.2 Experiments of figure 3.1.4 (Chapter 2)

3.2.1 Experiment A

Sesamol (14 mg, 1 mmol) and its analogous coumarin (18.6 mg, 1 mmol) were placed in a Schlenk-flask. Three cycle vacuum/argon were performed in order to ensure inert conditions. BMIM NTf_2 (0.75 ml) was added and the mixture stirred for 5 minutes. Then, $IPrAuNTf_2$ (1.8 mg, 0.002 mmol) was added to the

Schlenk and the reactor placed at 40°C by a thermostatic oil-bath. After 6h a sample was taken and dissolved in 0.5 ml of $CDCl_3$ for ^1H NMR analysis.

3.2.2 Experiment B

Sesamol (13.4 mg, 0.1 mmol) and its analogous coumarin (18.4 mg, 0.1 mmol) were placed in a Schlenk-flask. Three cycle vacuum/argon were performed in order to ensure inert conditions. Propiolic acid (35 mg, 0.5 mmol) in 0.75 ml BMIM NTf_2 was added to the Schlenk and the reactor placed under stirring in a thermostatic oil-bath at 40°C. After 6h a sample was taken and dissolved in 0.5 ml of $CDCl_3$ for ^1H NMR analysis.

3.2.3 Experiment C

Sesamol (13.9 mg, 0.1 mmol) and its analogous coumarin (19.0 mg, 0.1 mmol) were placed in a Schlenk-flask. Three cycle vacuum/argon were performed in order to ensure inert conditions. BMIM NTf_2 (0.75 ml) was added and the mixture stirred for 5 minutes. $IPrAuNTf_2$ (1.8 mg, 0.002 mmol) was added to the Schlenk and the reactor placed at 40°C by a thermostatic oil-bath. After 6h a sample was taken and dissolved in 0.5 ml of $CDCl_3$ for ^1H NMR analysis. After 3h a sample was taken and dissolved in 0.5 ml of $CDCl_3$ for ^1H NMR. At this point, $HBF_4{\cdot}Et_2O$ (0.035 ml, 0.25 mmol) was added and another ^1H NMR spectrum was taken after further 3h reaction time.

3.3 Intramolecular hydroarylation: evaluation of possible contributes by the acid co-catalyst

The correct quantities of substrate (0.5 mmol) was weighed and placed in a flame-dried Schlenk-flask. BMIM NTf_2 (0.75 ml) was added together to di-methoxyethane (0.05 ml, 0.48 mmol) and the acid co-catalyst (0.1 or 0.25 mmol)*. After a t_0 NMR check was performed, the flask was placed in a thermostatic bath at 40°C and the reaction was monitored by ^1H NMR taking aliquots at different times in 0.5 ml of $CDCl_3$.

* $HNTf_2$ or $HBF_4{\cdot}Et_2O$

4. Characterization data

4.1 (P,C)-ligands

8-Di-isopropyl-phosphino-1-iodonaphtalene

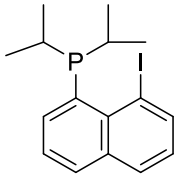

^{1}H NMR (300 MHz, C_6D_6): δ = 0.94 (dd, 6H), 1.15 (dd, 6H), 2.08 [(pseudo)sept-d, 2H], 6.59 (pseudo-t, 2H), 7.39−7.45 (m, 2H), 7.60− 7.65 (m, 1H), 8.24 (dd, 1H) ppm ; **^{31}P{^{1}H} (121 MHz, C_6D_6):** δ = 7.9 ppm; [69]

8-Di-phenyl-phosphino-1-iodonaphtalene

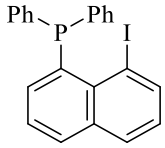

^{1}H NMR (300 MHz, $CDCl_3$): δ 8.30 (dd, 1H), 7.86 (dtd, 1H), 7.80 (dd, 1H), 7.24 – 7.36 (m, 12H), 7.09 (dd, 1H) ppm ; **^{31}P{^{1}H} NMR (121 MHz, $CDCl_3$):** δ -12.6 (s) ppm; [19]

4.2 (P,C)-AuX_2 complexes

8-Di-isopropyl-phosphino-naphtalen-1-yl-bis-iodo Au(III) cyclometallated complex

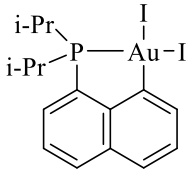

^{1}H NMR (300 MHz, C_6D_6): δ 9.96 (d, 1H), 7.51 (dd, 1H), 7.36 (dd, 1H), 7.08 (t, 1H), 6.88-7.01 (m, 2H), 2.71 (m, 2H), 0.96 (d, 3H), 0.89 (d, 3H), 0.63 (d, 3H), 0.57 (d, 3H); **^{31}P{^{1}H} NMR (121 MHz, C_6D_6):** δ 85.0 (s) ppm; [70]

8-Di-phenyl-phosphino-naphtalen-1-yl-bis-iodo Au(III) cyclometallated complex

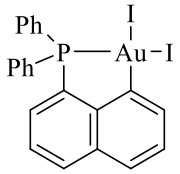

^{1}H NMR (300 MHz, $CDCl_3$): δ 9.37 (ddd, 1H), 8.00 – 8.06 (m, 1H), 7.78 – 7.91 (m, 5H), 7.45 – 7.66 (m, 9H); **^{31}P{^{1}H} NMR (121 MHz, $CDCl_3$):** δ 51.8 (s) ppm; [19]

8-Di-isopropyl-phosphino-naphtalen-1-yl-bis-trifluoroacetate Au(III) cyclometallated complex

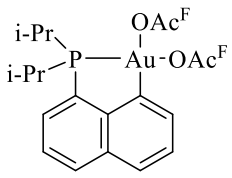

^{1}H NMR (300 MHz, CD_2Cl_2): δ 8.14 (ddd, 1H), 7.92 (dd, 1H), 7.77 (ddd, 1H), 7.74 (ddd, 1H), 7.70 (ddd, 1H), 7.53 (t, 1H), 3.10 (heptd, 2H), 1.40 (dd, 6H), 1.39 (dd, 6H) ppm ; **^{31}P{^{1}H} NMR (121 MHz, CD_2Cl_2):** δ 109.38 (s) ppm ; **^{19}F{^{1}H} NMR (282 MHz, CD_2Cl_2):** δ -74.2 (bs, OAc^F trans to P), -74.6 (s, OAc^F trans to C) ppm; [54]

8-Di-penyl-phosphino-naphtalen-1-yl-bis-trifluoroacetate Au(III) cyclometallated complex

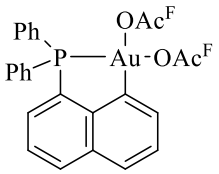

^{1}H NMR (300 MHz, CD_2Cl_2): δ 8.17 (ddd, 1H), 7.96 (dd, 1H), 7.87-7.82 (m, 5H), 7.79-7.74 (m, 3H), 7.72 (ddd, 1H), 7.62 (m, 4H), 7.56 (t, 1H) ppm ; **^{31}P{^{1}H} NMR (121 MHz, CD_2Cl_2):** δ 64.94 (s) ppm ; **^{19}F NMR (282 MHz, CD_2Cl_2):** δ -74.17 (brs, OAcF trans to P), -74.56 (bs, OAcF trans to C) ppm; [54]

4.3 Aryl alkynoates and aryl alkynyl ethers

3,4-Methylendioxy-phenyl 3-phenylpropiolate

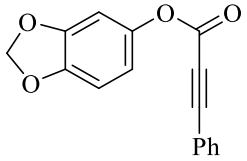

^{1}H NMR (300 MHz, $CDCl_3$): δ 7.7-7.4 (m, 5H), 6.83 (d, 1H, $^{3}J_{orto}$= 8.4Hz), 6.74 (d, 1H, $^{4}J_{meta}$= 2.4Hz), 6.67 (dd, 1H, $^{3}J_{orto}$= 8.4Hz, $^{4}J_{meta}$= 2.4Hz), 6.02(s, 2H) ppm;

3,4-Methylendioxy-phenyl propiolate

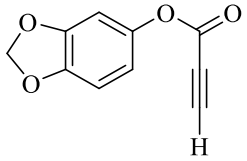

^{1}H NMR (300 MHz, $CDCl_3$): δ 6.78 (d, J = 8.4 Hz, 1H), 6.66 (d, J = 2.4 Hz, 1H), 6.59 (dd, J = 8.4 and 2.4 Hz, 1H), 6.00 (s, 2H), 3.06 (s, 1H) ppm; [52]

4-Methoxyphenyl 3-phenylpropiolate

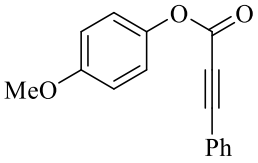

^{1}H NMR (300 MHz, $CDCl_3$): δ 7.63 (d, *J* = 7.2 Hz, 2H), 7.49 (t, *J* = 7.2 Hz, 1H), 7.40 (t, *J* = 7.2 Hz, 2H), 7.12 (d, *J* = 8.8 Hz, 2H), 6.93 (d, *J* = 8.8 Hz, 2H), 3.81 (s, 3H) ppm; [65]

4-Methoxyphenyl propiolate

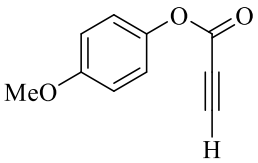

^{1}H NMR (300 MHz, $CDCl_3$): δ 7.07 (d, J = 8.4 Hz, 2H), 6.90 (d, J = 8.4 Hz, 2H), 3.80 (s, 3H), 3.06 (s, 1H) ppm; [65]

7-Methoxynaphtalen-2-yl pripiolate

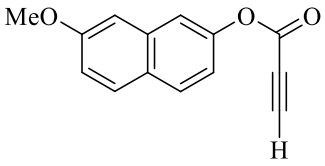

^{1}H NMR (300 MHz, $CDCl_3$): δ 7.79 (d, J = 8.8 Hz, 1H), 7.74 (d, J = 8.8 Hz, 1H), 7.52 (s, 1H), 7.17−7.08 (m, 3H), 3.92 (s, 3H), 3.10 (s, 1H) ppm; [52]

6-Methoxynaphtalen-2-yl pripiolate

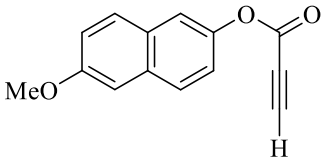

^{1}H NMR (300MHz, $CDCl_3$): δ 7.76 (d, *J* = 7.9 Hz, 1H), 7.71 (d, *J* = 7.9 Hz, 1H), 7.56 (d, *J* = 2.4 Hz, 1H), 7.25 (d, *J* = 2.5 Hz, 1H), 7.21 (dd, *J* = 6.1, 2.5 Hz, 1H), 7.18-7.14 (m, 1H), 3.92 (s, 3H), 3.09 (s, 1H) ppm;

Phenyl 3-phenylpropiolate

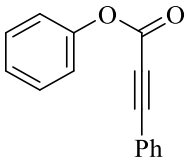

^{1}H NMR (300 MHz, $CDCl_3$): δ 7.59-7.66 (m, 2H), 7.36-7.5 (m, 5H), 7.15-7.23 (m, 3H) ppm; [71]

Phenyl propiolate

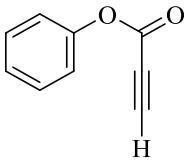

^{1}H NMR (300 MHz, $CDCl_3$): δ 7.32 (t, J = 7.7 Hz, 2H), 7.19 (t, J = 7.7 Hz, 1H), 7.07 (d, J = 7.7 Hz, 2H), 2.99 (s, 1H) ppm; [52]

Biphenyl-4-yl 3-phenylpropiolate

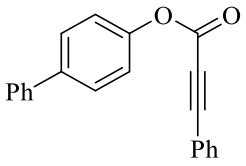

^{1}H NMR (300 MHz, $CDCl_3$): δ 7.64 (t, *J* = 7.6 Hz, 4H), 7.58 (d, *J* = 7.6 Hz, 2H), 7.52 – 7.35 (m, 6H), 7.29 –7.26 (m, 2H) ppm; [72]

Biphenyl-4-yl propiolate

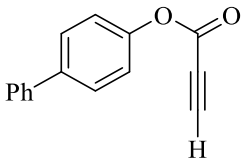

^{1}H NMR (300 MHz, $CDCl_3$): δ 7.64 (s, 1H), 7.62 (s, 1H), 7.59 (s, 1H), 7.57 (s, 1H), 7.47 (t, *J* = 7.8 Hz, 2H), 7.38 (s, 1H), 7.26 (s, 1H), 7.24 (s, 1H), 3.12 (s, 1H) ppm; [73]

4-bromophenyl 3-phenylpropiolate

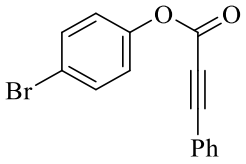

^{1}H NMR (300 MHz, $CDCl_3$): δ 7.62–7.64 (m, 2H), 7.48–7.55 (m, 3H), 7.39–7.43 (m, 2H), 7.08–7.12 (m, 2H) ppm; [71]

Phenyl propargyl ether

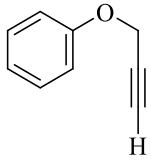

^{1}H NMR (300MHz, $CDCl_3$): δ 7.32 (t, 2H), 6.96-7.0 (m, 3H), 4.7 (d, 2H), 2.52 (t, 1H) ppm; [74]

4-methoxyphenyl propargyl ether

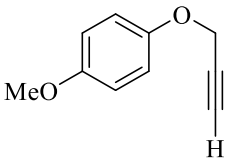

^{1}H NMR (300 MHz, $CDCl_3$): δ 6.93 (d, *J* = 8.8 Hz, 2H), 6.85 (d, *J* = 8.8 Hz, 2H), 4.64 (d, *J* = 2.2 Hz, 2H), 3.77 (s, 3H), 2.51 (t, *J* = 2.4 Hz, 1H) ppm; [75]

3,4-Methylendioxy-phenyl 3-phenyl-2-propynyl ether

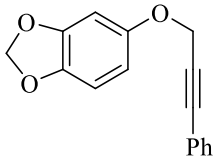

^{1}H NMR (300 MHz, $CDCl_3$): δ 7.46–7.43 (m, 2H), 7.34–7.29 (m, 3H), 6.74 (d, *J* = 8.0 Hz, 1H), 6.63 (d, *J* = 3.7 Hz, 1H), 6.48 (dd, *J* = 8.5, 2.5 Hz, 1H), 5.93 (s, 2H), 4.84 (s, 2H) ppm; [76]

4.4 Coumarins and 2H-chromenes

8-Phenyl-6H-[1,3]dioxolo[4,5-g]chromen-6-one

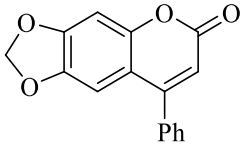

^{1}H NMR (300 MHz, $CDCl_3$): δ 7.52-7.50 (m, 3H), 7.45-7.39 (m, 2H), 6.88 (s, 1H), 6.82 (s, 1H), 6.23 (s, 1H), 6.05 (s, 2H) ppm; [77]

8-Propyl-6H-[1,3]dioxolo[4,5-g]chromen-6-one

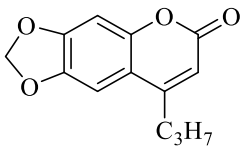

^{1}H NMR (300 MHz, $CDCl_3$): δ 6.97 (1H, s), 6.81 (1H, s), 6.13 (1H, s), 6.05 (2H, d, O-CH_2-O), 2,64 (2H, t), 1.70 (2H, m), 1.03 (3H, t) ppm; [78]

6H-[1,3]Dioxolo[4,5-g]chromen-6-one

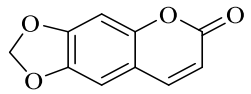

^{1}H NMR (300 MHz, $CDCl_3$): δ 7.58 (d, J = 9.5 Hz, 1H), 6.83 (s, 2H), 6.28 (d, J = 9.5 Hz, 1H), 6.07 (s, 2H) ppm; [52]

7,8-Dihydro-8-(6-hydroxy-1,3-benzodioxol-5-yl)-6H-1,3-dioxol-[4,5-g][1]benzopyran-6-one

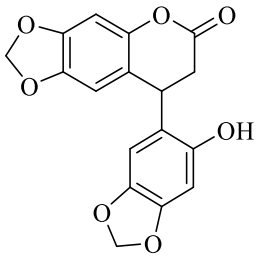

^{1}H NMR (300 MHz, DMSO-d_6): δ 9.57 (s, 1H, OH), 6.84 (s, 1H, ArH), 6.59 (s, 1H, ArH), 6.48 (s, 1H, ArH), 6.19 (s, 1H, ArH), 6.01 (s, 2H, OCH_2O), 5.86 (s, 2H, OCH_2O), 4.45 (t, 1H), 2.99 (dd, 1H), 2.95 (dd, 1H) ppm ; [55][79]

5,6,7-trimethyl-4-phenyl-2H-chromen-2-one

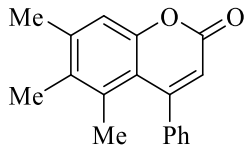

^{1}H NMR (300 MHz, DMSO-d_6): δ 7.4-7.2 (m, Ph, 5H), 7.16 (s, vinyl, 1H), 6.16 (s, Ar-H, 1H), 2.35 (s, CH_3, 3H), 2.09 (s, CH3, 3H), 1.68 (s, CH_3, 3H) ppm; [58]

5,6,7-trimethyl-2H-chromen-2-one

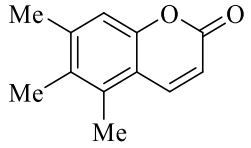

^{1}H NMR (300 MHz, $CDCl_3$): δ = 7.94 (d, J = 9.9 Hz, 1H), 6.97 (s, 1H), 6.32 (d, J = 9.9 Hz, 1H), 2.40 (s, 3H), 2.34 (s, 3H), 2.21 (s, 3H) ppm; [80]

5,6,7-trimethoxy-4-phenyl-2H-chromen-2-one

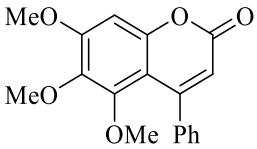

^{1}H NMR (300 MHz, $CDCl_3$) δ7.41 (m, 3H, aryl), 7.32 (m, 2H, aryl), 6.73 (s, 1H, aryl), 6.06 (s, 1H, vinyl), 3.94 (s, 3H, OCH_3), 3.79 (s, 3H, OCH_3), 3.26 (s, 3H, OCH_3) ppm; [49]

6-tertbutyl-4-phenyl-2H-chromen-2-one

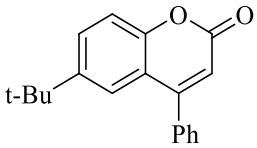

^{1}H NMR (300 MHz, $CDCl_3$): δ 7.60 (dd, 1H, aryl), 7.54 (m, 6H, aryl), 7.35 (d, 1H, aryl), 6.36 (s, 1H, vinyl), 1.27 (s, 9H, tert-butyl) ppm; [49]

6-tertbutyl-2H-chromen-2-one

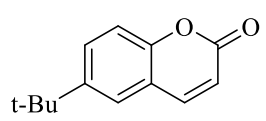

^{1}H NMR (300 MHz, $CDCl_3$): δ7.71 (d, 1H, vinyl) 7.60 (dd, 1H, aryl), 7.45 (d,1H, aryl), 7.27 (d, 1H, aryl), 6.41 (d, 1H, vinyl), 1.36 (s, 9H, t-butyl) ppm; [49][80]

4-(5-*tert*-Butyl-2-hydroxyphenyl)-6-*tert*-butylchroman-2-one

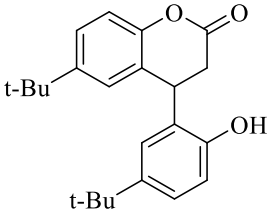

^{1}H NMR (300 MHz, $CDCl_3$): δ 7.32 (dd, J = 2.2, 8.5 Hz, 1H), 7.11–7.07 (m, 3H), 6.79 (d, J = 2.2 Hz, 1H), 6.66 (d, J = 8.3Hz, 1H), 5.50 (br s, 1H), 4.69 (t, J = 6.4 Hz, 1H), 3.19 (dd, J = 6.4, 16.1 Hz, 1H), 3.01 (dd, J = 6.4, 16.1 Hz, 1H), 1.25 (s, 9H), 1.17 (s, 9H) ppm; [81]

6-Methoxy-4-phenyl-2H-chromen-2-one

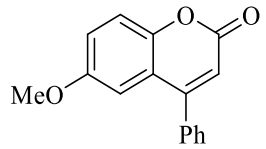

^{1}H NMR (300 MHz, $CDCl_3$): δ 7.53 (m, 3H), 7.46 (m, 2H), 7.34 (d, J = 9.0 Hz, 1H), 7.13 (dd, J = 9.0 and 3.0 Hz, 1H), 6.93 (d, J = 3.0 Hz, 1H), 6.38 (s, 1H), 3.74 (s, 3H) ppm; [52]

6-Methoxy-2H-chromen-2-one

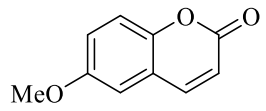

^{1}H NMR (300 MHz, $CDCl_3$): δ 7.65 (d, J = 9.6 Hz, 1H), 7.2 (d, J = 9.0 Hz, 1H), 7.11 (dd, J = 9.0 and 2.9 Hz, 1H), 6.91 (d, J = 2.9 Hz, 1H), 6.42 (d, J = 9.6 Hz, 1H), 3.85 (s, 3H) ppm; [52]

9-Methoxy-3H-benzo[f]chromen-3-one

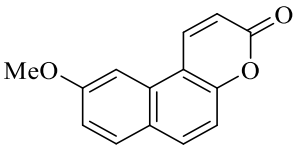

^{1}H NMR (300 MHz, $CDCl_3$): δ 8.44 (d, J = 9.8 Hz, 1H), 7.91 (d, J = 8.9 Hz, 1H), 7.81 (d, J = 8.9 Hz, 1H), 7.51 (d, J = 2.4 Hz, 1H), 7.32 (d, J = 8.9 Hz, 1H), 7.22 (dd, J = 8.9 and 2.4 Hz, 1H), 6.55 (d, J = 9.8 Hz, 1H), 4.00 (s, 3H) ppm; [52]

8-Methoxy-3H-benzo[f]chromen-3-one

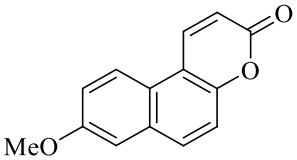

^{1}H NMR (300 MHz, $CDCl_3$): δ 8.41 (d, J = 9.8 Hz, 1H), 8.11 (d, J = 9.2 Hz, 1H), 7.87 (d, J = 9.0 Hz, 1H), 7.43 (d, J = 9.0 Hz, 1H), 7.34 (dd, J = 9.2 and 2.4 Hz, 1H), 7.21 (d, J = 2.4 Hz, 1H), 6.55 (d, J = 9.8 Hz, 1H), 3.95 (s, 3H); [82]

4-Phenyl-*2H*-chromen-*2*-one

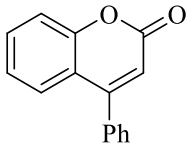

^{1}H NMR (300 MHz, $CDCl_3$): δ 7.58-7.40 (m, 8H), 7.26-7.21 (m, 1H), 6.39 (s, 1H) ppm; [83]

2H-Chromen-2-one

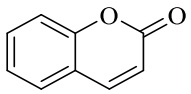

^{1}H NMR (300 MHz, $CDCl_3$): δ 7.64 (d, J = 9.6 Hz, 1H), 7.45 (t, J = 7.9 Hz, 1H), 7.42 (d, J = 7.9 Hz, 1H), 7.25 (d, J = 7.9 Hz, 1H), 7.21 (t, J = 7.9 Hz, 1H), 6.39 (d, J = 9.6 Hz, 1H); [52]

4,6-Diphenyl-2H-chromen-2-one

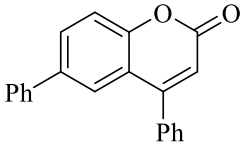

^{1}H NMR (300 MHz, $CDCl_3$): δ 7.77 (d, 1H), 7.67 (s, 1H), 7.54-7.35 (m, 11H), 6.42 (s, 1H) ppm; [72]

6-Phenyl-2H-chromen-2-one

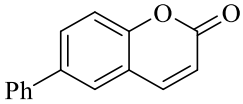

^{1}H NMR (300 MHz, $CDCl_3$): δ 7.77–7.72 (m, 2H), 7.66 (d, 1H), 7.58–7.56 (m, 2H), 7.49–7.45 (m, 2H), 7.40–7.37 (m, 2H), 6.46 (d, 1H) ppm; [84]

6-Bromo-2H-chromen-2-one

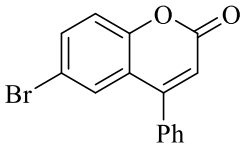

^{1}H NMR (300 MHz, $CDCl_3$): δ 7.59-7.66 (m, 2H), 7.55-7.57 (m, 3H), 7.43-7.45 (m, 2H), 7.30 (d, *J* = 8.8 Hz, 1H), 6.41 (s, 1H) ppm; [83]

2H-Chromene

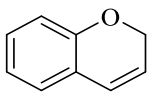

^{1}H NMR (300 MHz, $CDCl_3$): δ 7.08 (t, J = 7.3 Hz, J = 8.1 Hz, 1 H, CH_{arom}), 6.94 (d, J = 7.3 Hz, 1 H, CH_{arom}), 6.86 (t, J = 7.4 Hz, J = 7.3 Hz, 1 H, CH_{arom}), 6.77 (d, J = 8.1 Hz, 1 H, CH_{arom}), 6.42 (d, J = 8.1 Hz, 1 H, CH), 5.78-5.74 (m, 1 H, CH), 4.82 (dd, J = 1.8 Hz, J = 1.4 Hz, 2 H, CH_2) ppm; [85]

6-Methoxy-2H-chromene

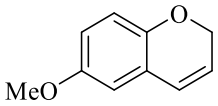

^{1}H NMR (300 MHz, $CDCl_3$): δ 6.65 (d, 1H), 6.59 (s, 1H), 6.47 (d, 1H), 6.31 (s, 1H), 5.73 (dt, 1H), 4.67 (dd, 2H), 3.67 (s, 3H) ppm; [86]

8-Phenyl-6H-[1,3]dioxolo[4,5-g]chromene

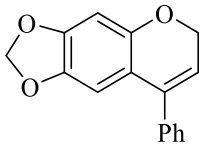

The product need to be isolated and characterized

4.5 Z-aryl alkenes

Ethyl 2-(2',4',6'-trimethoxyphenyl)-2-phenyl-(Z)-propenoate

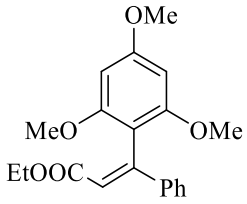

^{1}H NMR (300 MHz, $CDCl_3$): δ 7.36-7.27 (m, 5H), 6.51 (s, 1H), 6.20 (s, 2H), 4.10 (q, 2H), 3.87 (s, 3H), 3.64 (s, 6H), 1.14 (t, 3H) ppm; [54]

4.6 Spyrocycles

4-Phenyl-1-oxaspiro[4,5]deca-3.5,8-trien-2,7-dione

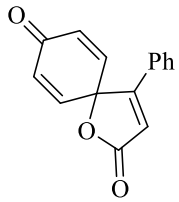

^{1}H NMR (300 MHz, $CDCl_3$): *δ* 7.52–7.46 (m, 3H), 7.42–7.37 (m, 2H), 6.72 (d, *J* = 10.2 Hz, 2H), 6.57 (s, 1H), 6.51 (d, *J* = 9.9 Hz, 2H) ppm; [65]

1-Oxaspiro[4,5]dec-3.5,8-trien-2,7-dione

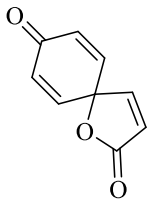

^{1}H NMR (300 MHz, $CDCl_3$): δ 7.17 (d, J = 5.7 Hz, 1H), 6.55 (d, J = 10.2 Hz, 2H), 6.41 (d, J = 10.2 Hz, 2H), 6.36 (d, J = 5.7 Hz, 1H); [65]

4.7 Hydration/decarboxylation products of alkynes

Phenylacetylene

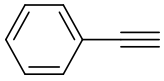

^{1}H NMR (300 MHz, $CDCl_3$): δ 7.51 (m, 2H), 7.32 (m, 3H), 3.08 (s, 1H) ppm; [87]

Acetophenone

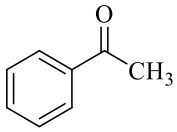

^{1}H NMR (300 MHz, $CDCl_3$): δ 7.97–7.94 (m, 2H), 7.55 (tt, 1H, J = 7.3, 1.5), 7.47–7.43 (m, 2H), 2.59 (s, 3H) ppm; [88]

3-Oxo-3-phenyl-propanoic acid

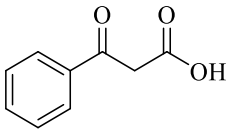

^{1}H NMR (300 MHz, $CDCl_3$): δ 8.05–7.88 (m, 2H), 7.55 – 7.42 (m, 3H), 4.08 (d, J = 1.4 Hz, 2H) ppm; [89]

Ethyl 3-oxo-3-phenyl-propanoate

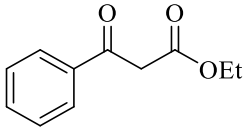

^{1}H NMR (300 MHz, $CDCl_3$): δ 7.94 (d, 2H), 7.57-7.61 (m, 1H), 7.46-7.50 (m, 2H), 4.22 (q, J=7.2 Hz, 2H), 3.99 (s, 2H), 2.45 (t, J=7.2 Hz, 3H); [90][91]

2-Pentanone

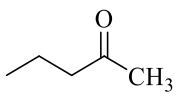

^{1}H NMR (300 MHz, $CDCl_3$): 2.38 (t, 2H), 2.13 (s, 3H), 1.53 (sept, 2H), 0.89 (t, 3H) ppm; [90][92]

4.8 3,4-methylendioxyphenyl 3-phenylpropiolate full characterization

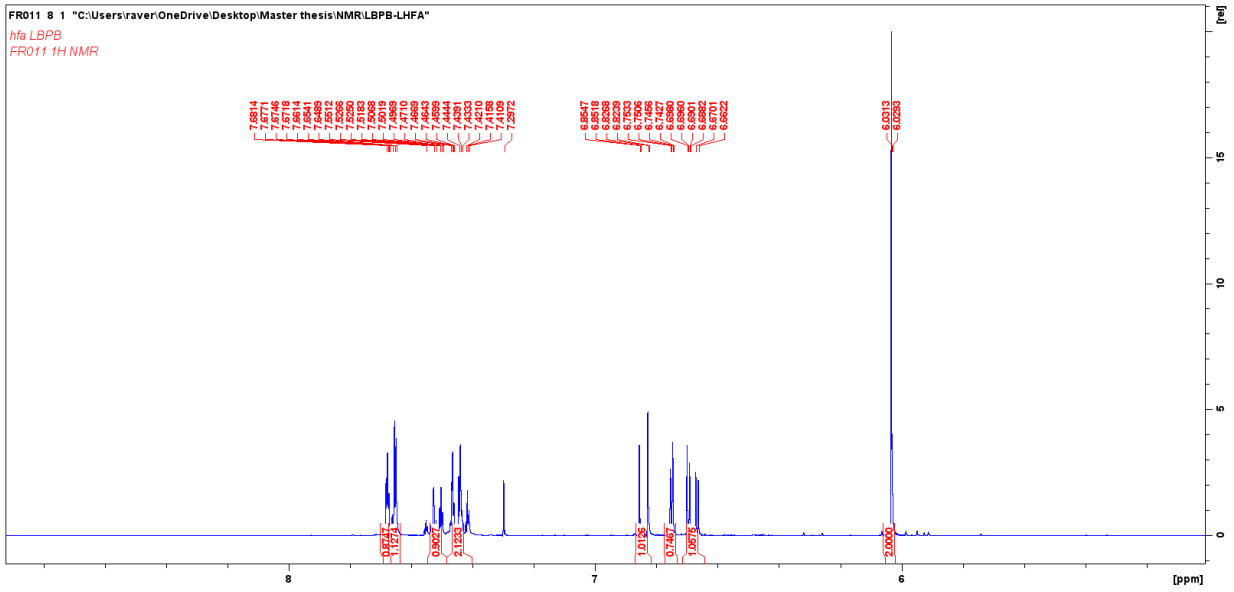

Figure 4.8.1 ^{1}H NMR (300MHz, $CDCl_3$)

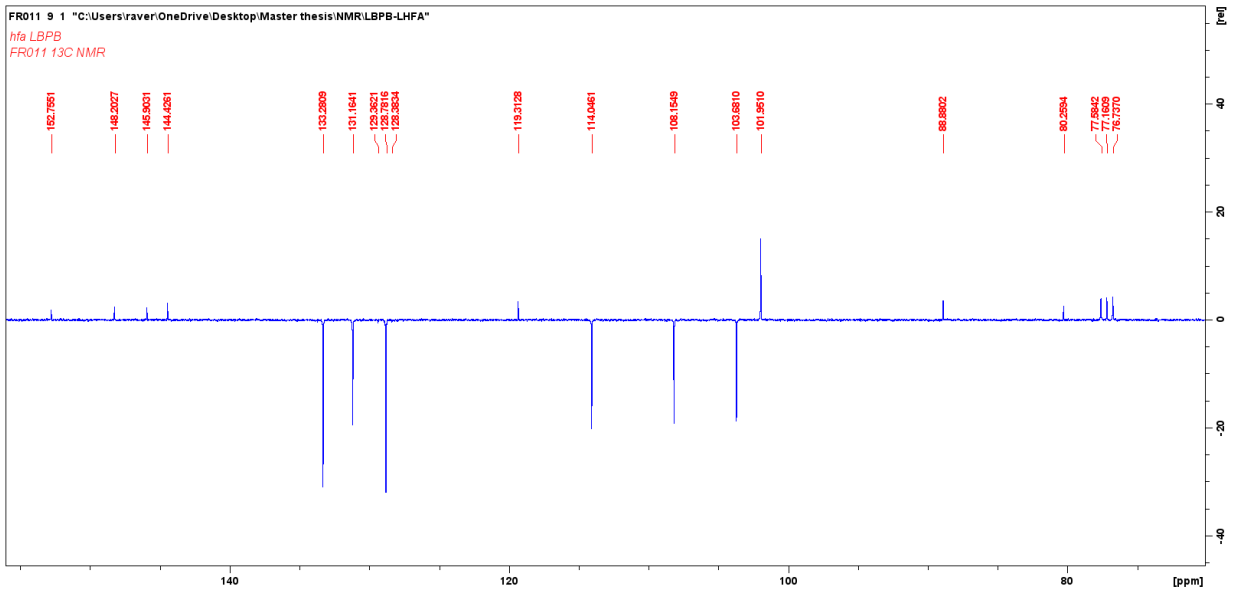

Figure 4.8.2 $^{13}C\{^{1}H\}$ NMR (75.5 MHz, $CDCl_3$)

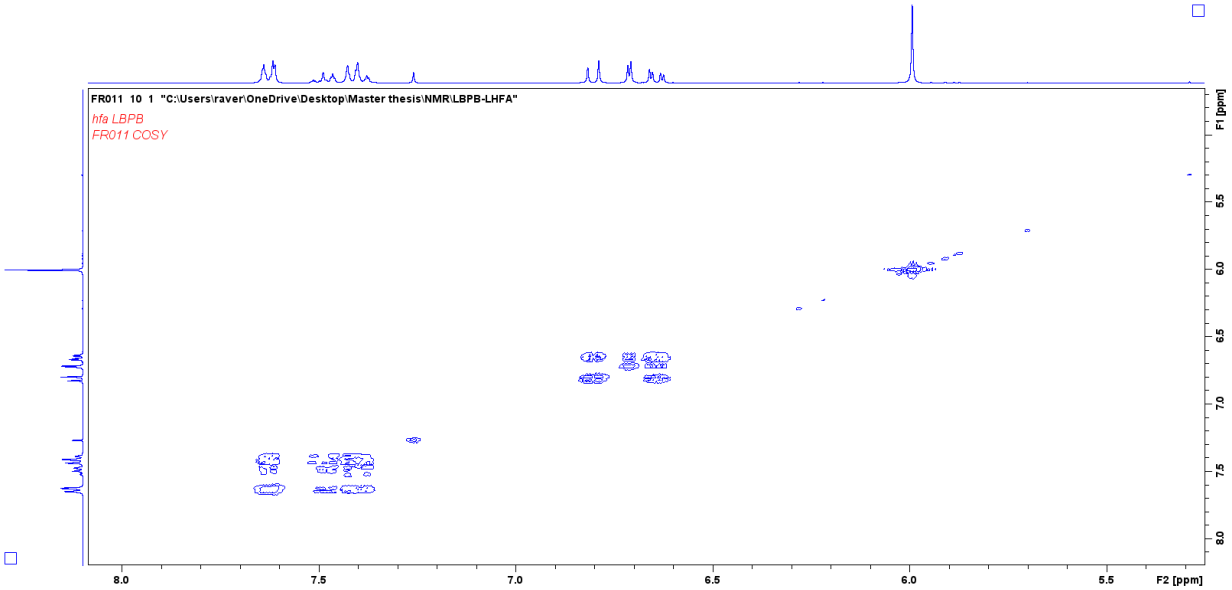

Figure 4.8.3 COSY for determining three-bond-distance H-H correlations

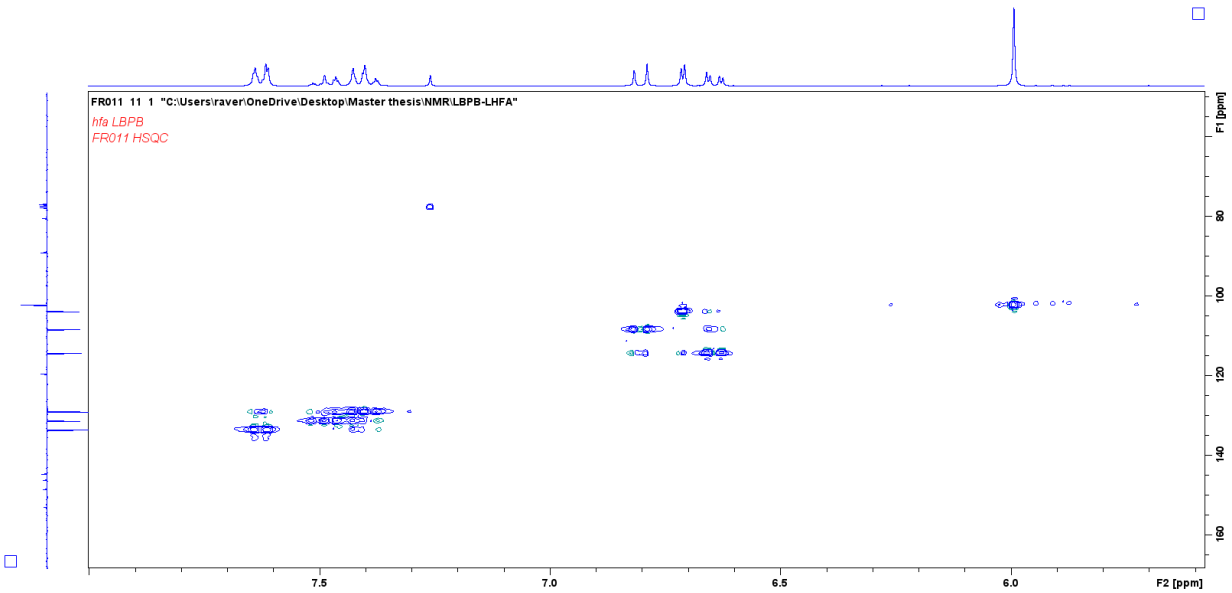

Figure 4.8.4 HSQC for determini single-bond-distance H-C correlations

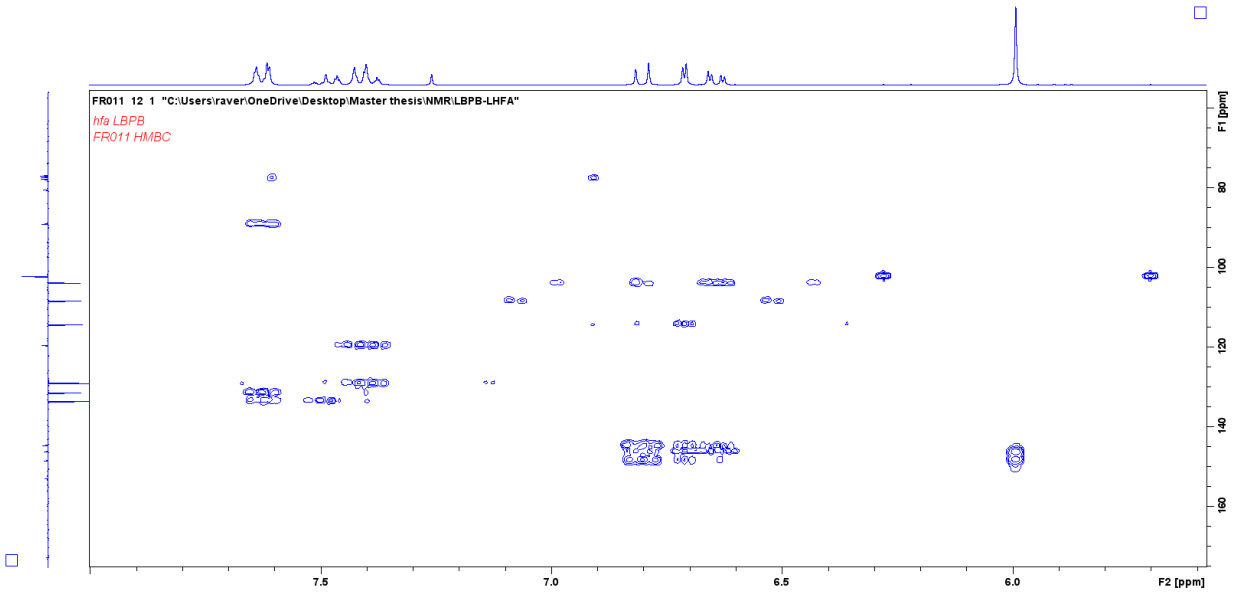

Figure 4.8.5 HMBC for determinig multiple-bond-distance H-C correlations

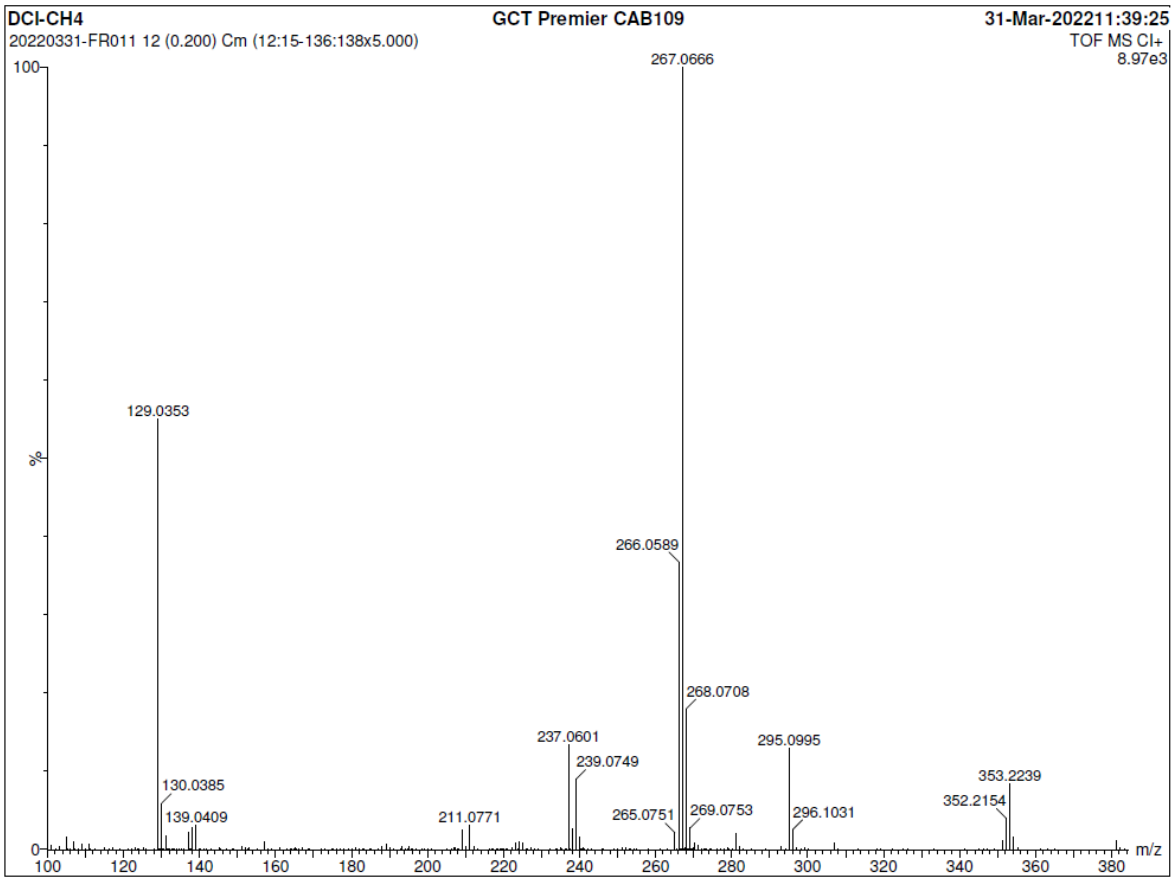

Figure 4.8.6 Positive mode DCl-CH_4/TOF-MS analysis

Single Mass Analysis
Tolerance = 5.0 PPM / DBE: min = -1.5, max = 80.0
Element prediction: Off

Monoisotopic Mass, Odd and Even Electron Ions
22 formula(e) evaluated with 1 results within limits (all results (up to 1000) for each mass)
Elements Used:
C: 0-100 H: 0-100 O: 0-5

DCI-CH4 GCT Premier CAB109 31-Mar-202211:39:25
20220331-FR011 12 (0.200) Cm (12:15-136:138x5.000) TOF MS CI+
8.97e+003

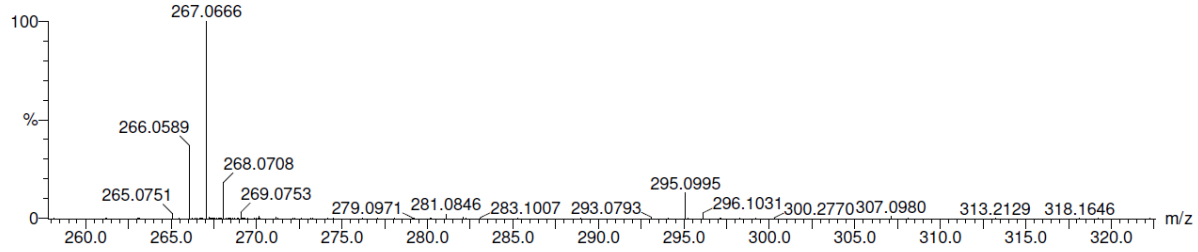

Minimum:				-1.5		
Maximum:		1.4	5.0	80.0		
Mass	Calc. Mass	mDa	PPM	DBE	i-FIT	Formula
266.0589	266.0579	1.0	3.8	12.0	4588.9	C16 H10 O4

Figure 4.8.7 Exact mass determination

Bibliography

[1] T. J. Colacot, J. Matthey, *Platin. Met. Rev.* **2011**, *55*, 84–90.

[2] R. Grubbs, *Angew. Chemie* **2006**, *45*, 3760–3765.

[3] R. R. Schrock, *Angew. Chemie - Int. Ed.* **2006**, *45*, 3748–3759.

[4] R. Noyori, *Adv. Synth. Catal.* **2003**, *345*, 15–32.

[5] K. B. Sharpless, *Angew. Chemie - Int. Ed.* **2002**, *41*, 2024–2032.

[6] A. Fürstner, P. W. Davies, *Angew. Chemie - Int. Ed.* **2007**, *46*, 3410–3449.

[7] R. G. Pearson, *J. Am. Chem. Soc.* **1963**, *85*, 3533–3539.

[8] J. Chatt, L. A. Ducanson, *J. Am. Chem. Soc.* **1952**, 2939–2947.

[9] M. S. Nechaev, V. M. Rayon, G. Frenking, *J. Phys. Chem. A* **2004**, *108*, 3134–3142.

[10] R. H. Hertwig, W. Koch, D. Schröder, H. Schwarz, J. Hrušák, P. Schwerdtfeger, *J. Phys. Chem.* **1996**, *100*, 12253–12260.

[11] C. Jia, W. Lu, J. Oyamada, T. Kitamura, K. Matsuda, M. Irie, Y. Fujiwara, *J. Am. Chem. Soc.* **2000**, *122*, 7252–7263.

[12] A. Fürstner, H. Szillat, B. Gabor, R. Mynott, *J. Am. Chem. Soc.* **1998**, *120*, 8305–8314.

[13] A. Fürstner, *Acc. Chem. Res.* **2014**, *47*, 925–938.

[14] A. Fürstner, *Chem. Soc. Rev.* **2009**, *38*, 3208–3221.

[15] D. J. Gorin, F. D. Toste, *Nature* **2007**, *446*, 395–403.

[16] M. A. Carvajal, J. J. Novoa, S. Alvarez, *J. Am. Chem. Soc.* **2004**, *126*, 1465–1477.

[17] K. M. Altus, J. A. Love, *Commun. Chem.* **2021**, *4*, 1–11.

[18] M. Joost, A. Zeineddine, L. Estévez, S. Mallet-Ladeira, K. Miqueu, A. Amgoune, D. Bourissou, *J. Am. Chem. Soc.* **2014**, *136*, 14654–14657.

[19] J. Guenther, S. Mallet-Ladeira, L. Estevez, K. Miqueu, A. Amgoune, D. Bourissou, *J. Am. Chem. Soc.* **2014**, *136*, 1778–1781.

[20] D. Munz, D. Meyer, T. Strassner, *Organometallics* **2013**, *32*, 3469–3480.

[21] C. Jia, D. Piao, J. Oyamada, W. Lu, T. Kitamura, Y. Fujiwara, *Science (80-.).* **2000**, *287*, 1992–1995.

[22] D. Zargarian, H. Alper, *Organometallics* **1993**, *12*, 712–724.

[23] C. Jia, T. Kitamura, Y. Fujiwara, *J. Synth. Org. Chem.* **2001**, *59*, 1052–1061.

[24] C. Nevado, A. M. Echavarren, *Synthesis (Stuttg).* **2005**, *2*, 167–182.

[25] A. S. K. Hashmi, *Chem. Rev.* **2007**, *107*, 3180–3211.

[26] A. S. K. Hashmi, F. D. Toste, *Modern Gold Catalyzed Synthesis*, **2012**.

[27] D. J. Gorin, N. R. Davis, F. D. Toste, *J. Am. Chem. Soc.* **2005**, *127*, 11260–11261.

[28] V. Mamane, P. Hannen, A. Fürstner, *Chem. - A Eur. J.* **2004**, *10*, 4556–4575.

[29] A. Fürstner, V. Mamane, *J. Org. Chem.* **2002**, *67*, 6264–6267.

[30] M. T. Reetz, K. Sommer, *European J. Org. Chem.* **2003**, 3485–3496.

[31] W. Wang, G. B. Hammond, B. Xu, *J. Am. Chem. Soc.* **2012**, *134*, 5697–5705.

[32] H. Tinnermann, C. Wille, M. Alcarazo, *Angew. Chemie - Int. Ed.* **2014**, *53*, 8732–8736.

[33] Z. Shi, C. He, *J. Org. Chem.* **2004**, *69*, 3669–3671.

[34] J. Schießl, J. Schulmeister, A. Doppiu, E. Wörner, M. Rudolph, R. Karch, A. S. K. Hashmi, *Adv. Synth. Catal.* **2018**, *360*, 2493–2502.

[35] P. W. Davies, N. Martin, *Org. Lett.* **2009**, *11*, 2293–2296.

[36] A. Homs, C. Obradors, D. Leboeuf, A. M. Echavarren, *Adv. Synth. Catal.* **2014**, *356*, 221–228.

[37] A. Zhdanko, M. E. Maier, *ACS Catal.* **2015**, *5*, 5994–6004.

[38] D. Weber, M. R. Gagné, *Org. Lett.* **2009**, *11*, 4962–4965.

[39] D. Wang, R. Cai, S. Sharma, J. Jirak, S. K. Thummanapelli, N. G. Akhmedov, H. Zhang, X. Liu, J. L. Petersen, X. Shi, *J. Am. Chem. Soc.* **2012**, *134*, 9012–9019.

[40] K. R. Seddon, *J. Chem. Tech. Biotechnol.* **1997**, *50*, 1–6.

[41] N. V. Plechkova, K. R. Seddon, *Chem. Soc. Rev.* **2008**, *37*, 123–150.

[42] H. Olivier-Bourbigou, Y. Chauvin, *Multiph. Homog. Catal.* **2008**, 406–412.

[43] R. Sheldon, *Chem. Commun.* **2001**, *1*, 2399–2407.

[44] J. Dupont, R. F. De Souza, P. A. Z. Suarez, *Chem. Rev.* **2002**, *102*, 3667–3692.

[45] Y. Chauvin, L. Mussmann, H. Olivier, *Angew. Chemie (International Ed. English)* **1996**, *34*, 2698–2700.

[46] A. Biffis, C. Tubaro, M. Baron, *Chem. Rec.* **2016**, 1742–1760.

[47] J. H. Do, H. N. Kim, J. Yoon, J. S. Kim, H. J. Kim, *Org. Lett.* **2010**, *12*, 932–934.

[48] K. Szwaczko, *Inorganics* **2022**, *10*.

[49] C. Jia, D. Piao, T. Kitamura, Y. Fujiwara, *J. Org. Chem.* **2000**, *65*, 7516–7522.

[50] O. Zaitceva, V. Bénéteau, D. S. Ryabukhin, I. I. Eliseev, M. A. Kinzhalov, B. Louis, A. V. Vasilyev, P. Pale, *Tetrahedron* **2020**, *76*, 1–9.

[51] R. S. Menon, A. D. Findlay, A. C. Bissember, M. G. Banwell, *J. Org. Chem.* **2009**, *74*, 8901–8903.

[52] A. Cervi, Y. Vo, C. L. L. Chai, M. G. Banwell, P. Lan, A. C. Willis, *J. Org. Chem.* **2021**, *86*, 178–198.

[53] M. Baron, A. Biffis, *European J. Org. Chem.* **2019**, *2019*, 3687–3693.

[54] C. Blons, S. Mallet-Ladeira, A. Amgoune, D. Bourissou, *Angew. Chemie - Int. Ed.* **2018**, *57*, 11732–11736.

[55] S. Bonfante, GOLD (I) -CATALYZED HYDROARYLATION REACTIONS IN IONIC LIQUIDS, **2019**.

[56] A. Marciniak, *Int. J. Mol. Sci.* **2010**, *11*, 1973–1990.

[57] S. H. Lee, S. B. Lee, *Chem. Commun.* **2005**, 3469–3471.

[58] P. Bax, Gold-Catalyzed Alkyne Hydroarylations: Applications to Coumarin Synthesis, **2021**.

[59] R. A. Daley, A. S. Morrenzin, S. R. Neufeldt, J. J. Topczewski, *J. Am. Chem. Soc.* **2020**, *142*, 13210–13218.

[60] H. Li, S. Liu, Y. Huang, X. H. Xu, F. L. Qing, *Chem. Commun.* **2017**, *53*, 10136–10139.

[61] N. Ibrahim, M. H. Vilhelmsen, M. Pernpointner, F. Rominger, A. S. K. Hashmi, *Organometallics* **2013**, *32*, 2576–2583.

[62] H. Li, S. Liu, Y. Huang, X. H. Xu, F. L. Qing, *Chem. Commun.* **2017**, *53*, 10136–10139.

[63] Z. Li, Z. Shi, C. He, *J. Organomet. Chem.* **2005**, *690*, 5049–5054.

[64] P. A. Vadola, D. Sames, *J. Org. Chem.* **2012**, *77*, 7804–7814.

[65] M. D. Aparece, P. A. Vadola, *Org. Lett.* **2014**, *16*, 6008–6011.

[66] S. J. Pastine, S. W. Youn, D. Sames, *Org. Lett.* **2003**, *5*, 1055–1058.

[67] C. Nevado, A. M. Echavarren, *Chem. - A Eur. J.* **2005**, *11*, 3155–3164.

[68] G. R. Fulmer, A. J. M. Miller, N. H. Sherden, H. E. Gottlieb, A. Nudelman, B. M. Stoltz, J. E. Bercaw, K. I. Goldberg, *Organometallics* **2010**, *29*, 2176–2179.

[69] S. Bontemps, M. Devillard, S. Mallet-Ladeira, G. Bouhadir, K. Miqueu, D. Bourissou, *Inorg. Chem.* **2013**, *52*, 4714–4720.

[70] F. Rekhroukh, R. Brousses, A. Amgoune, D. Bourissou, *Angew. Chemie - Int. Ed.* **2015**, *54*, 1266–1269.

[71] S. Sau, P. Mal, *Chem. Commun.* **2021**, *57*, 9228–9231.

[72] M. L. N. Rao, A. Kumar, *Tetrahedron* **2014**, *70*, 6995–7005.

[73] M. Bio, G. Nkepang, Y. You, *Chem. Commun.* **2012**, *48*, 6517–6519.

[74] S. Bhuyan, A. Gogoi, J. Basumatary, G. B. Roy, *European J. Org. Chem.* **2022**, 1–6.

[75] I. Volchkov, D. Lee, *J. Am. Chem. Soc.* **2013**, *135*, 5324–5327.

[76] J. S. Tian, Y. He, Z. Y. Gao, X. Liu, S. F. Dong, P. Wu, T. P. Loh, *Org. Lett.* **2021**, *23*, 6594–6598.

[77] Z. Wang, X. Li, L. Wang, P. Li, *Tetrahedron* **2019**, *75*, 1044–1051.

[78] P. Olaya, N. E. Vergel, J. L. López, D. Viña, M. F. Guerrero, *Braz. J. Pharm. Sci.* **2020**, 1–10.

[79] T. Ziegler, H. Mohler, **1987**, 373–378.

[80] P. K. Hota, A. Jose, S. K. Mandal, *Organometallics* **2017**, *36*, 4422–4431.

[81] R. A. Kunkalkar, R. A. Fernandes, *Chem. Commun.* **2019**, *55*, 2313–2316.

[82] Y. S. Hon, T. W. Tseng, C. Y. Cheng, *Chem. Commun.* **2009**, 5618–5620.

[83] Y. Yang, J. Han, X. Wu, S. Xu, L. Wang, *Tetrahedron Lett.* **2015**, *56*, 3809–3812.

[84] H. Choi, J. Kim, K. Lee, *Tetrahedron Lett.* **2016**, *57*, 3600–3603.

[85] J. R. Bernardo, A. C. Fernandes, *Green Chem.* **2016**, *18*, 2675–2681.

[86] F. V. Gaspar, J. C. F. Barcellos, J. F. Cívicos, P. Merino, C. Nájera, P. R. R. Costa, *Tetrahedron* **2020**, *76*, 1–8.

[87] A. Modak, P. Bhanja, A. Bhaumik, *Chem. - A Eur. J.* **2018**, *24*, 14189–14197.

[88] A. Modak, A. Deb, T. Patra, S. Rana, S. Maity, D. Maiti, *Chem. Commun.* **2012**, *48*, 4253–4255.

[89] H. Hu, X. Wu, Y. Qiu, C. Wang, W. Wang, G. Yue, H. Wang, J. Feng, G. Wang, H. Ni, P. Zou, *Org. Lett.* **2022**, *24*, 832–836.

[90] X. Zeng, Y. Xu, J. Liu, Y. Deng, *Org. Lett.* **2021**, *23*, 9058–9062.

[91] Y. Gao, W. Qin, M. Q. Tian, X. Zhao, X. H. Hu, *Adv. Synth. Catal.* **2022**, *364*, 2241–2247.

[92] S. D. Mürtz, N. Kurig, F. J. Holzhäuser, R. Palkovits, *Green Chem.* **2021**, *23*, 8428–8433.